

Braun

8176
54-4-49

NACA TN 3120

TECH LIBRARY KAFB, NM
0065987

NATIONAL ADVISORY COMMITTEE FOR AERONAUTICS

TECHNICAL NOTE 3120

SPAN LOAD DISTRIBUTIONS RESULTING FROM CONSTANT VERTICAL
ACCELERATION FOR THIN SWEPTBACK TAPERED
WINGS WITH STREAMWISE TIPS

SUPERSONIC LEADING AND TRAILING EDGES

By Isabella J. Cole and Kenneth Margolis

Langley Aeronautical Laboratory
Langley Field, Va.



Washington
January 1954

TECHNICAL NOTE
AFL 2811



TECHNICAL NOTE 3120

SPAN LOAD DISTRIBUTIONS RESULTING FROM CONSTANT VERTICAL
ACCELERATION FOR THIN SWEEPBACK TAPERED
WINGS WITH STREAMWISE TIPS

SUPERSONIC LEADING AND TRAILING EDGES

By Isabella J. Cole and Kenneth Margolis

SUMMARY

On the basis of the linearized supersonic-flow theory, equations for the span load distribution resulting from constant vertical acceleration (that is, linear variation of angle of attack with time) are derived for a series of thin sweptback tapered wings with streamwise tips. The analysis is valid at Mach numbers for which the wing leading and trailing edges are supersonic. A minor restriction is that the Mach line from the leading edge of either wing tip may not intersect the remote half wing.

The computational results of the investigation are presented in a series of charts from which the span loadings may be obtained for given values of aspect ratio, taper ratio, leading-edge sweepback, and Mach number. For illustrative purposes, variations of the spanwise distribution of circulation (which is proportional to the span load distribution) with several plan-form parameters and Mach number are shown, in addition to some typical chordwise and spanwise pressure distributions.

INTRODUCTION

The aerodynamicist requires detailed information on the load distribution over the component surfaces of an airframe. One of the most important considerations is the distribution of load along the wing span. This information can be used directly to obtain the forces and moments acting on the wing itself and to estimate roughly the load on isolated vertical tails (for corresponding motions) and isolated horizontal tails; in addition, knowledge of the span load distribution is a prime requirement for the solution of problems relating to loads and aeroelasticity and for flow-field and other aerodynamic calculations. Thus, much effort has been devoted to developing methods of calculation

and utilizing these methods to obtain detailed load information throughout the range of flight speeds for wings of various plan forms undergoing several types of motion.

Some of the more recent contributions to the literature on span load distributions at supersonic speeds are references 1 to 4. The general plan form considered in these references has arbitrary aspect ratio, taper ratio, and sweepback; the wing tips are parallel to the axis of wing symmetry. At Mach numbers for which the wing leading edge is subsonic, equations and charts for the span load distributions resulting from constant angle of attack, steady rolling, steady pitching, and constant vertical acceleration are given in reference 1; the case of constant sideslip is treated in reference 2. At Mach numbers for which the wing leading edge is supersonic, corresponding information is given for constant angle of attack, steady rolling, and steady pitching in reference 3; calculations for the sideslip motion are given in reference 4. (Restrictions common to references 1 to 4 inclusive are that the wing trailing edge is supersonic and that the Mach line from the leading edge of either tip may not intersect the remote half wing.) The span loading due to constant vertical acceleration for the supersonic-leading-edge condition has not been previously considered; the present paper contributes this information.

Equations are derived herein for the spanwise distribution of circulation (which is proportional to the span load) due to constant vertical acceleration, that is, linear variation of angle of attack with time. The type of wing plan form considered is that used in references 1 to 4; namely, wings of arbitrary aspect ratio, taper ratio, and sweepback, and with wing tips that may be termed "streamwise" for this motion. The analysis is valid at supersonic speeds for which the wing leading and trailing edges are supersonic, provided the Mach line from the leading edge of one tip does not intersect the opposite half wing.

The numerical results of the investigation are presented in a series of charts from which fairly rapid estimations of the load distribution may be obtained for given values of the parameters aspect ratio, taper ratio, leading-edge sweepback, and Mach number. Several illustrative variations of the load distribution with Mach number and wing geometry as well as some typical chordwise and spanwise pressure distributions are also presented.

SYMBOLS

x, y Cartesian coordinates (see fig. 1)
 V free-stream velocity

ρ	density of air
M	free-stream Mach number
μ	Mach angle
B	cotangent of Mach angle, $\sqrt{M^2 - 1}$
b	wing span
c_r	root chord
e	spanwise coordinate of intersection of trailing edge of wing and Mach line from wing apex
g	spanwise coordinate of intersection of trailing edge of wing and Mach line reflected from wing tip
h	spanwise coordinate of intersection of trailing edge of wing and Mach line from leading edge of wing tip
λ	taper ratio, $\frac{\text{Tip chord}}{\text{Root chord}}$
A	aspect ratio, $\frac{2b}{c_r(1 + \lambda)}$
Λ	angle of sweep (see fig. 1)
$m = \cot \Lambda_{LE}$	
$k = \frac{\cot \Lambda_{TE}}{\cot \Lambda_{LE}} = \frac{AB(1 + \lambda)}{AB(1 + \lambda) - 4mB(1 - \lambda)}$	
α	angle of attack
q	steady pitching velocity about the y-axis, positive as shown in figure 1
t	time
$\dot{\alpha}$	rate of change of α with time $\left(\frac{d\alpha}{dt}\right)$; positive $\dot{\alpha}$ indicates an acceleration downward
ΔP	difference due to constant vertical acceleration between upper- and lower-surface pressures; positive in sense of lift
$(\Delta P)_{\alpha=1}$	difference due to unit angle of attack between upper- and lower-surface pressures; positive in sense of lift

- $(\Delta P)_{q=1}$ difference due to unit pitching velocity about the y-axis between upper- and lower-surface pressures; positive in sense of lift
- ϕ perturbation velocity potential due to constant vertical acceleration, evaluated on upper surface of wing
- $\phi_{\alpha=1}$ perturbation velocity potential due to unit angle of attack, evaluated on upper surface of wing
- $\phi_{q=1}$ perturbation velocity potential due to unit pitching velocity about y-axis, evaluated on upper surface of wing
- Γ circulation due to constant vertical acceleration at any spanwise station y , defined by equation (3)
- Γ_1, Γ_2 components of circulation due to constant vertical acceleration; $\Gamma = \Gamma_1 + \Gamma_2$
- Γ_{α} circulation due to angle of attack
- Γ_q circulation due to steady pitching velocity about y-axis

Subscripts:

- LE refers to leading edge or evaluation along leading edge
- TE refers to trailing edge or evaluation along trailing edge

All angles are measured in radians unless otherwise indicated.

ANALYSIS

Scope

The motion considered in the present paper has been commonly termed constant vertical acceleration; it is a time dependent motion that involves a linear variation of angle of attack with time. Expressions for the span load distribution associated with such a motion are derived and calculations based on these expressions are presented for a generalized family of isolated wings (see fig. 1). The wings are uncambered and have vanishingly small thickness; the plan form is of arbitrary sweepback and taper ratio with wing tips parallel to the axis of wing symmetry (streamwise tips). The analysis is carried out within the framework of the linearized supersonic-flow theory and is applicable at those supersonic speeds for which the wing leading and trailing edges are supersonic, subject to the relatively minor restriction that the Mach line from the leading edge of either wing tip does not intersect the remote half wing.

Derivation of Equations

The spanwise distribution of circulation Γ for unyawed wings is related to the integrated chordwise pressure distribution (span loading) by the relationship

$$\Gamma = \frac{1}{\rho V} \int_{x_{LE}}^{x_{TE}} \Delta P \, dx \quad (1)$$

It should be mentioned that the span loading and the spanwise distribution of circulation are sometimes used interchangeably. As is apparent from equation (1), these two quantities are proportional to each other. Based on an application of the linearized supersonic-flow theory, the lifting pressure ΔP for the motion considered (that is, a positive $\dot{\alpha}$) has been shown previously (for example, eq. (13) of ref. 5) to be expressible as follows:

$$\Delta P = \frac{\dot{\alpha}}{B^2} \left[M^2 (\Delta P)_{q=1} - \frac{M^2 x}{V} (\Delta P)_{\alpha=1} - 2\rho(\phi)_{\alpha=1} \right] \quad (2)$$

where $(\Delta P)_{q=1}$ is the lifting pressure for positive unit pitching velocity about the y-axis and where $(\Delta P)_{\alpha=1}$ and $(\phi)_{\alpha=1}$ are the lifting pressure and perturbation velocity potential, respectively, due to positive unit angle of attack. Equation (1) may then be rewritten:

$$\Gamma = \frac{\dot{\alpha}}{B^2 \rho V} \int_{x_{LE}}^{x_{TE}} \left[M^2 (\Delta P)_{q=1} - \frac{M^2 x}{V} (\Delta P)_{\alpha=1} - 2\rho(\phi)_{\alpha=1} \right] dx \quad (3)$$

It is known (for example, see ref. 3) that

$$\int_{x_{LE}}^{x_{TE}} (\Delta P)_{q=1} \, dx = 2\rho V (\phi_{q=1})_{TE} \quad (4)$$

and

$$\int_{x_{LE}}^{x_{TE}} (\Delta P)_{\alpha=1} dx = 2\rho V (\phi_{\alpha=1})_{TE} \quad (5)$$

Upon integration by parts of the middle term of equation (3), utilization of equations (4) and (5), and combination of terms, equation (3) becomes

$$\Gamma = 2\alpha \left[\frac{M^2}{B^2} (\phi_{q=1})_{TE} - \frac{M^2}{VB^2} x_{TE} (\phi_{\alpha=1})_{TE} + \frac{1}{V} \int_{x_{TE}}^{x_{LE}} (\phi)_{\alpha=1} dx \right] \quad (6)$$

According to equation (1), the following relationships are valid:

$$(\Gamma_q)_{q=1} = \frac{1}{\rho V} \int_{x_{LE}}^{x_{TE}} (\Delta P)_{q=1} dx \quad (7)$$

and

$$(\Gamma_\alpha)_{\alpha=1} = \frac{1}{\rho V} \int_{x_{LE}}^{x_{TE}} (\Delta P)_{\alpha=1} dx \quad (8)$$

It then follows from equations (4) and (5) that

$$(\Gamma_q)_{q=1} = 2(\phi_{q=1})_{TE} \quad (9)$$

and

$$(\Gamma_\alpha)_{\alpha=1} = 2(\phi_{\alpha=1})_{TE} \quad (10)$$

Equation (6) may now be expressed in the following convenient manner (since Γ_q and Γ_α are directly proportional to q and α , respectively):

$$\Gamma = \dot{\alpha} \left[\frac{(b/2)^2 M^2}{B} \frac{\Gamma_q}{Bq(b/2)^2} - \frac{M^2 (b/2)^2}{B} \frac{AB(1+\lambda) \frac{y}{b/2} + 4kmB}{kmBAB(1+\lambda)} \frac{\Gamma_\alpha}{V\alpha \frac{b}{2}} + \frac{2}{V} \int_{x_{LE}}^{x_{TE}} (\phi)_{\alpha=1} dx \right] \quad (11)$$

where x_{TE} has been replaced by its functional equivalent

$$x_{TE} = \frac{B \frac{b}{2} \left[\frac{y}{b/2} AB(1+\lambda) + 4mBk \right]}{AB(1+\lambda)Bmk} \quad (12)$$

Formulas and charts for the quantities $\frac{\Gamma_q}{Bq(b/2)^2}$ and $\frac{\Gamma_\alpha}{V\alpha \frac{b}{2}}$ appearing in equation (11) are presented in reference 3. Thus, only the integral $\int_{x_{LE}}^{x_{TE}} (\phi)_{\alpha=1} dx$ remains to be evaluated. Expressions for the potential $(\phi)_{\alpha=1}$ for the various wing regions formed by the Mach line and plan-form boundaries may be obtained from reference 6 (the value of α therein being replaced by unity).

For convenience in calculations and presentation of results, equation (11) for the spanwise distribution of circulation Γ is subdivided into two components, Γ_1 and Γ_2 , such that $\Gamma = \Gamma_1 + \Gamma_2$. The components are as follows:

$$\Gamma_1 = \frac{M^2 \dot{\alpha} (b/2)^2}{B} \left[\frac{\Gamma_q}{Bq(b/2)^2} - \frac{AB(1+\lambda) \frac{y}{b/2} + 4kmB}{kmBAB(1+\lambda)} \frac{\Gamma_\alpha}{V\alpha \frac{b}{2}} \right] \quad (13)$$

$$\Gamma_2 = \dot{\alpha} B (b/2)^2 \int_{x_{LE}}^{x_{TE}} \frac{2(\phi)_{\alpha=1}}{BV(b/2)^2} dx \quad (14)$$

Formulas for the quantities $\frac{B\Gamma_1}{\dot{\alpha}(b/2)^2 M^2}$ and $\frac{\Gamma_2}{B\dot{\alpha}(b/2)^2}$, which are functions of the parameters AB , Bm , λ , and the nondimensional spanwise coordinate $\frac{y}{b/2}$, are presented in table I for the combinations of Mach lines and plan forms considered. The mathematical expressions required in the use of table I are given in the appendix.

RESULTS AND DISCUSSION

Equations have been derived in the preceding analysis for the spanwise distribution of circulation resulting from constant vertical acceleration of isolated sweptback wings of arbitrary aspect ratio and taper ratio with streamwise tips. The analysis is valid at those supersonic speeds for which the wing leading and trailing edges are supersonic, subject to the additional minor restriction that the Mach line from the leading edge of one wing tip does not intersect the remote half wing.

The pressure distributions obtained over the wing for the motion considered are of interest. For illustrative purposes some chordwise and spanwise pressure distributions, calculated from equation (2), are presented in figures 2 and 3, respectively. (The expressions for $(\Delta P)_{q=1}$, $(\Delta P)_{\alpha=1}$, and $(\phi)_{\alpha=1}$ required for the calculations were obtained from tables V, III, and II, respectively, of reference 7 - in which both q and α therein were replaced by unity.)

Calculations of the spanwise distribution of circulation have been made for values of AB from 3 to 20 for $\lambda = 0, 0.25, 0.50, 0.75$, and 1.0; for $\lambda = 1.0$ calculations for $AB = 2$ have also been included. The range of Bm considered is from 1.0 to ∞ . Results of the numerical calculations are presented in a series of charts (figs. 4 to 9) so that, for given values of the parameters aspect ratio, taper ratio, leading-edge sweepback, and Mach number, the circulation components Γ_1 and Γ_2 (and hence Γ) may be readily obtained. An index to these charts is given in table II.

In order to illustrate the variation of the spanwise distribution of circulation with different parameters, several specific examples have been chosen; the results are presented in figure 10.

The results presented herein for constant vertical acceleration $\dot{\alpha}$ may, of course, be combined with the results of reference 3 for steady pitching q to obtain an estimate of the span load distribution for a slowly (first-order frequency) oscillating wing, that is, $q + \dot{\alpha}$ motion.

CONCLUDING REMARKS

On the basis of an application of linearized supersonic-flow theory, equations have been derived for the spanwise loading on isolated wings resulting from a linear angle-of-attack variation with time at supersonic flight speeds.

The types of wing considered have sweptback leading edges, either sweptback or sweptforward trailing edges, and tips that are parallel to the axis of wing symmetry (streamwise tips). The analysis is applicable, in general, at those supersonic speeds for which the wing leading and trailing edges are supersonic.

Computational results are presented in the form of generalized design curves which permit fairly rapid estimation of the spanwise distribution of circulation (or span load distribution) for broad ranges of the parameters aspect ratio, taper ratio, leading-edge sweepback, and Mach number.

The results obtained herein may be combined with corresponding results previously reported for the steady pitching case to obtain the span load distribution for a slowly (first-order frequency) oscillating wing.

Langley Aeronautical Laboratory,
National Advisory Committee for Aeronautics,
Langley Field, Va., October 13, 1953.

APPENDIX

LIST OF FUNCTIONS TO BE USED IN CONJUNCTION WITH TABLE I

In order to avoid repetition of cumbersome mathematical expressions appearing in the circulation equations of table I, a system of capital-letter symbols has been used therein to denote various functions. The letters and their functional equivalents are as follows:

$$\begin{aligned}
 D &= -\frac{4 \left[AB(1+\lambda) \frac{y}{b/2} + 4k \right]}{kA^2B^2(1+\lambda)^2\pi} \sqrt{\frac{1}{k^2} \left(\frac{y}{b/2} \right)^2 A^2B^2(1+\lambda)^2(1-k^2) + 8kAB(1+\lambda) \frac{y}{b/2} + 16k^2} + \\
 &\quad \frac{8}{3\pi} \left[\frac{y}{b/2} + \frac{4k}{AB(1+\lambda)} \right] \sqrt{\frac{y^2}{(b/2)^2} \frac{(1-k^2)}{k^2} + \frac{8}{kAB(1+\lambda)} \frac{y}{b/2} + \frac{16}{A^2B^2(1+\lambda)^2}} \\
 E &= \frac{2}{\pi} \left\{ -\frac{y^2}{(b/2)^2} \cosh^{-1} \left[\frac{\frac{y}{b/2} + \frac{4k}{AB(1+\lambda)}}{k \frac{y}{b/2}} \right] + \frac{\frac{y}{b/2} + \frac{4k}{AB(1+\lambda)}}{k} \sqrt{\left[\frac{\frac{y}{b/2} + \frac{4k}{AB(1+\lambda)}}{k} \right]^2 - \frac{y^2}{(b/2)^2}} \right\} \\
 F &= \frac{2\sqrt{2}}{3\pi} \left\{ -\frac{1}{k} \left[\frac{19y}{b/2} + \frac{4k}{AB(1+\lambda)} \right] + \frac{y}{b/2} - 2 \right\} \sqrt{\frac{1 - \frac{y}{b/2} \left[\frac{y}{b/2} (1+k) + \frac{4k}{AB(1+\lambda)} \right]}{k}} \\
 G &= \frac{2}{\pi} \left\{ -\frac{y^2}{(b/2)^2} \cosh^{-1} \left(\frac{2 - \frac{y}{b/2}}{\frac{y}{b/2}} \right) + \left(2 - \frac{y}{b/2} \right) \sqrt{\left(2 - \frac{y}{b/2} \right)^2 - \frac{y^2}{(b/2)^2}} + \right. \\
 &\quad \left. \frac{4}{3} \sqrt{2 \left(1 - \frac{y}{b/2} \right) \left\{ -2\sqrt{2} + \left[\frac{y}{b/2} + \frac{\frac{y}{b/2} + \frac{4k}{AB(1+\lambda)}}{k} \right]^{3/2} \right\}} \right\} \\
 H &= -\frac{2 \left[AB(1+\lambda) \frac{y}{b/2} + 4k \right]}{\pi B k^2 A^2 B^2 (1+\lambda)^2 \sqrt{B^2 m^2 - 1}} \left\{ \left[\frac{4Bmk + AB(1+\lambda)(1-k) \frac{y}{b/2}}{Bm \left[AB(1+\lambda)(1-k) \frac{y}{b/2} + 4mBk \right]} \cos^{-1} \frac{AB(1+\lambda)(1-B^2 m^2 k) \frac{y}{b/2} + 4mBk}{Bm \left[AB(1+\lambda)(1-k) \frac{y}{b/2} + 4mBk \right]} \right. \right. \\
 &\quad \left. \left[\frac{4mBk + AB(1+\lambda)(1+k) \frac{y}{b/2}}{Bm \left[AB(1+\lambda)(1+k) \frac{y}{b/2} + 4mBk \right]} \cos^{-1} \frac{AB(1+\lambda)(1+B^2 m^2 k) \frac{y}{b/2} + 4mBk}{Bm \left[AB(1+\lambda)(1+k) \frac{y}{b/2} + 4mBk \right]} \right\} + \frac{2}{\pi k m B (B^2 m^2 - 1)} \left[\frac{y}{b/2} + \frac{4k m B}{AB(1+\lambda)} \right] \times \\
 &\quad \sqrt{\frac{1}{k^2} \left[\frac{y^2}{(b/2)^2} (1 - B^2 m^2 k^2) + \frac{8k m B}{AB(1+\lambda)} \frac{y}{b/2} + \frac{16B^2 m^2 k^2}{A^2 B^2 (1+\lambda)^2} \right]} + \frac{1}{2k \sqrt{B^2 m^2 - 1}} \left\{ \frac{y^2}{(b/2)^2} (k-1) [2 - B^2 m^2 (k+1)] + \right. \\
 &\quad \left. \frac{8mBk}{AB(1+\lambda)} (k + B^2 m^2 - 2) \frac{y}{b/2} + \frac{16B^2 m^2 k^2}{A^2 B^2 (1+\lambda)^2} (B^2 m^2 - 2) \right\} \cos^{-1} \frac{\frac{y}{b/2} (1 - B^2 m^2 k) + \frac{4mBk}{AB(1+\lambda)}}{Bm \left[(1-k) \frac{y}{b/2} + \frac{4mBk}{AB(1+\lambda)} \right]} +
 \end{aligned}$$

(Equation continued on next page)

$$\begin{aligned}
& \left\{ \frac{y^2}{(b/2)^2} (k+1) [-2 - B^2 m^2 (k-1)] + \frac{8Bmk}{AB(1+\lambda)} (B^2 m^2 - 2 - k) \frac{y}{b/2} + \right. \\
& \left. \frac{16B^2 m^2 k^2}{A^2 B^2 (1+\lambda)^2} (B^2 m^2 - 2) \right\} \cos^{-1} \frac{\frac{y}{b/2} (1 + B^2 m^2 k) + \frac{4mBk}{AB(1+\lambda)}}{Bm \left[\frac{y}{b/2} (1+k) + \frac{4mBk}{AB(1+\lambda)} \right]} \Bigg] \\
J = & \frac{2}{\pi \sqrt{B^2 m^2 - 1}} \left[\frac{1}{2} \left\{ \frac{\left[\frac{y}{b/2} + \frac{4mBk}{AB(1+\lambda)} \right]^2}{k^2 mB} + \frac{1}{Bm} \frac{y^2}{(b/2)^2} \right\} + \frac{\frac{y}{b/2} + \frac{4mBk}{AB(1+\lambda)}}{kmB} \frac{y}{b/2} \right) \cos^{-1} \frac{\frac{y}{b/2} (1 + B^2 m^2 k) + \frac{4kmB}{AB(1+\lambda)}}{Bm \left[\frac{y}{b/2} (1+k) + \frac{4kmB}{AB(1+\lambda)} \right]} \right. \\
& \left. - \frac{1}{2} \left\{ \frac{\left[\frac{y}{b/2} + \frac{4kmB}{AB(1+\lambda)} \right]^2}{k^2 mB} + \frac{1}{Bm} \frac{y^2}{(b/2)^2} \right\} + \frac{\frac{y}{b/2} + \frac{4mBk}{AB(1+\lambda)}}{kmB} \frac{y}{b/2} \right) \cos^{-1} \frac{\frac{y}{b/2} (1 - B^2 m^2 k) + \frac{4kmB}{AB(1+\lambda)}}{Bm \left[\frac{y}{b/2} (1-k) + \frac{4kmB}{AB(1+\lambda)} \right]} \right. \\
& \left. - \frac{y^2}{(b/2)^2} \frac{\sqrt{B^2 m^2 - 1}}{Bm} \cosh^{-1} \frac{\frac{y}{b/2} + \frac{4mBk}{AB(1+\lambda)}}{kmB \frac{y}{b/2}} \right] \\
L = & \frac{2}{\pi kmB (B^2 m^2 - 1)} \left(\frac{1}{2k \sqrt{B^2 m^2 - 1}} \left[\frac{y^2}{(b/2)^2} (k+1) [-2 - B^2 m^2 (k-1)] + \frac{8Bmk}{AB(1+\lambda)} (-k + B^2 m^2 - 2) \frac{y}{b/2} + \right. \right. \\
& \left. \frac{16B^2 m^2 k^2 (B^2 m^2 - 2)}{A^2 B^2 (1+\lambda)^2} - \frac{2(B^2 m^2 - 1) \left[AB(1+\lambda) \frac{y}{b/2} + 4kmB \right] \left[4kmB + AB(1+\lambda) (1+k) \frac{y}{b/2} \right]}{A^2 B^2 (1+\lambda)^2} \right] \times \\
& \cos^{-1} \frac{\frac{y}{b/2} (1 - k + 2mBk) + \frac{4mBk}{AB(1+\lambda)} - 2k(mB - 1)}{\frac{y}{b/2} (1+k) + \frac{4mBk}{AB(1+\lambda)}} + \frac{2k \sqrt{B^2 m^2 - 1}}{3} \left[\frac{y}{b/2} (-12 + B^2 m^2 k + 4mB + \right. \\
& \left. 2B^3 m^3 k + 5m^2 B^2) + (4Bmk - 2B^2 m^2 k - 2B^3 m^3 k) + \frac{4mBk(-12 + 4mB + 5m^2 B^2)}{AB(1+\lambda)} \right] \times \\
& \left. \left[\frac{1}{k(mB + 1)} \left\{ - \frac{y^2}{(b/2)^2} (1 + Bmk) + \frac{y}{b/2} \left[\frac{4mBk}{AB(1+\lambda)} - k + 2mBk + 1 \right] + \frac{4mBk}{AB(1+\lambda)} + k - kmB \right\} \right] \right)
\end{aligned}$$

$$\begin{aligned}
N = & \frac{2}{\pi \sqrt{B^2 m^2 - 1}} \left[\left(\frac{y}{b/2} + \frac{4kmB}{AB(1+\lambda)} \left[\frac{y}{b/2} + \frac{1}{2k} \left[\frac{y}{b/2} + \frac{4kmB}{AB(1+\lambda)} \right] \right] \right) + \right. \\
& \left. \frac{1}{2Bm} \frac{y^2}{(b/2)^2} \cos^{-1} \frac{y \left(\frac{1}{k} + 2Bm - 1 \right) + 2(1 - Bm) + \frac{4mB}{AB(1+\lambda)}}{\frac{y}{b/2} \left(\frac{1}{k} + 1 \right) + \frac{4mB}{AB(1+\lambda)}} - \frac{y^2}{(b/2)^2} \frac{\sqrt{B^2 m^2 - 1}}{Bm} \cosh^{-1} \frac{2 - \frac{y}{b/2}}{\frac{y}{b/2}} \right. \\
& \left. \frac{6 \left(\frac{y}{b/2} + \frac{2}{3} \right)}{3Bm} \sqrt{\left(1 - \frac{y}{b/2} \right) (B^2 m^2 - 1)} + \frac{1}{3mB} \left[\left(\frac{y}{k} + 2mB + 3 \right) \frac{y}{b/2} - 2(Bm - 1) + \frac{20mB}{AB(1+\lambda)} \right] \times \right. \\
& \left. \sqrt{(Bm - 1) \left(1 - \frac{y}{b/2} \right) \left[\frac{y}{b/2} \left(\frac{1}{k} + Bm \right) - (Bm - 1) + \frac{4mB}{AB(1+\lambda)} \right]} \right] \\
P = & - \frac{2 \left[AB(1+\lambda) \frac{y}{b/2} + 4kmB \right]}{Bmk^2 A^2 B^2 (1+\lambda)^2 \sqrt{B^2 m^2 - 1}} \left[4mBk + AB(1+\lambda)(1-k) \frac{y}{b/2} \right] + \frac{1}{k^2 mB (B^2 m^2 - 1)^{3/2}} \left[\frac{y^2}{(b/2)^2} (k-1) + \right. \\
& \left. \frac{8mBk}{AB(1+\lambda)} (k + B^2 m^2 - 2) \frac{y}{b/2} + \frac{16B^2 m^2 k^2 (B^2 m^2 - 2)}{A^2 B^2 (1+\lambda)^2} \right] \\
Q = & \frac{1}{k^2 mB \sqrt{B^2 m^2 - 1}} \left[\frac{y}{b/2} (1-k) + \frac{4kmB}{AB(1+\lambda)} \right]^2 \\
R = & \frac{2}{\pi k mB (B^2 m^2 - 1)} \left(\frac{1}{2k \sqrt{B^2 m^2 - 1}} \left[\left[\frac{y^2}{(b/2)^2} (k-1) \left[2 - B^2 m^2 (k+1) \right] + \frac{8Bmk}{AB(1+\lambda)} (k + B^2 m^2 - 2) \frac{y}{b/2} + \right. \right. \right. \\
& \left. \left. \frac{16B^2 m^2 k^2 (B^2 m^2 - 2)}{A^2 B^2 (1+\lambda)^2} - \frac{2(B^2 m^2 - 1) \left[AB(1+\lambda) \frac{y}{b/2} + 4kmB \right] \left[4mBk + AB(1+\lambda)(1-k) \frac{y}{b/2} \right]}{A^2 B^2 (1+\lambda)^2} \right] \right) \times \\
& \cos^{-1} \frac{\frac{y}{b/2} (1+k + 2Bmk) + \frac{4mBk}{AB(1+\lambda)} - 2k(mB + 1)}{\frac{y}{b/2} (1-k) + \frac{4mBk}{AB(1+\lambda)}} + \frac{2k \sqrt{B^2 m^2 - 1}}{3} \left[\frac{y}{b/2} (-12 - B^2 m^2 k - 4mB - \right. \\
& \left. 2B^3 m^3 k + 5B^2 m^2) + (4Bkm + 2B^2 m^2 k - 2B^3 m^3 k) + \frac{4mBk(-12 - 4mB + 5B^2 m^2)}{AB(1+\lambda)} \right] \times \\
& \left. \sqrt{\frac{1}{k(Bm - 1)} \left\{ - \frac{y^2}{(b/2)^2} (1 + Bmk) + \frac{y}{b/2} \left[- \frac{4mBk}{AB(1+\lambda)} + k + 2mBk + 1 \right] + \frac{4mBk}{AB(1+\lambda)} - k - Bmk \right\}} \right)
\end{aligned}$$

$$T = \frac{1}{\pi \sqrt{B^2 m^2 - 1}} \left(- \frac{(mB + 1)^2 \left(1 - \frac{y}{b/2}\right)^2}{2mB} \pi + \frac{\left[\frac{y}{b/2}(1 - k) + \frac{4mBk}{AB(1 + \lambda)}\right]^2}{2k^2 mB} \times \right. \\ \left. \cos^{-1} \frac{\frac{y}{b/2}(1 + 2mBk + k) - 2k(Bm + 1) + \frac{4Bkm}{AB(1 + \lambda)}}{\frac{y}{b/2}(1 - k) + \frac{4kmB}{AB(1 + \lambda)}} + \left[\frac{\frac{y}{b/2}(1 - 2Bmk - 3k) + 2k(Bm + 1)}{6kmB} + \right. \right. \\ \left. \left. \frac{2\left[\frac{y}{b/2}(1 + Bmk) - k(Bm + 1) + \frac{4mBk}{AB(1 + \lambda)}\right]}{3kmB} \right] \frac{2\sqrt{Bm + 1}}{\sqrt{k}} \sqrt{\left[\frac{y}{b/2}(1 + Bmk) - k(Bm + 1) + \frac{4mBk}{AB(1 + \lambda)}\right] \left(1 - \frac{y}{b/2}\right)} \right)$$

$$U = - \frac{16}{A^2 B^2 (1 + \lambda)^2} \left[1 - \frac{y}{b/2}(1 - \lambda) \right]^2$$

$$W = \frac{16}{A^2 B^2 (1 + \lambda)^2} \left[1 - \frac{y}{b/2}(1 - \lambda) \right]^2$$

$$U' = - \frac{16}{\pi A^2 B^2 (1 + \lambda)^2} \left[1 - \frac{y}{b/2}(1 - \lambda) \right]^2 \cos^{-1} \frac{AB(1 + \lambda) \left(\frac{y}{b/2} - 1\right) + 2 \left[1 - (1 - \lambda) \frac{y}{b/2} \right]}{2 \left[1 - (1 - \lambda) \frac{y}{b/2} \right]} +$$

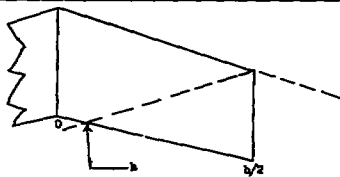
$$\frac{\frac{8y}{b/2} + 4AB(1 + \lambda) \left(\frac{y}{b/2} - 1\right)}{3 [AB(1 + \lambda)]^{3/2}} \sqrt{\left\{ \left(\frac{y}{b/2} - 1\right) AB(1 + \lambda) + 4 \left[1 - (1 - \lambda) \frac{y}{b/2} \right] \right\} \left(1 - \frac{y}{b/2}\right)}$$

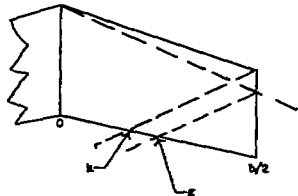
$$W' = \frac{2}{\pi} \left(\frac{8 \left[1 - \frac{y}{b/2}(1 - \lambda) \right]^2}{A^2 B^2 (1 + \lambda)^2} \cos^{-1} \left\{ \frac{AB(1 + \lambda) \left(\frac{y}{b/2} - 1\right)}{2 \left[1 - \frac{y}{b/2}(1 - \lambda) \right]} + 1 \right\} + \frac{4 \left[1 - \frac{y}{b/2}(1 - \lambda) \right] - 2AB(1 + \lambda) \left(\frac{y}{b/2} - 1\right)}{3AB(1 + \lambda)} \times \right. \\ \left. \sqrt{\frac{4 \left(1 - \frac{y}{b/2}\right) \left[1 - \frac{y}{b/2}(1 - \lambda) \right]}{AB(1 + \lambda)} - \left(1 - \frac{y}{b/2}\right)^2} + \frac{4 \left[1 - \frac{y}{b/2} \right]}{3} \left\{ \frac{y}{b/2} - 1 + \frac{4 \left[1 - \frac{y}{b/2}(1 - \lambda) \right]}{AB(1 + \lambda)} \right\}^{3/2} \right)$$

REFERENCES

1. Hannah, Margery E., and Margolis, Kenneth: Span Load Distributions Resulting From Constant Angle of Attack, Steady Rolling Velocity, Steady Pitching Velocity, and Constant Vertical Acceleration for Tapered Sweptback Wings With Streamwise Tips - Subsonic Leading Edges and Supersonic Trailing Edges. NACA TN 2831, 1952.
2. Margolis, Kenneth, Sherman, Windsor L., and Hannah, Margery E.: Theoretical Calculation of the Pressure Distribution, Span Loading, and Rolling Moment Due to Sideslip at Supersonic Speeds for Thin Sweptback Tapered Wings With Supersonic Trailing Edges and Wing Tips Parallel to the Axis of Wing Symmetry. NACA TN 2898, 1953.
3. Martin, John C., and Jeffreys, Isabella: Span Load Distributions Resulting From Angle of Attack, Rolling, and Pitching for Tapered Sweptback Wings With Streamwise Tips - Supersonic Leading and Trailing Edges. NACA TN 2643, 1952.
4. Sherman, Windsor L., and Margolis, Kenneth: Theoretical Calculations of the Effects of Finite Sideslip at Supersonic Speeds on the Span Loading and Rolling Moment for Families of Thin Sweptback Tapered Wings at an Angle of Attack. NACA TN 3046, 1953.
5. Ribner, Herbert S., and Malvestuto, Frank S., Jr.: Stability Derivatives of Triangular Wings at Supersonic Speeds. NACA Rep. 908, 1948. (Supersedes NACA TN 1572.)
6. Harmon, Sidney M., and Jeffreys, Isabella: Theoretical Lift and Damping in Roll of Thin Wings With Arbitrary Sweep and Taper at Supersonic Speeds - Supersonic Leading and Trailing Edges. NACA TN 2114, 1950.
7. Martin, John C., Margolis, Kenneth, and Jeffreys, Isabella: Calculations of Lift and Pitching Moments Due to Angle of Attack and Steady Pitching Velocity at Supersonic Speeds for Thin Sweptback Tapered Wings With Streamwise Tips and Supersonic Leading and Trailing Edges. NACA TN 2699, 1952.

TABLE I.- EXPRESSIONS FOR THE SPANWISE DISTRIBUTION OF CIRCULATION DUE TO CONSTANT VERTICAL ACCELERATION ($\Gamma = \Gamma_1 + \Gamma_2$)
 [Formulas for the parameters D, E, F, G, . . . H are given in appendix]

 $\frac{h}{b/2} = \frac{2k[\lambda b(1+\lambda) - 2]}{\lambda b(1+\lambda)(k+1)}$		
Range of $\frac{y}{b/2}$	Expression for components of circulation Γ along the span; Mach line coincident with leading edge	
	$\frac{\Gamma_1}{\partial^2(y/2)^2}$	$\frac{\Gamma_2}{2b(y/2)^2}$
$0 \leq \frac{y}{b/2} \leq \frac{h}{b/2}$	D	E
$\frac{h}{b/2} \leq \frac{y}{b/2} \leq 1$	F	G

 $\frac{h}{b/2} = \frac{k[\lambda b(1+\lambda)(km+1) - km^2]}{\lambda b(1+\lambda)(km+1)}$ $\frac{g}{b/2} = \frac{2kmk[\lambda b(1+\lambda) - 2]}{\lambda b(1+\lambda)(km+1)}$		
Range of $\frac{y}{b/2}$	Expression for components of circulation Γ along the span; Mach line intersecting tip	
	$\frac{\Gamma_1}{\partial^2(y/2)^2}$	$\frac{\Gamma_2}{2b(y/2)^2}$
$0 \leq \frac{y}{b/2} \leq \frac{h}{b/2}$	K	J
$\frac{h}{b/2} \leq \frac{y}{b/2} \leq \frac{g}{b/2}$	K + R - P	J + T - Q
$\frac{g}{b/2} \leq \frac{y}{b/2} \leq 1$	L	H

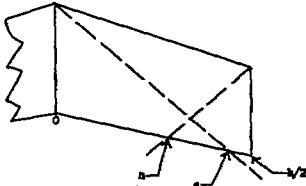
 $\frac{h}{b/2} = \frac{k[\lambda b(1+\lambda)(km+1) - km^2]}{\lambda b(1+\lambda)(km+1)}$ $\frac{g}{b/2} = \frac{kmk}{\lambda b(1+\lambda)(km-1)}$		
Range of $\frac{y}{b/2}$	Expression for components of circulation Γ along the span; Mach line from center intersecting trailing edge and intersecting Mach line from tip	
	$\frac{\Gamma_1}{\partial^2(y/2)^2}$	$\frac{\Gamma_2}{2b(y/2)^2}$
$0 \leq \frac{y}{b/2} \leq \frac{h}{b/2}$	K	J
$\frac{h}{b/2} \leq \frac{y}{b/2} \leq \frac{g}{b/2}$	K + R - P	J + T - Q
$\frac{g}{b/2} \leq \frac{y}{b/2} \leq 1$	R	T

TABLE I.- EXPRESSIONS FOR THE SPANWISE DISTRIBUTION OF CIRCULATION DUE TO CONSTANT VERTICAL ACCELERATION ($\Gamma = \Gamma_1 + \Gamma_2$) - Concluded

[Formulas for the parameters D, E, F, G, . . . W' are given in appendix]

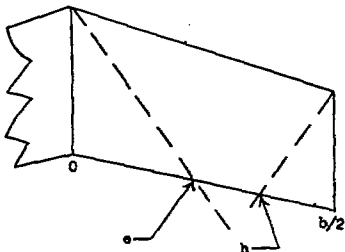
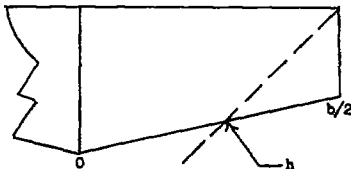
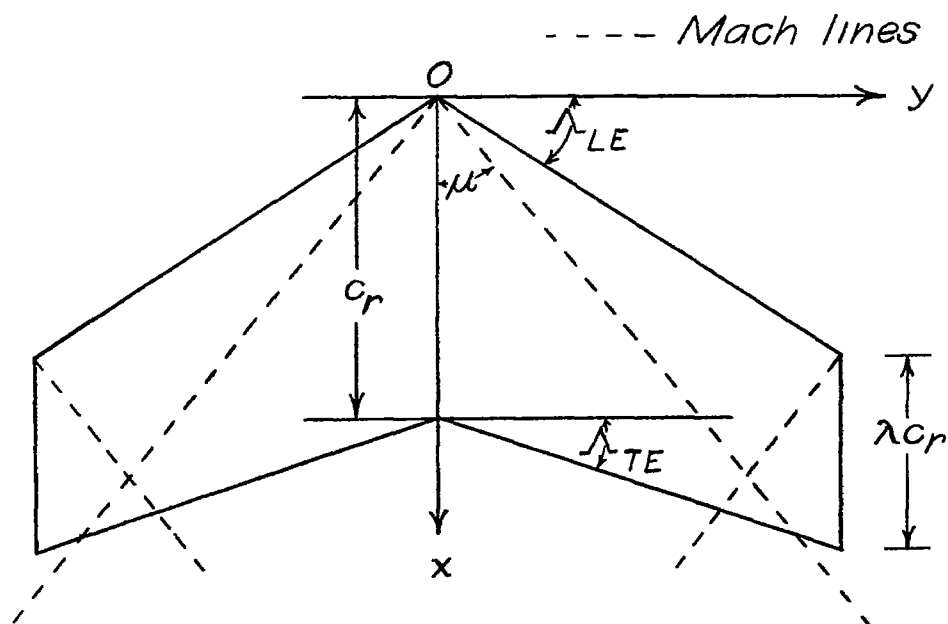
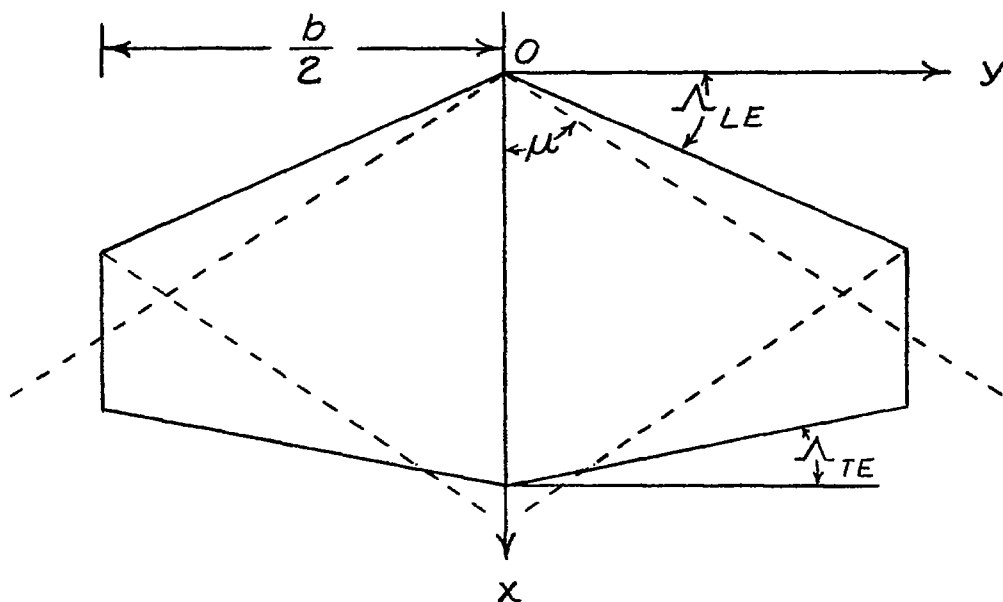
 $\frac{e}{b/2} = \frac{4\pi Bk}{AB(1 + \lambda)(Bk - 1)}$ $\frac{h}{b/2} = \frac{k[AB(1 + \lambda)(Bk + 1) - 4\pi B]}{AB(1 + \lambda)(Bk + 1)}$		
Range of $\frac{y}{b/2}$	Expression for components of circulation Γ along the span; Mach line from center intersecting trailing edge	
	$\frac{B\Gamma_1}{\cos^2(b/2)^2}$	$\frac{\Gamma_2}{Bk(b/2)^2}$
$0 \leq \frac{y}{b/2} \leq \frac{e}{b/2}$	H	J
$\frac{e}{b/2} \leq \frac{y}{b/2} \leq \frac{h}{b/2}$	P	Q
$\frac{h}{b/2} \leq \frac{y}{b/2} \leq 1$	R	T
 $\frac{h}{b/2} = \frac{AB(1 + \lambda) - 4}{AB(1 + \lambda) - 4(1 - \lambda)}$		
Range of $\frac{y}{b/2}$	Expression for components of circulation Γ along the span; unswept leading edge; Mach line from tip does not intersect remote half-wing	
	$\frac{B\Gamma_1}{\cos^2(b/2)^2}$	$\frac{\Gamma_2}{Bk(b/2)^2}$
$0 \leq \frac{y}{b/2} \leq \frac{h}{b/2}$	U	W
$\frac{h}{b/2} \leq \frac{y}{b/2} \leq 1$	U'	W'

TABLE II.- INDEX TO CHARTS FOR SPANWISE
DISTRIBUTION OF CIRCULATION

AB	Bm	Figure	AB	Bm	Figure
$\lambda = 0$			$\lambda = 0.75$		
4 to 20	1.0 to 5.0	4	3	1.0 to ∞	8(a)
3	1.0 to 3.0	5(a)	4	1.0 to ∞	8(b)
4	1.0 to ∞	5(b)	6	1.0 to ∞	8(c)
6	1.0 to ∞	5(c)	8	1.0 to ∞	8(d)
8	1.0 to ∞	5(d)	12	1.0 to ∞	8(e)
12	1.0 to ∞	5(e)	20	1.0 to ∞	8(f)
20	1.0 to ∞	5(f)	$\lambda = 1.00$		
$\lambda = 0.25$			2	1.0 to ∞	9(a)
3	1.0 to 7.0	6(a)	3	1.0 to ∞	9(b)
4	1.0 to ∞	6(b)	4	1.0 to ∞	9(c)
6	1.0 to ∞	6(c)	6	1.0 to ∞	9(d)
8	1.0 to ∞	6(d)	8	1.0 to ∞	9(e)
12	1.0 to ∞	6(e)	12	1.0 to ∞	9(f)
20	1.0 to ∞	6(f)	20	1.0 to ∞	9(g)
$\lambda = 0.50$					
3	1.0 to ∞	7(a)			
4	1.0 to ∞	7(b)			
6	1.0 to ∞	7(c)			
8	1.0 to ∞	7(d)			
12	1.0 to ∞	7(e)			
20	1.0 to ∞	7(f)			



(a) Sweptback trailing edge; positive Λ_{TE} .



(b) Sweptforward trailing edge; negative Λ_{TE} .

Figure 1.- Types of wing configurations analyzed. Supersonic leading and trailing edges; streamwise tips. Note that the Mach lines from the leading edge of the center section may intersect the tip or trailing edge and also that the Mach lines from the tip may not intersect the remote half-wing.

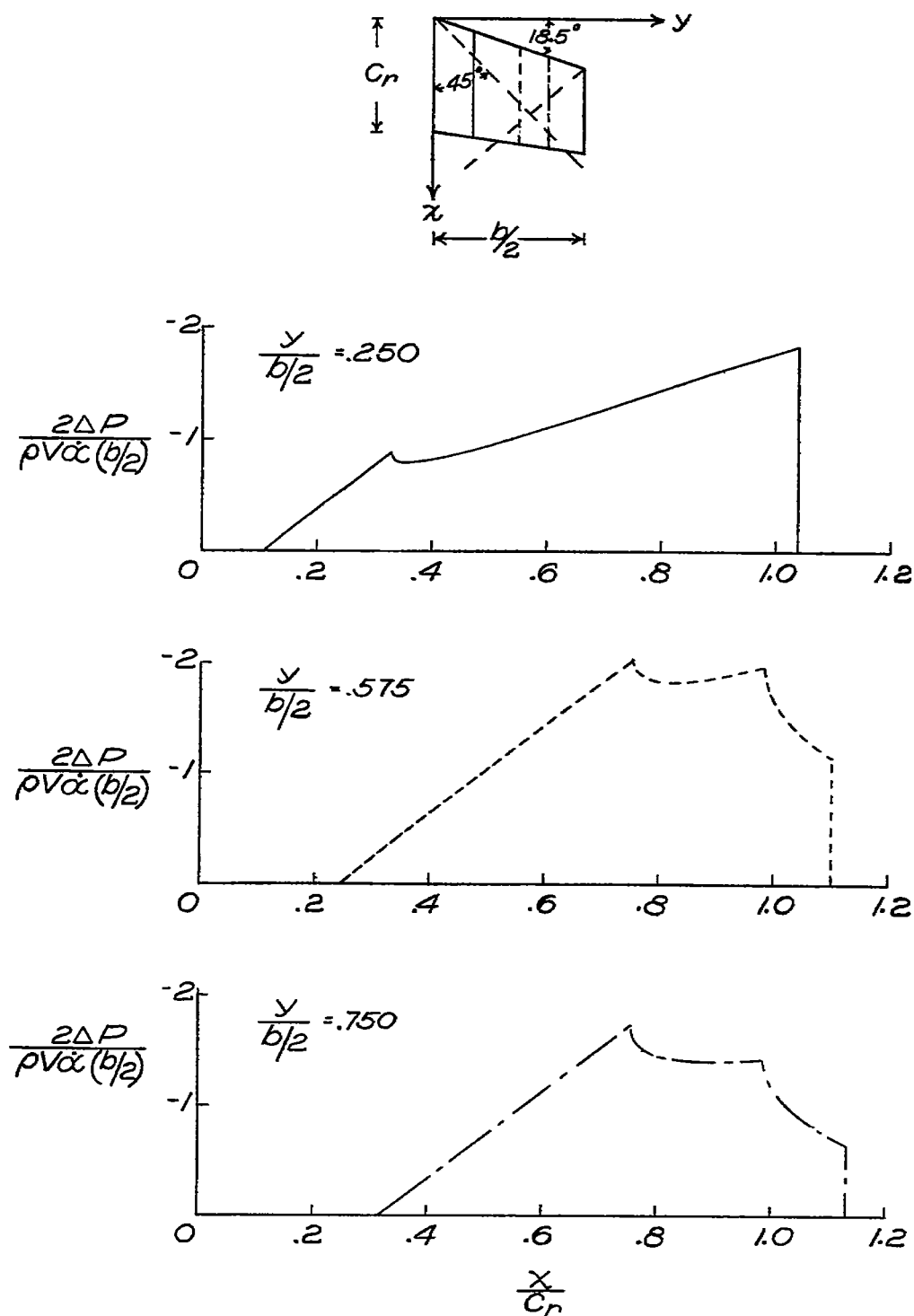


Figure 2.- Some typical chordwise pressure distributions. $A = 3$; $\Lambda_{LE} = 18.5^\circ$;
 $\lambda = 0.75$; $M = \sqrt{2}$.

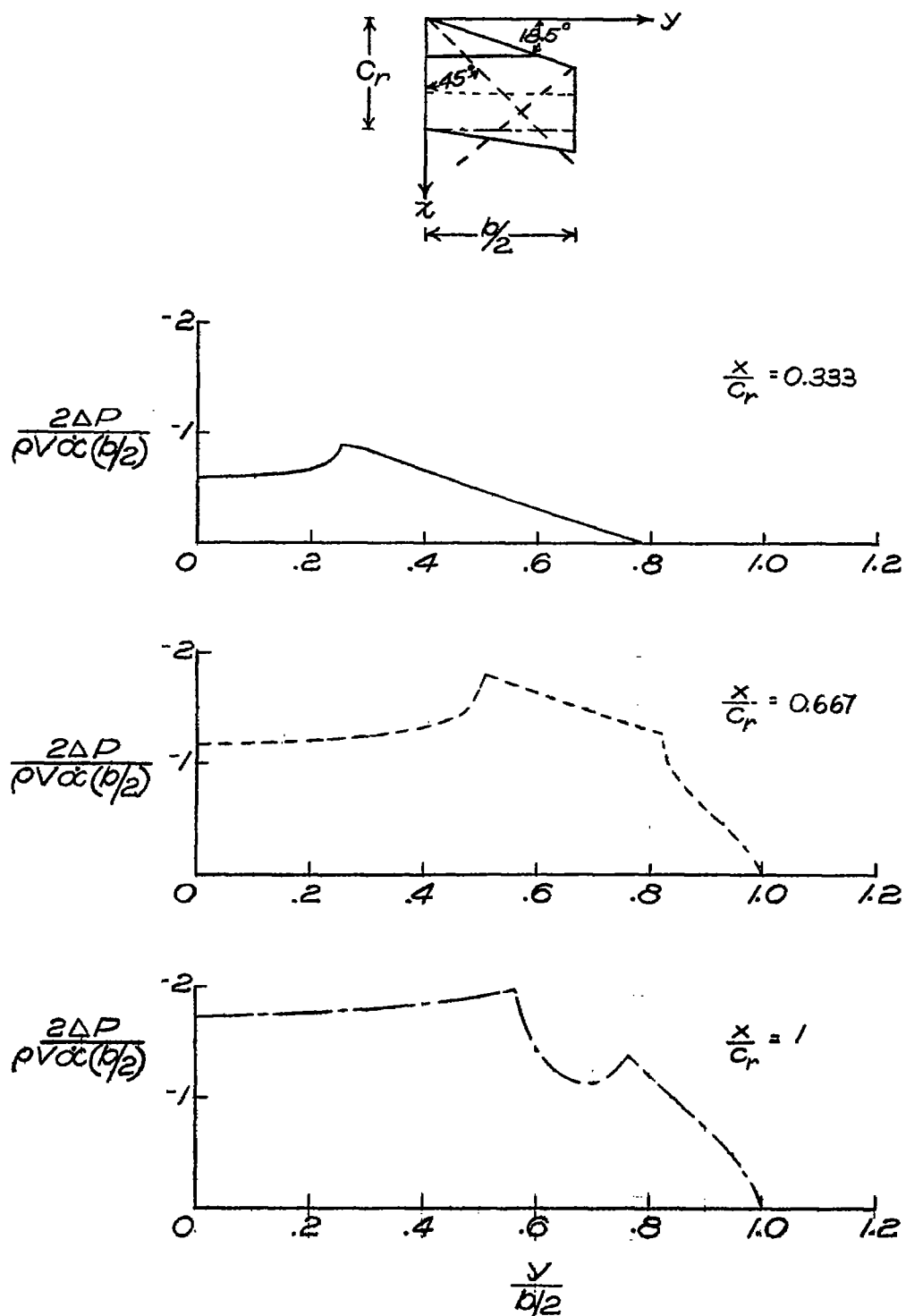


Figure 3.- Some typical spanwise pressure distributions. $A = 3$; $\Lambda_{LE} = 18.5^\circ$;
 $\lambda = 0.75$; $M = \sqrt{2}$.

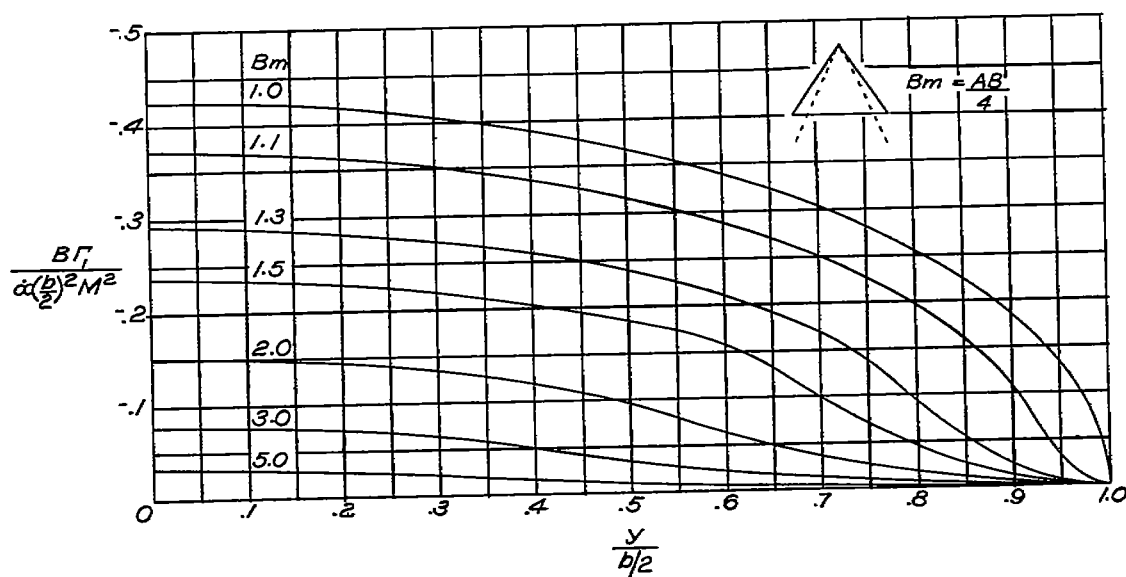
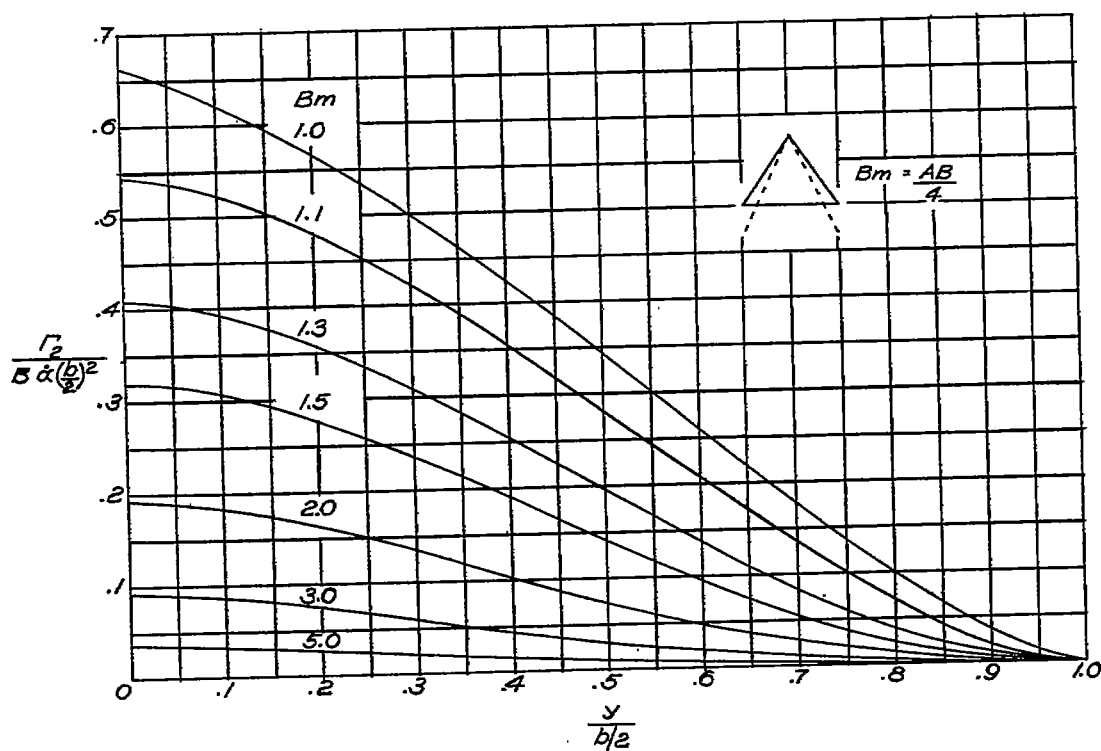
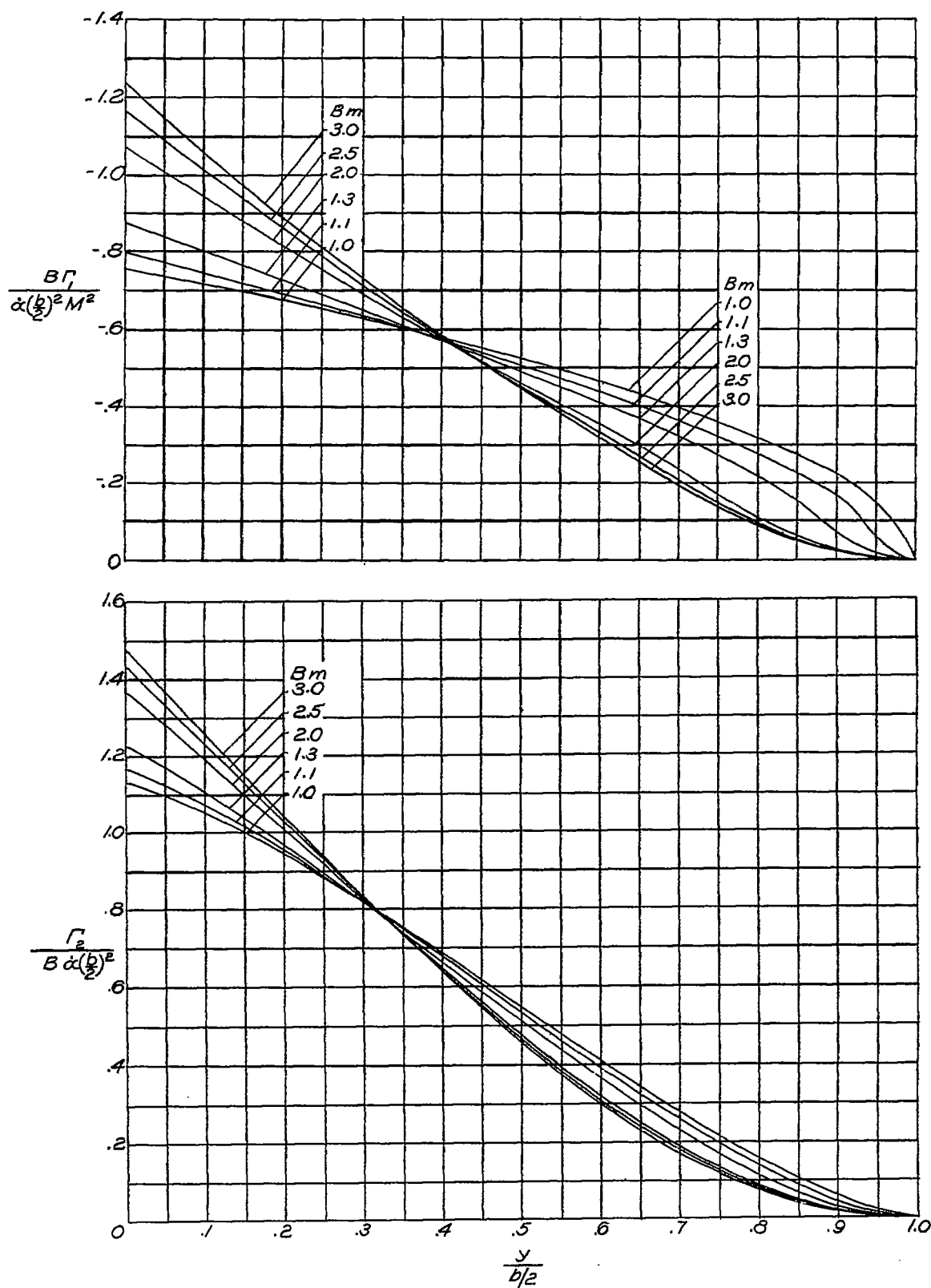
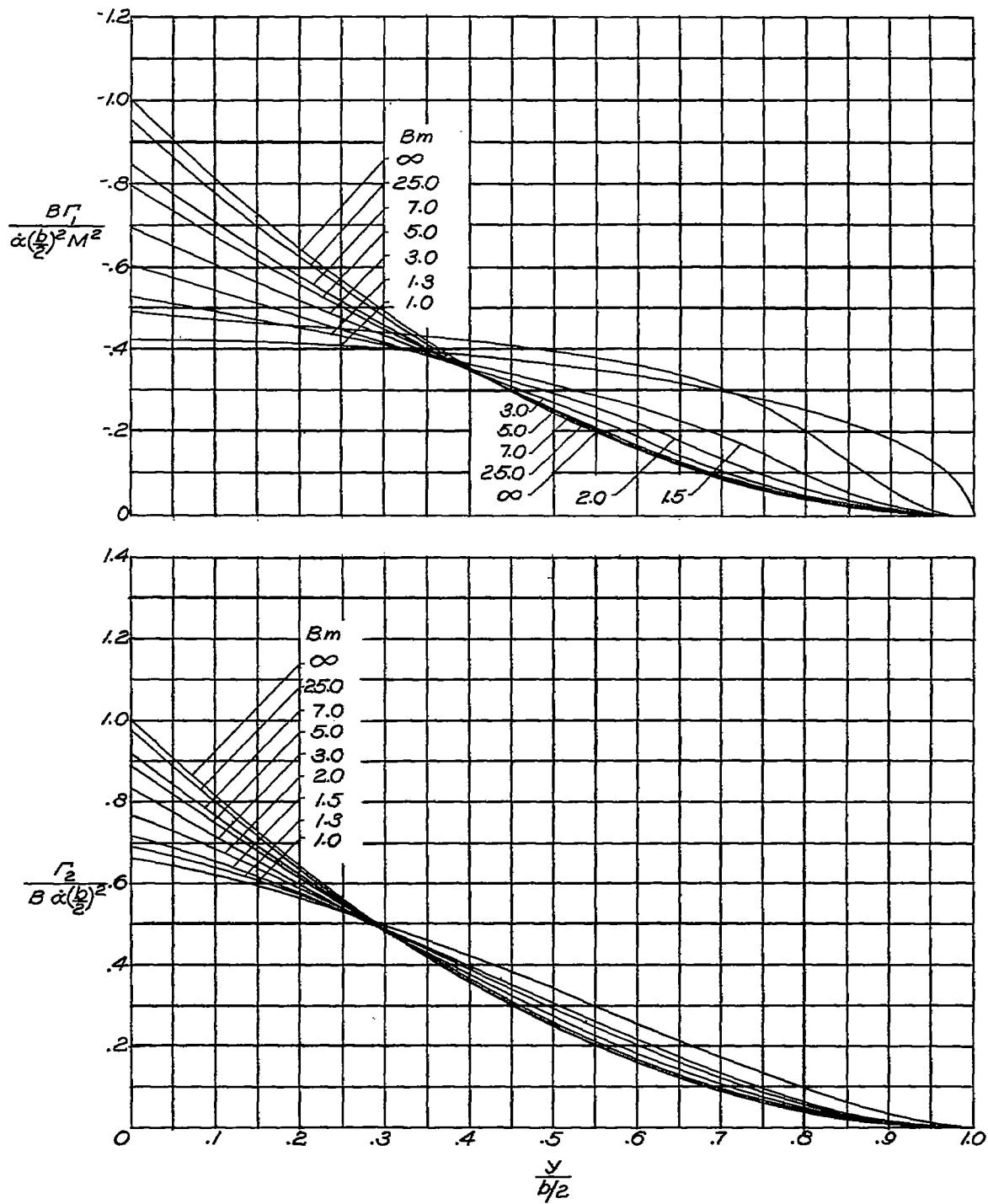
(a) Circulation component Γ_1 .(b) Circulation component Γ_2 .

Figure 4.- Distribution of circulation along span for delta wings.
 $\Gamma = \Gamma_1 + \Gamma_2$.



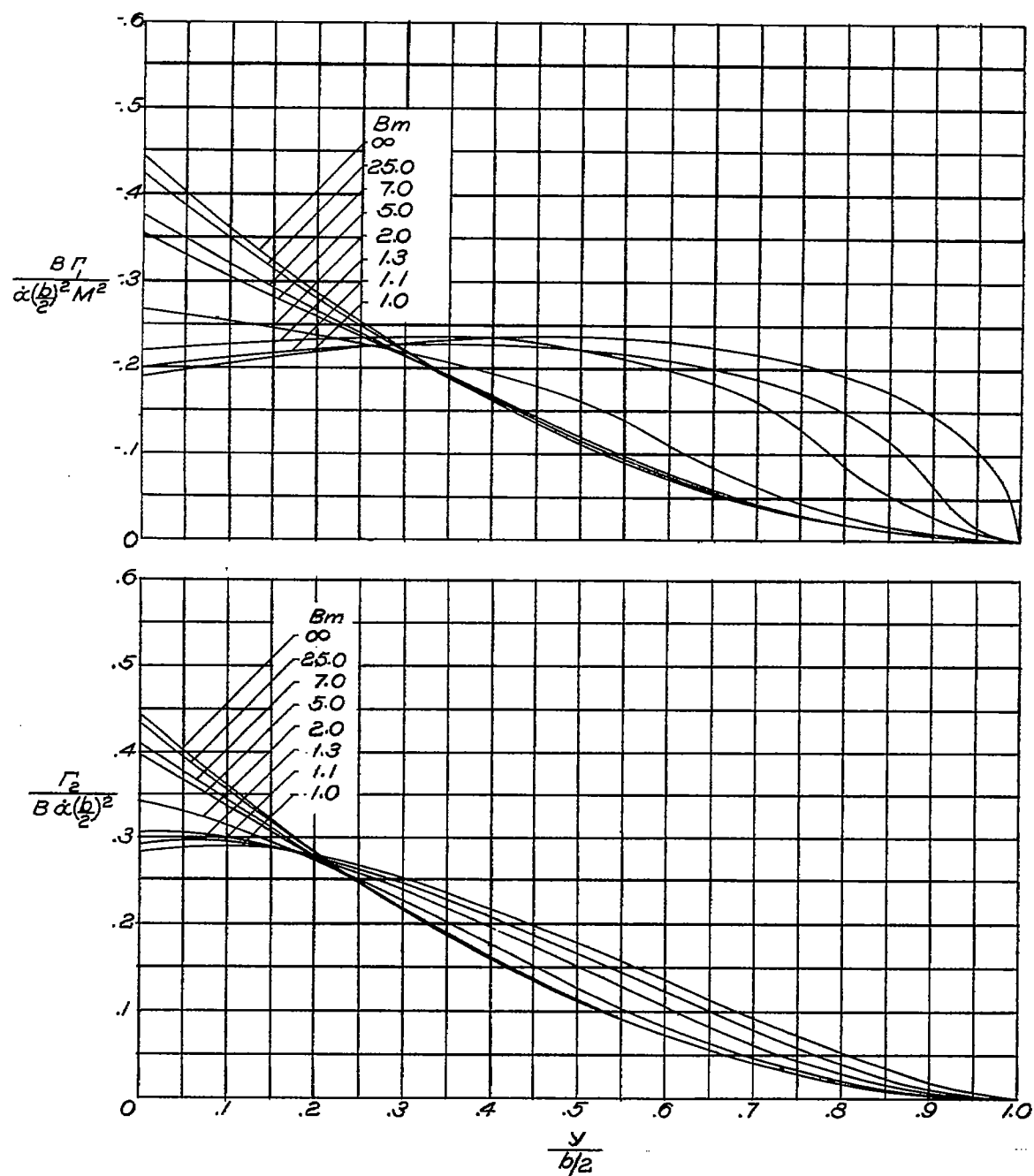
(a) $AB = 3$; $\lambda = 0$.

Figure 5.- Distribution of circulation along span for wings with $\lambda = 0$.
 $\Gamma = \Gamma_1 + \Gamma_2$.



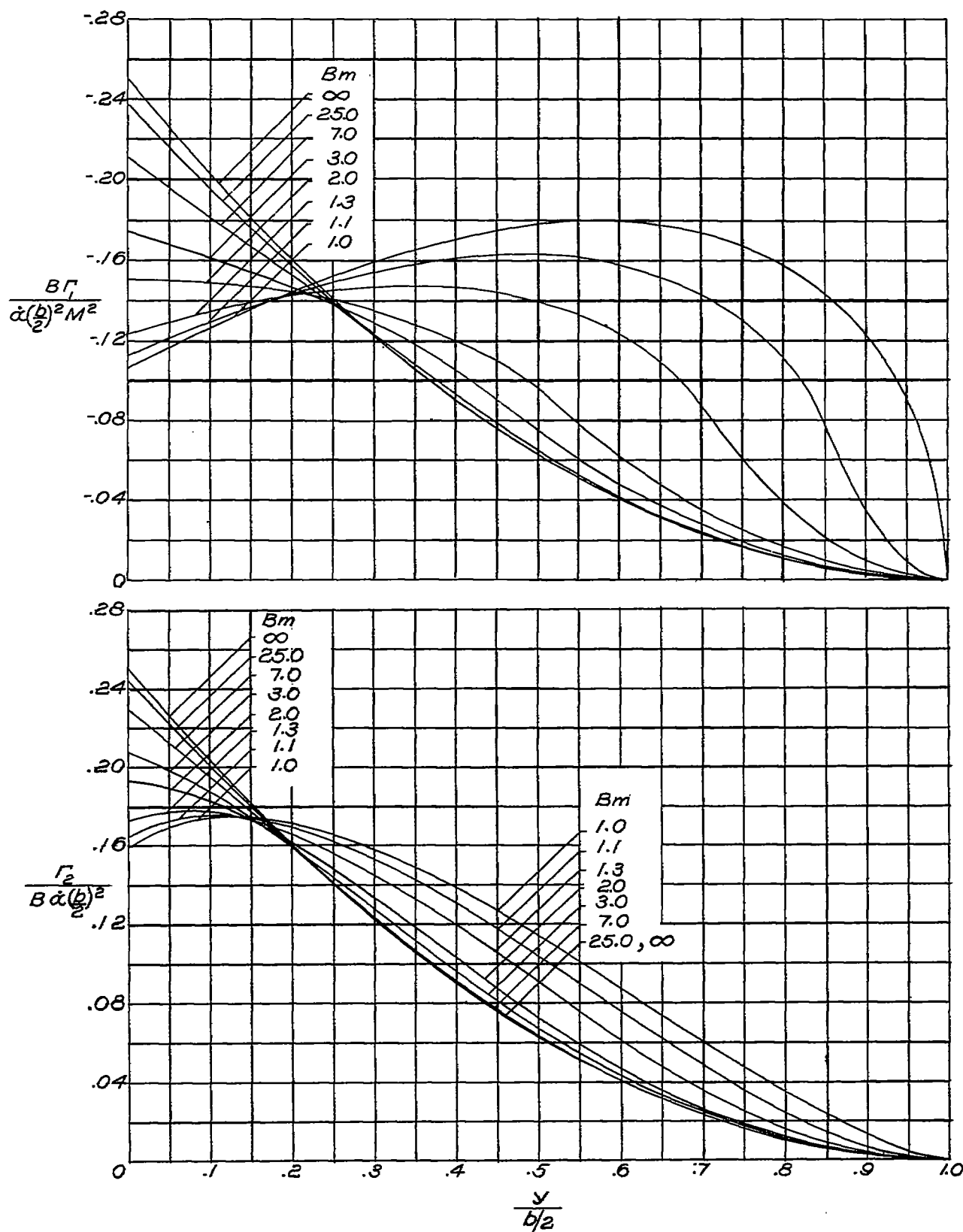
(b) $AB = 4$; $\lambda = 0$.

Figure 5.- Continued.



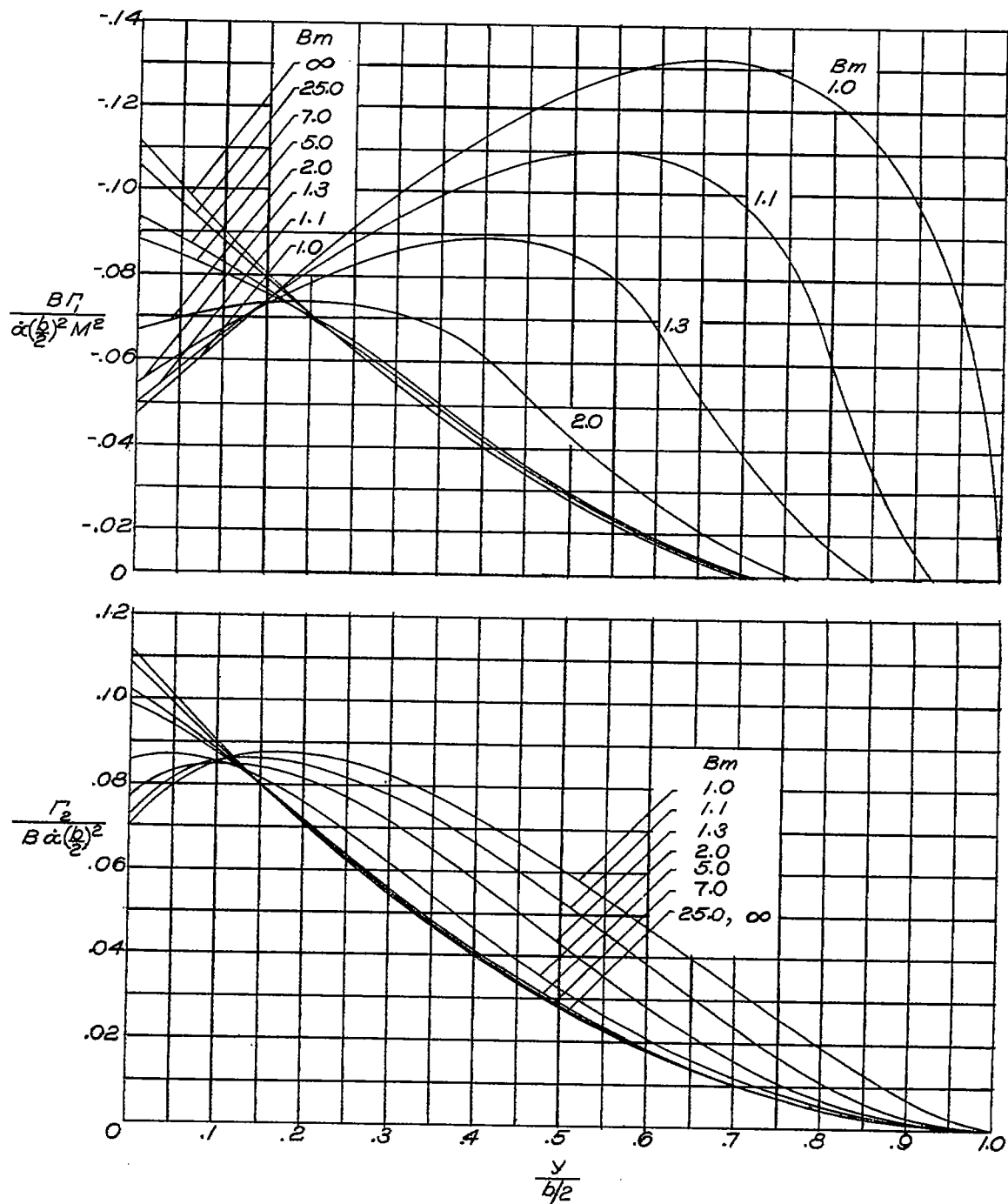
(c) $AB = 6$; $\lambda = 0$.

Figure 5.- Continued.



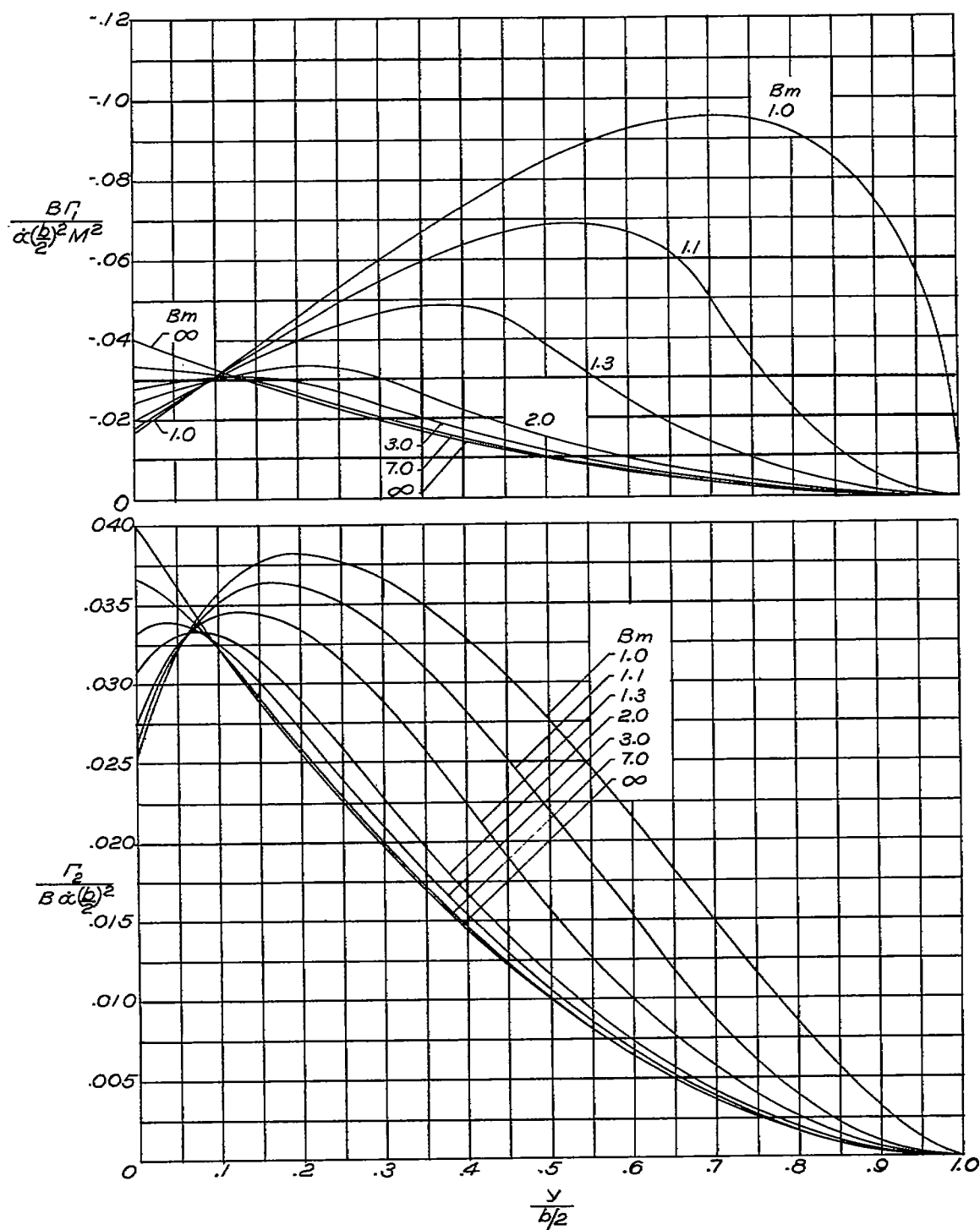
(d) $AB = 8$; $\lambda = 0$.

Figure 5.- Continued.



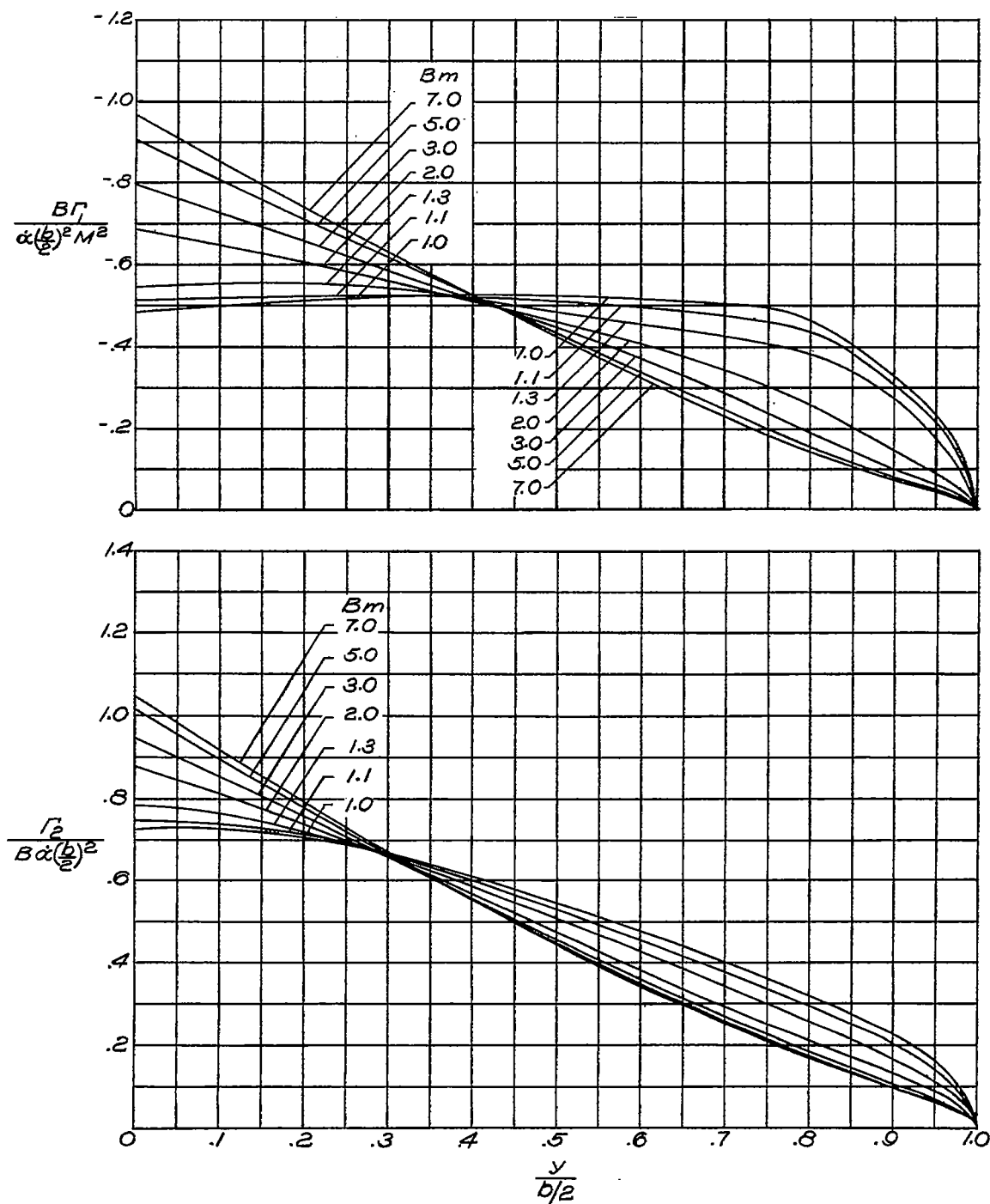
(e) $AB = 12$; $\lambda = 0$.

Figure 5.- Continued.



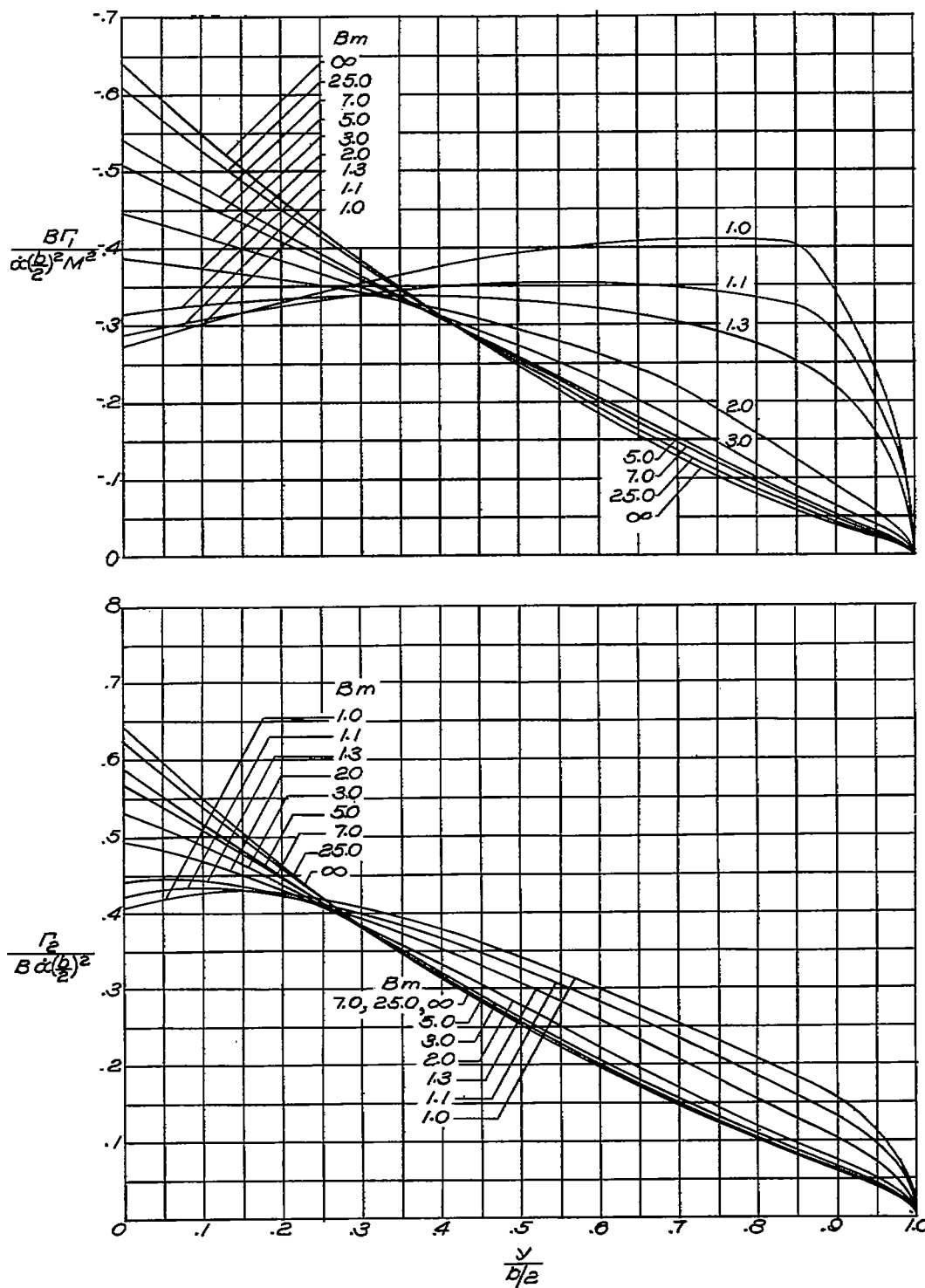
(f) $AB = 20$; $\lambda = 0$.

Figure 5.- Concluded.



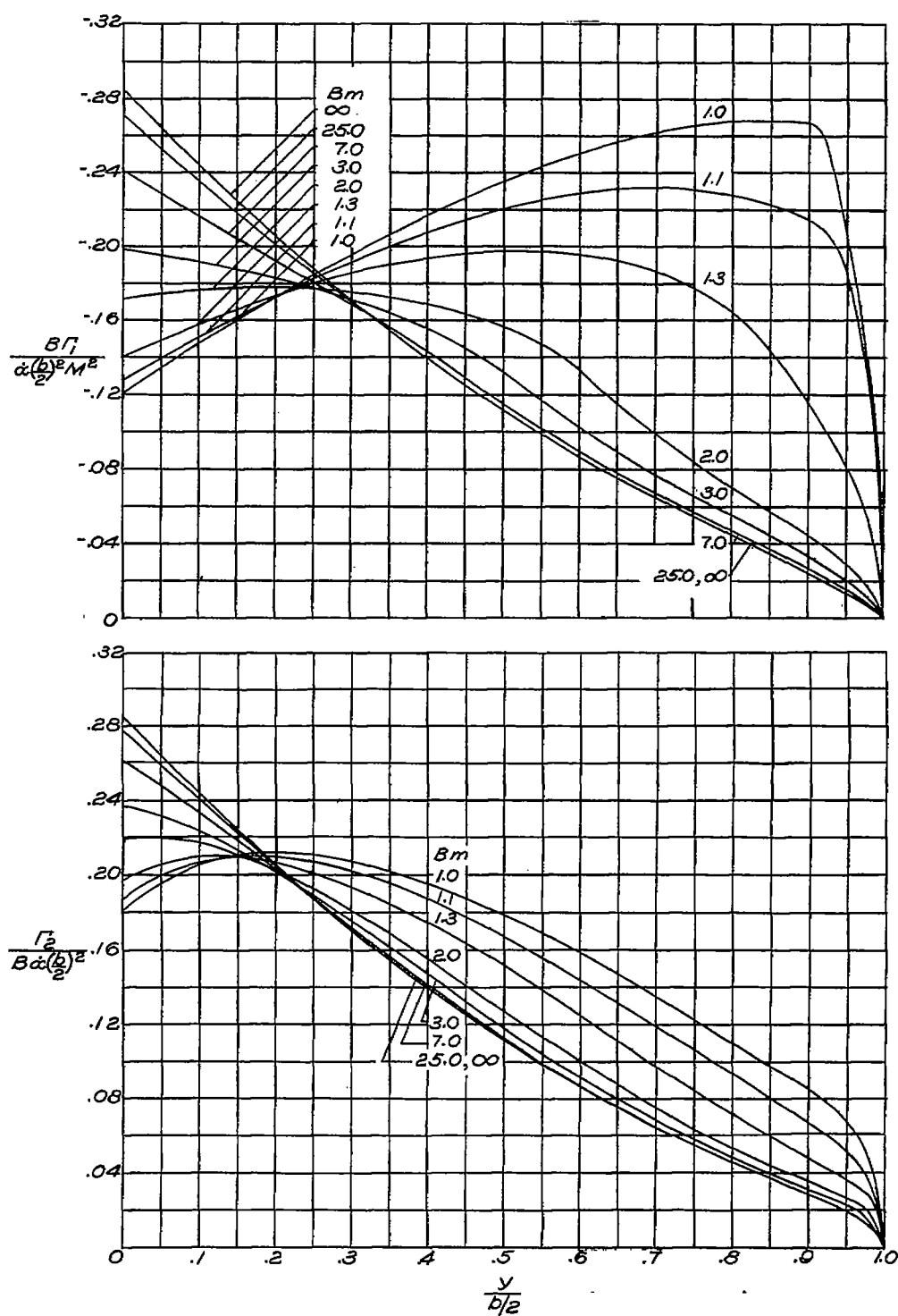
(a) $AB = 3$; $\lambda = 0.25$.

Figure 6.- Distribution of circulation along span for wings with $\lambda = 0.25$.
 $\Gamma = \Gamma_1 + \Gamma_2$.



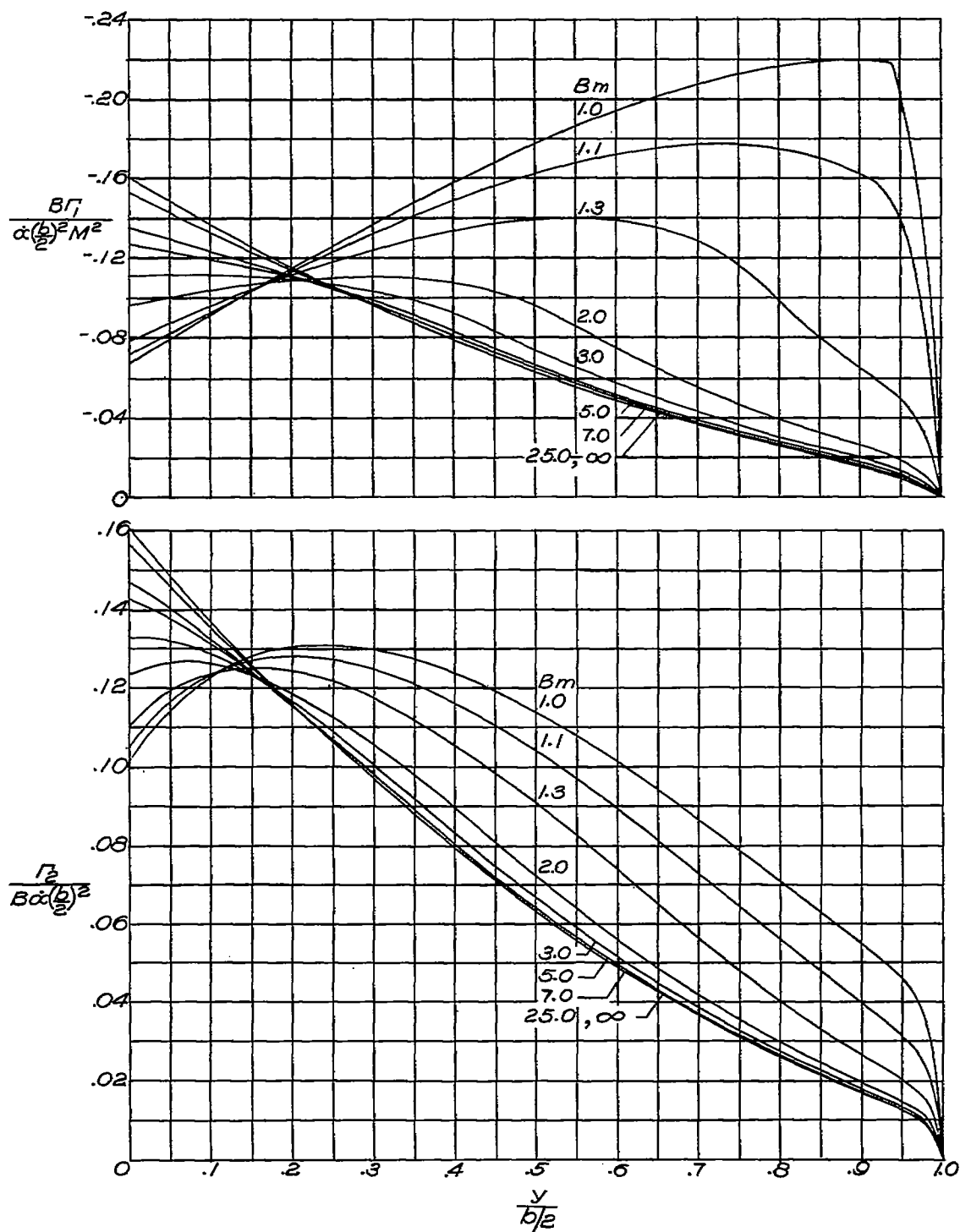
(b) $AB = 4$; $\lambda = 0.25$.

Figure 6.- Continued.



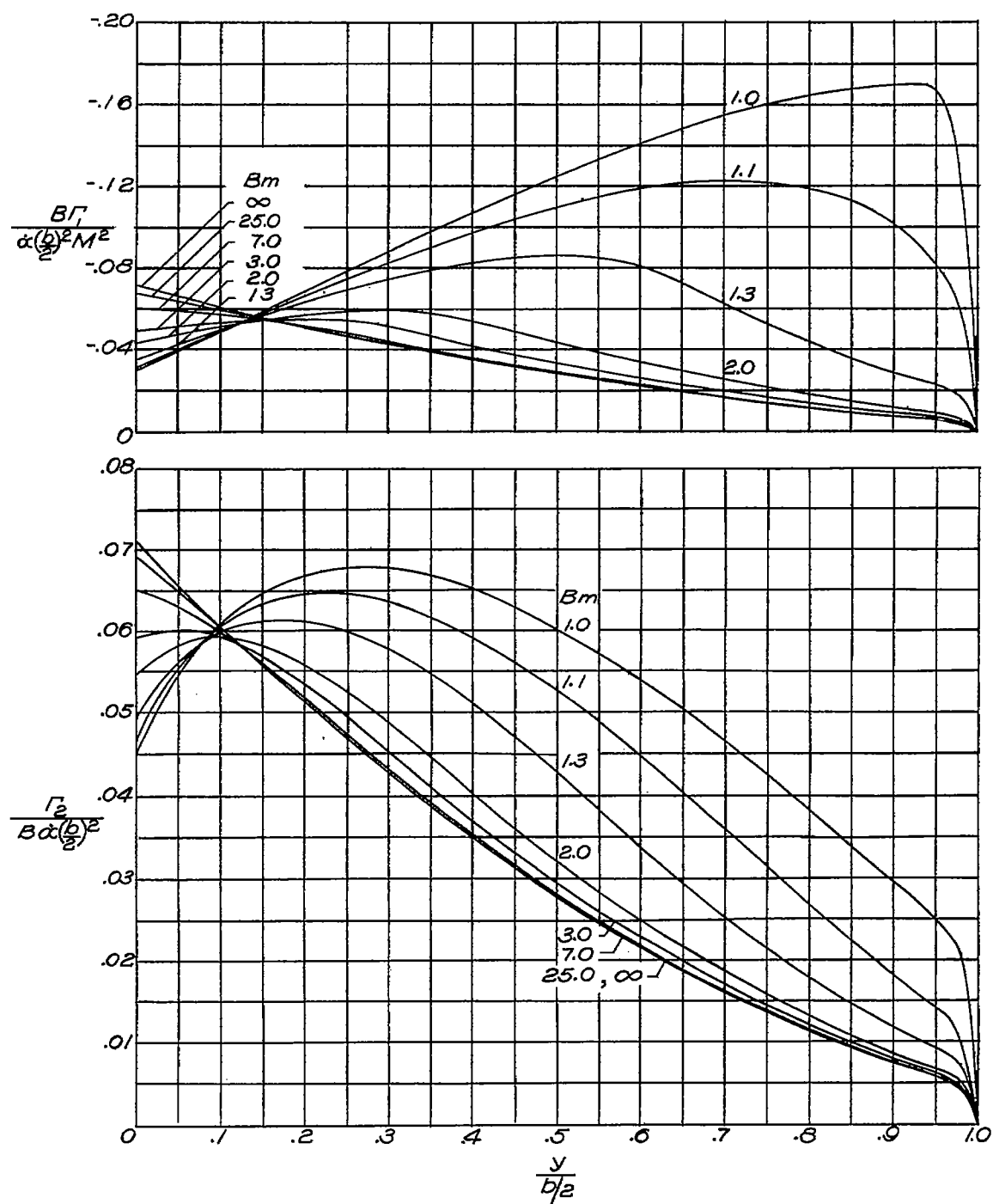
(c) $AB = 6$; $\lambda = 0.25$.

Figure 6.- Continued.



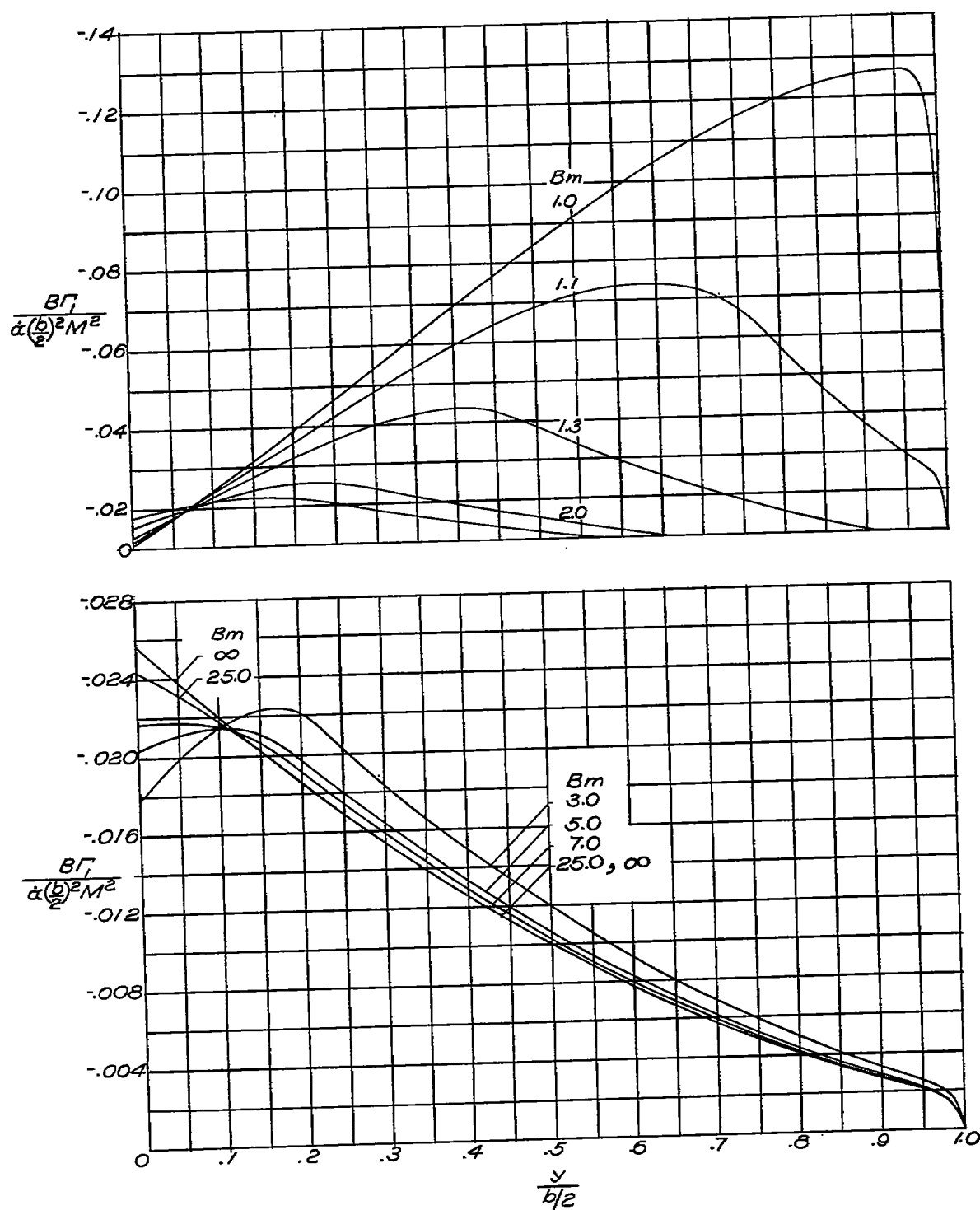
(d) $AB = 8$; $\lambda = 0.25$.

Figure 6.- Continued.



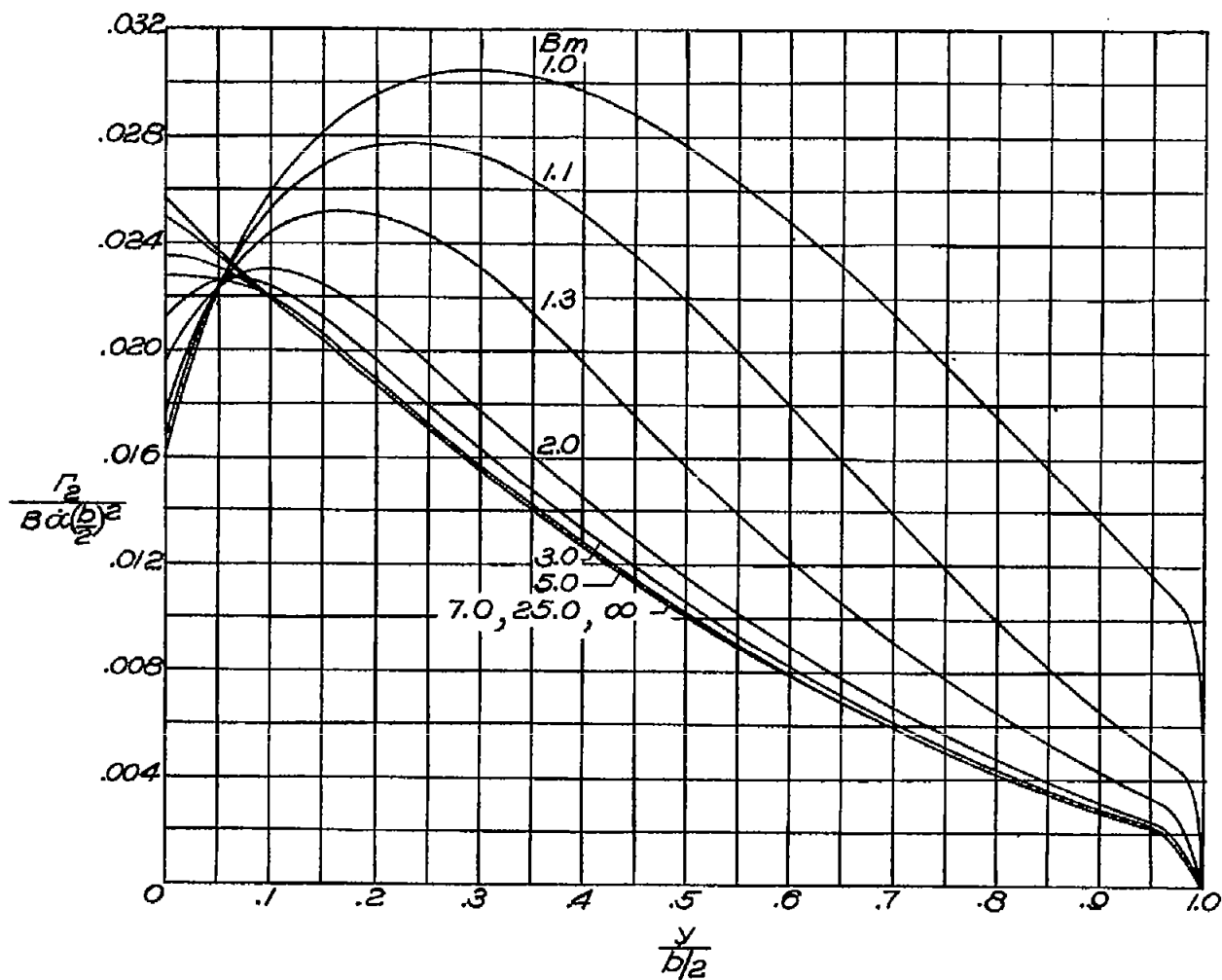
(e) $AB = 12$; $\lambda = 0.25$.

Figure 6.- Continued.



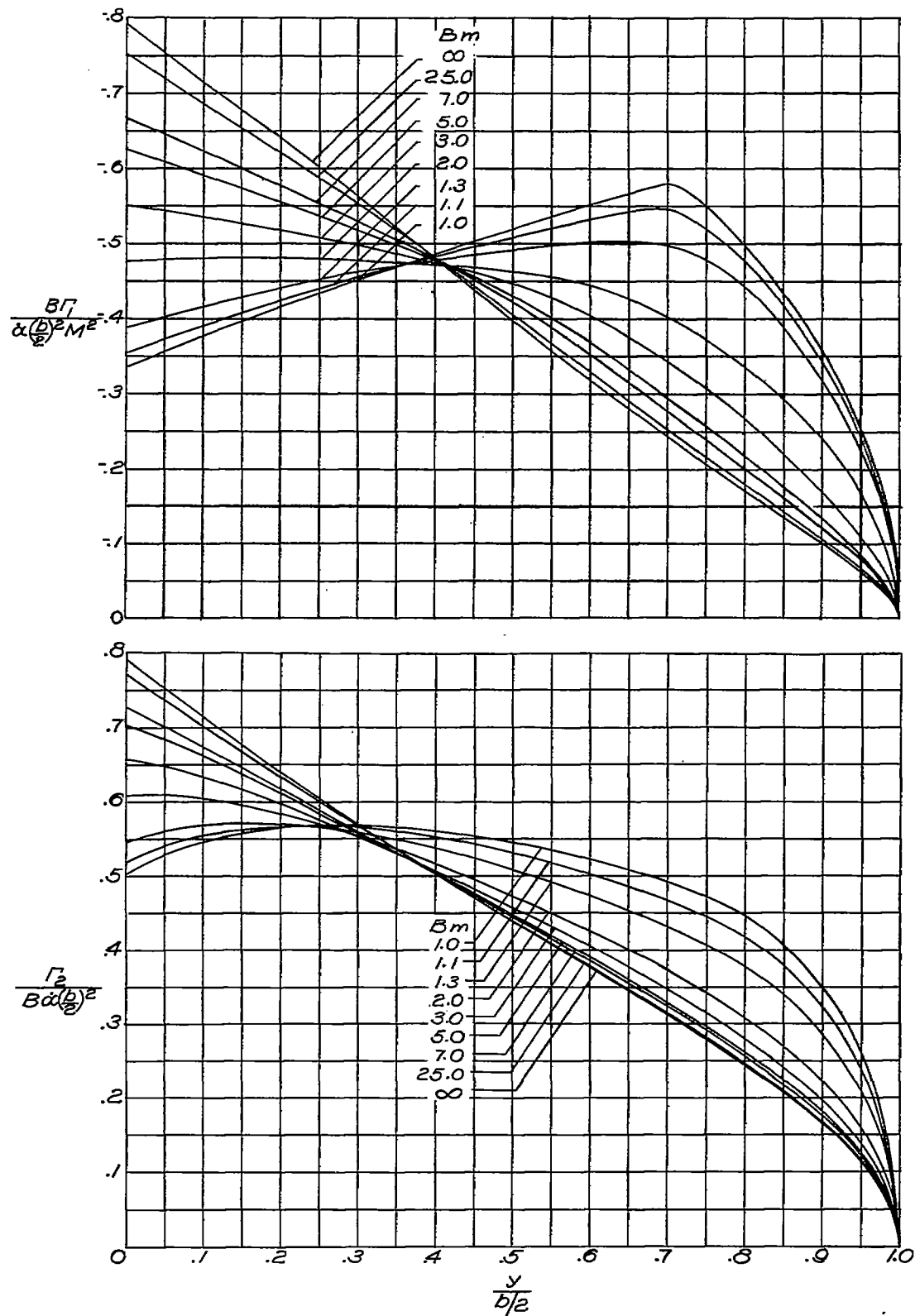
(f) $AB = 20$; $\lambda = 0.25$.

Figure 6.- Continued.



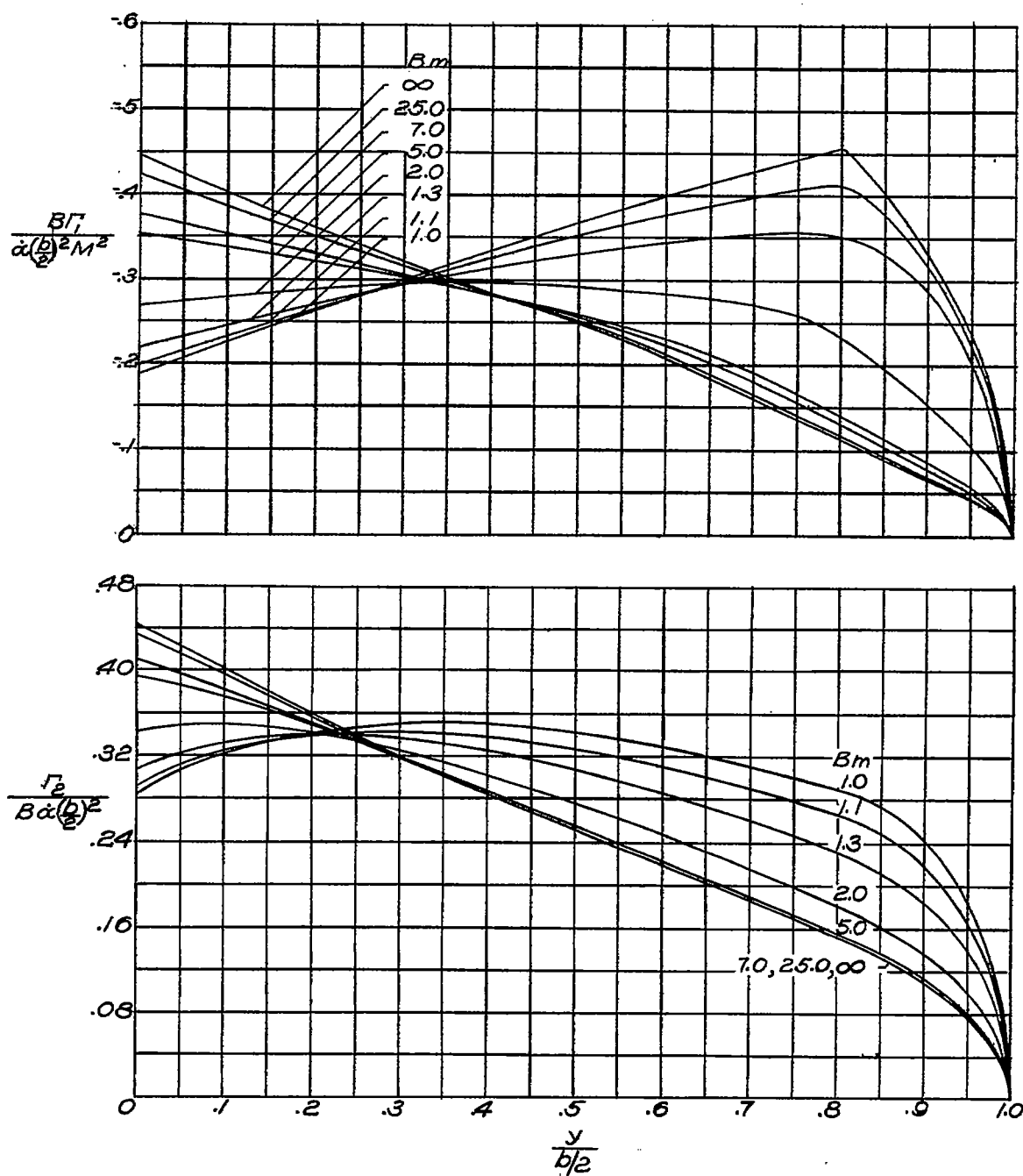
(f) $AB = 20$; $\lambda = 0.25$. Concluded.

Figure 6.- Concluded.



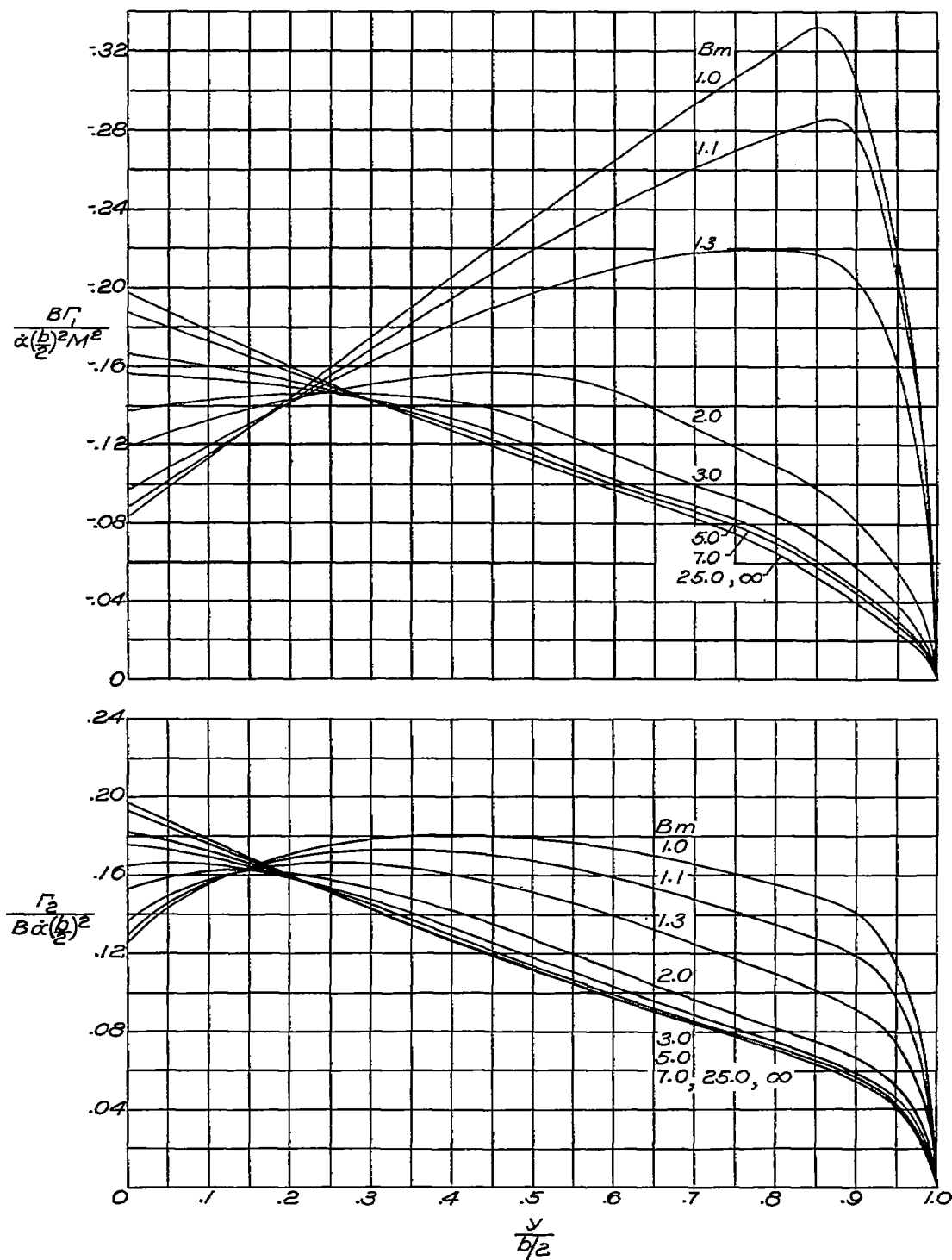
(a) $AB = 3$; $\lambda = 0.50$.

Figure 7.- Distribution of circulation along span for wings with $\lambda = 0.50$.
 $\Gamma = \Gamma_1 + \Gamma_2$.



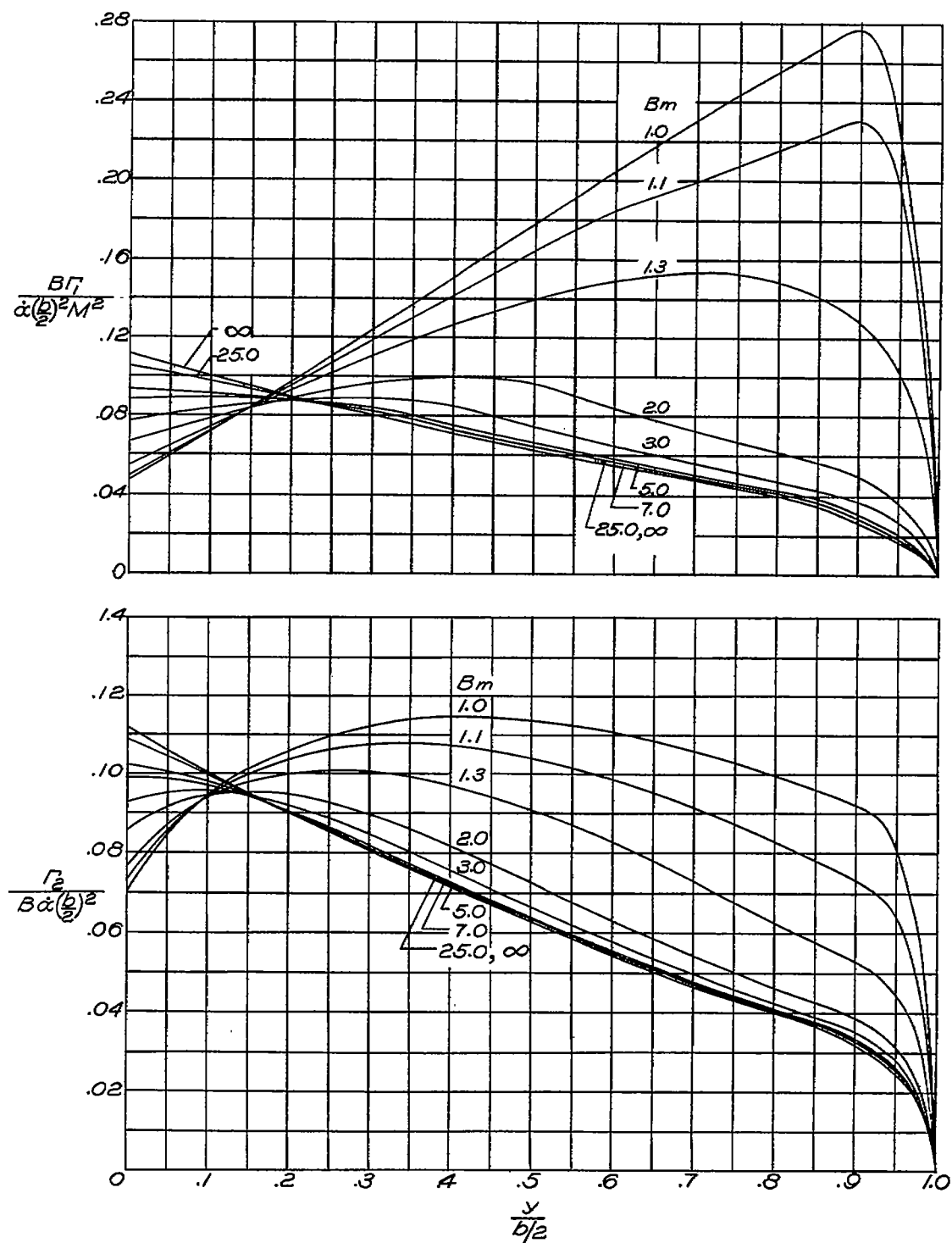
(b) $AB = 4$; $\lambda = 0.50$.

Figure 7.- Continued.



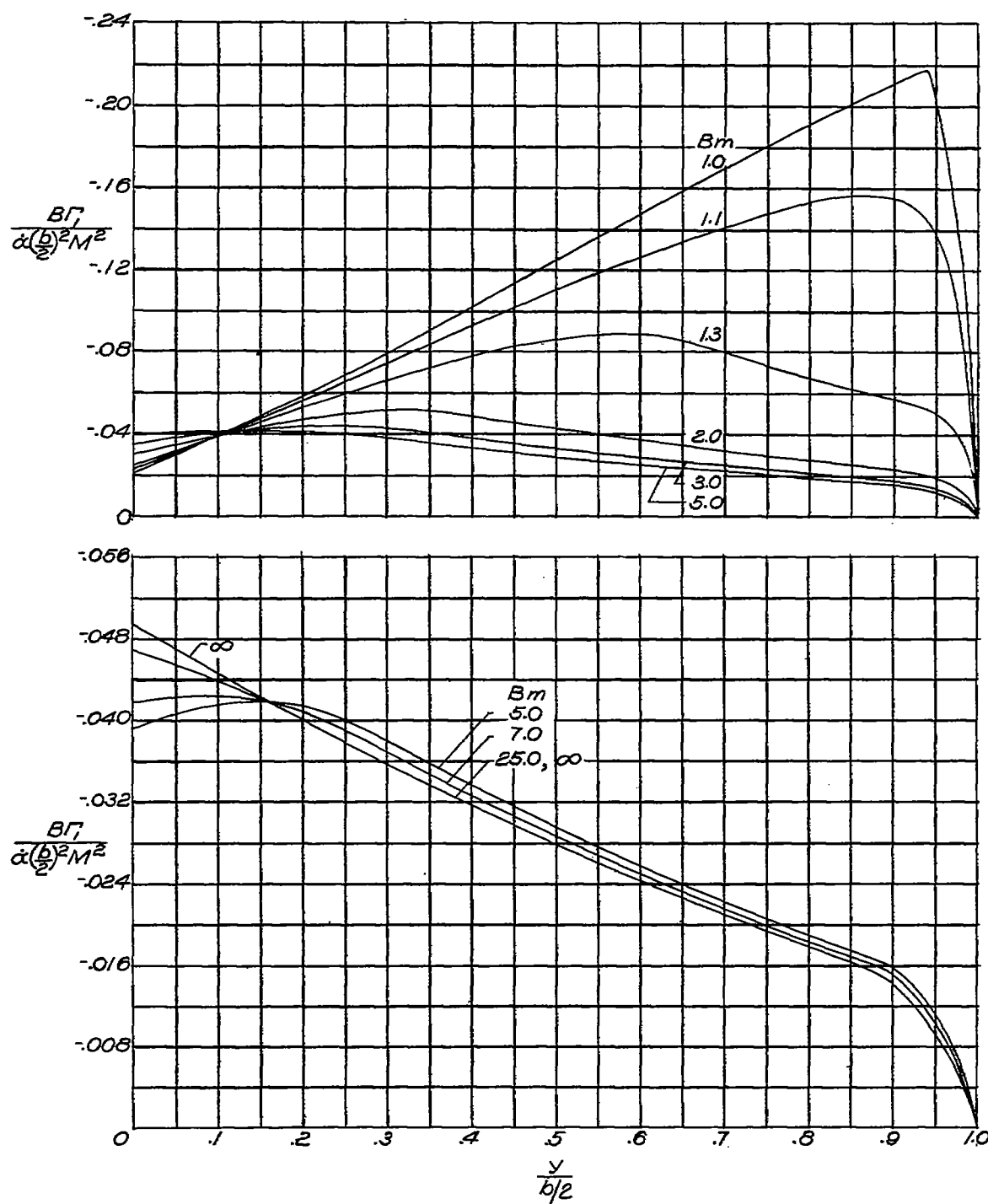
(c) $AB = 6$; $\lambda = 0.50$.

Figure 7.- Continued.



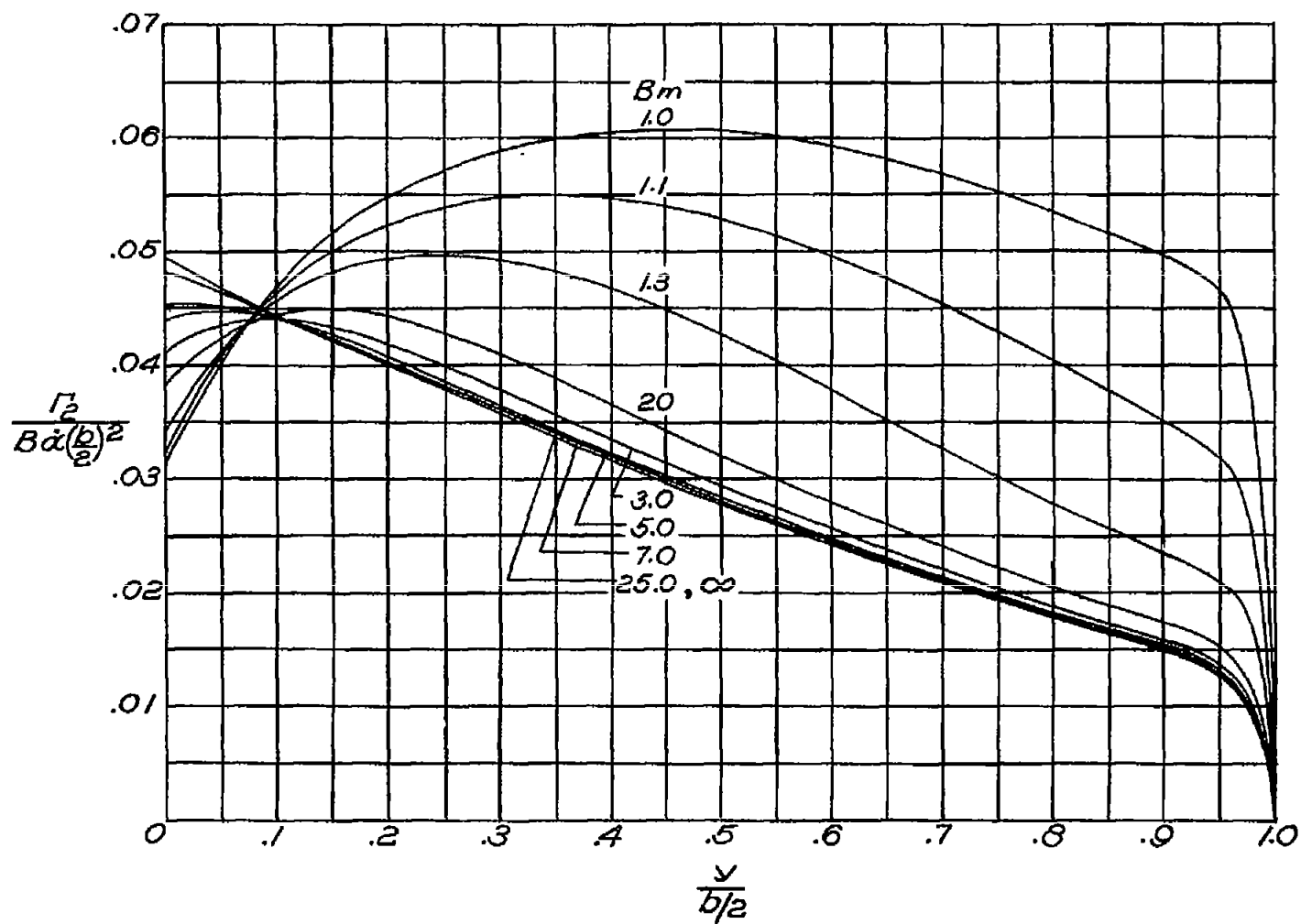
(d) $AB = 8; \lambda = 0.50.$

Figure 7.- Continued.



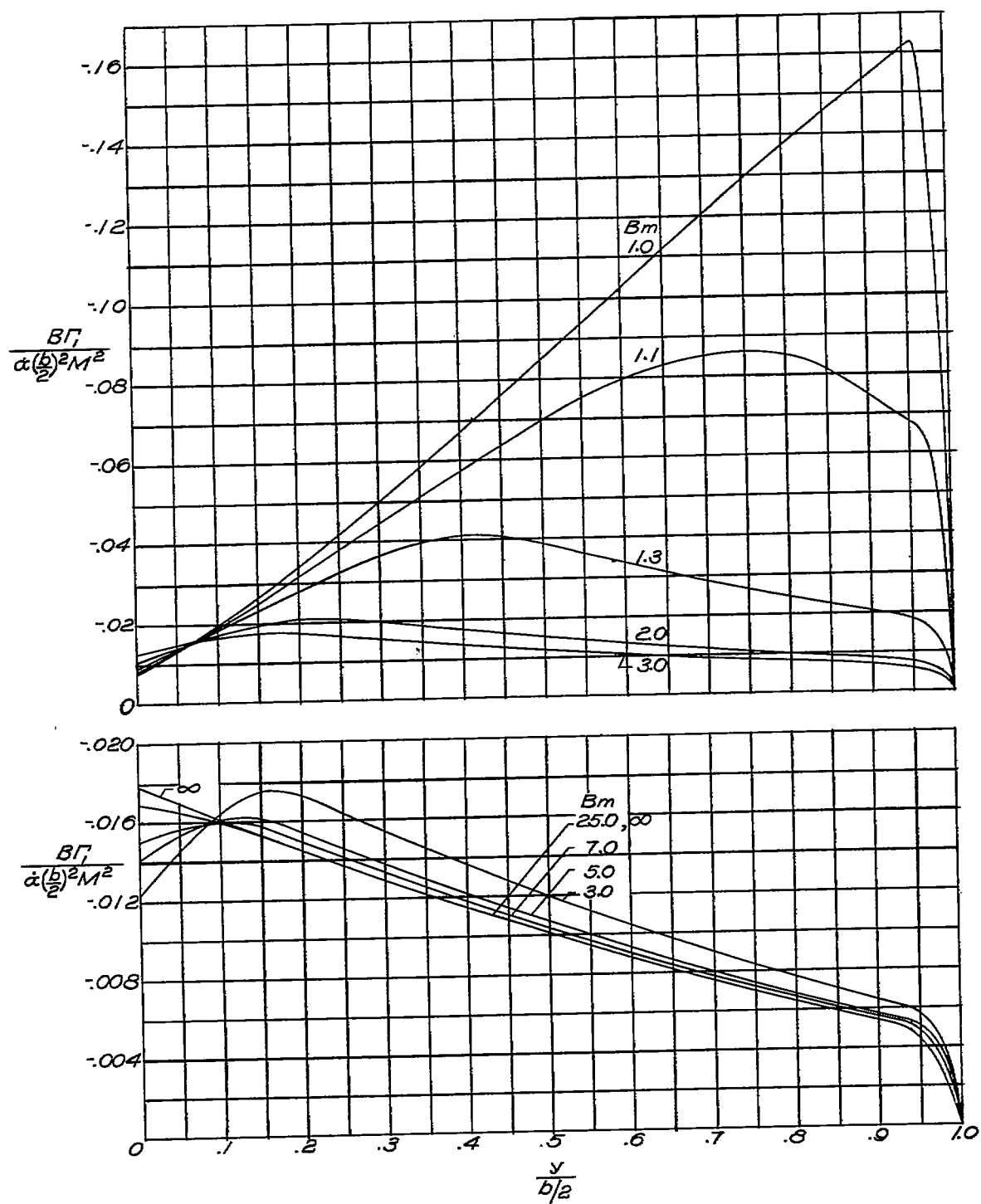
(e) $AB = 12$; $\lambda = 0.50$.

Figure 7.- Continued.



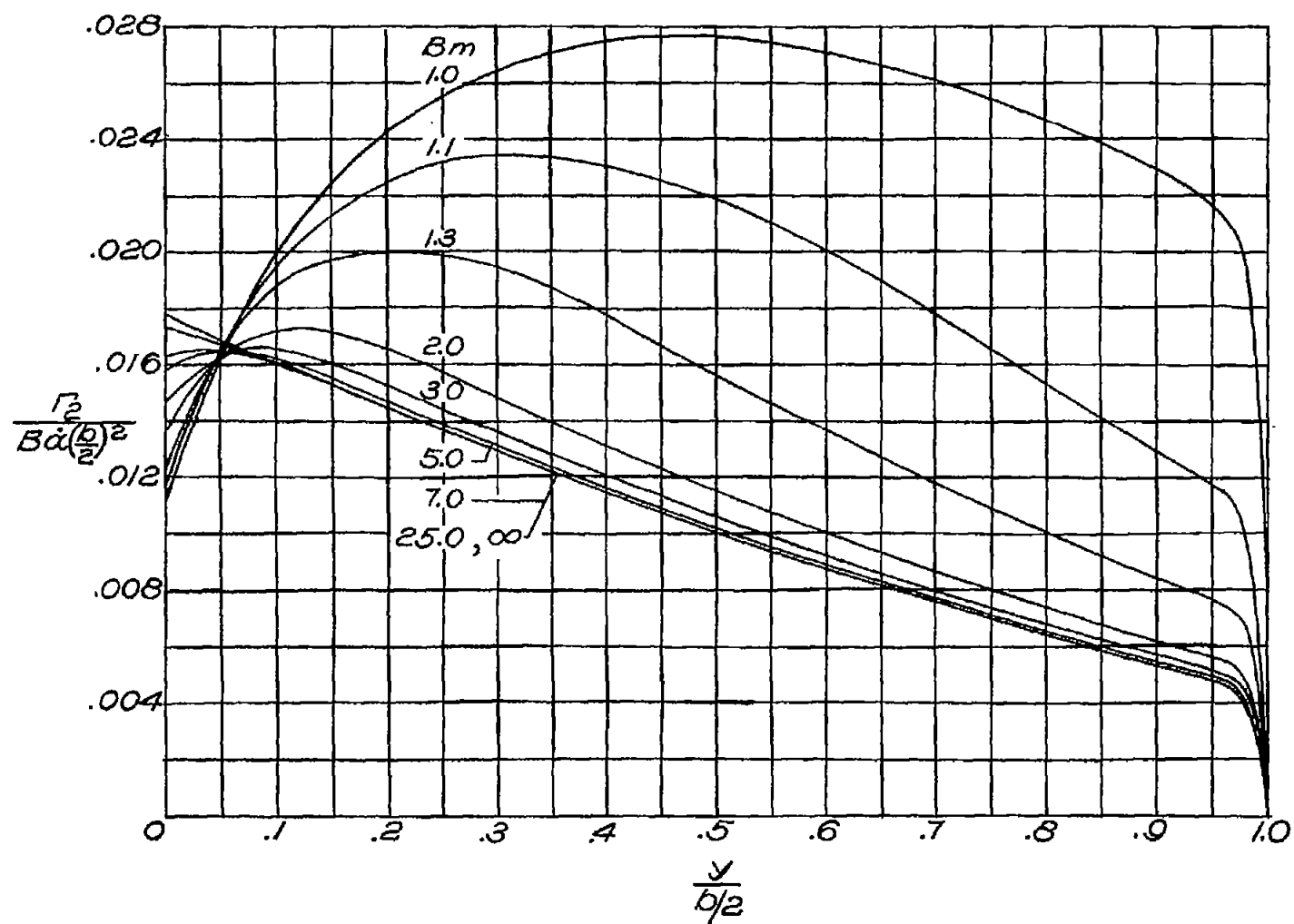
(e) $AB = 12$; $\lambda = 0.50$. Concluded.

Figure 7.- Continued.



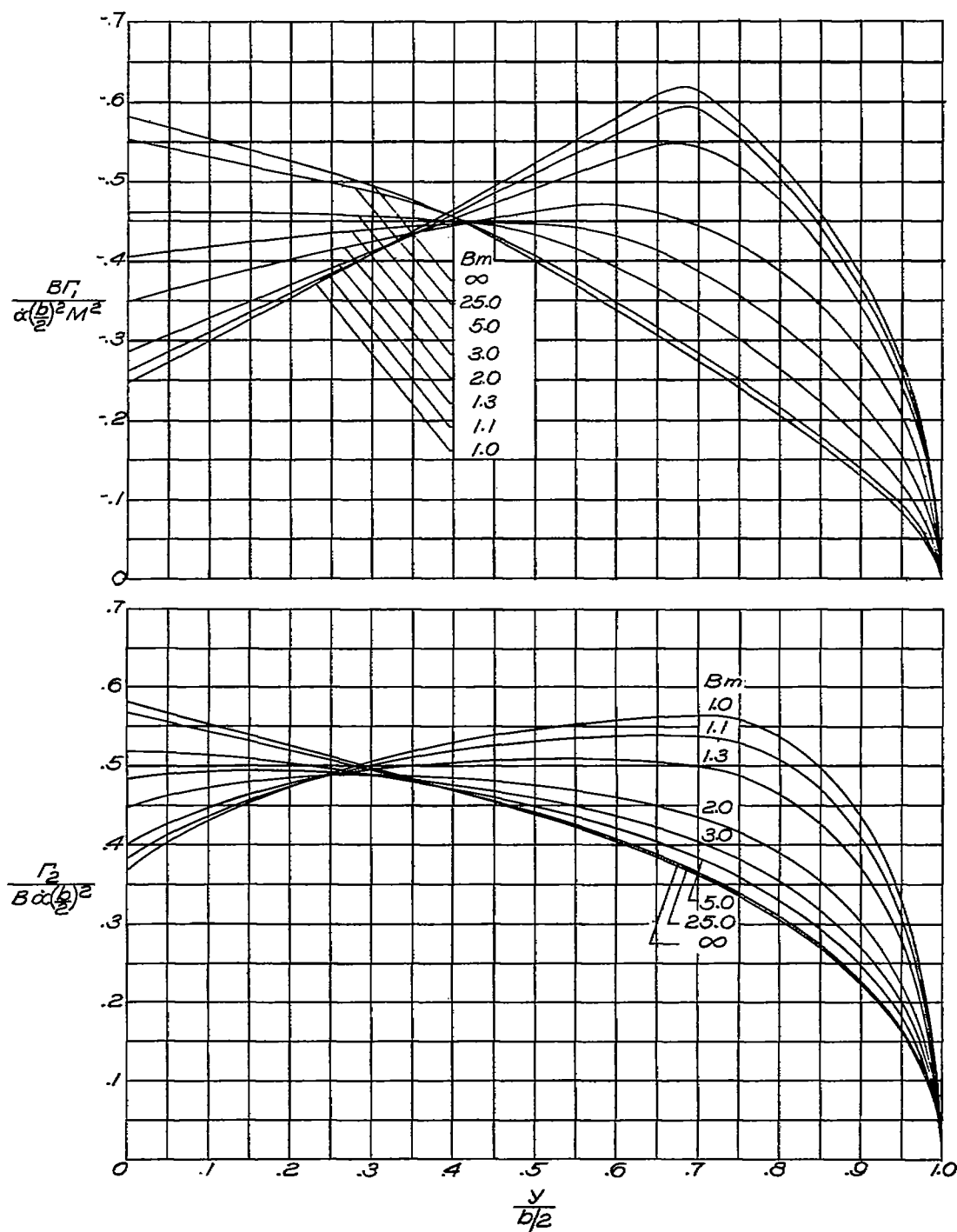
(f) $AB = 20$; $\lambda = 0.50$.

Figure 7.- Continued.



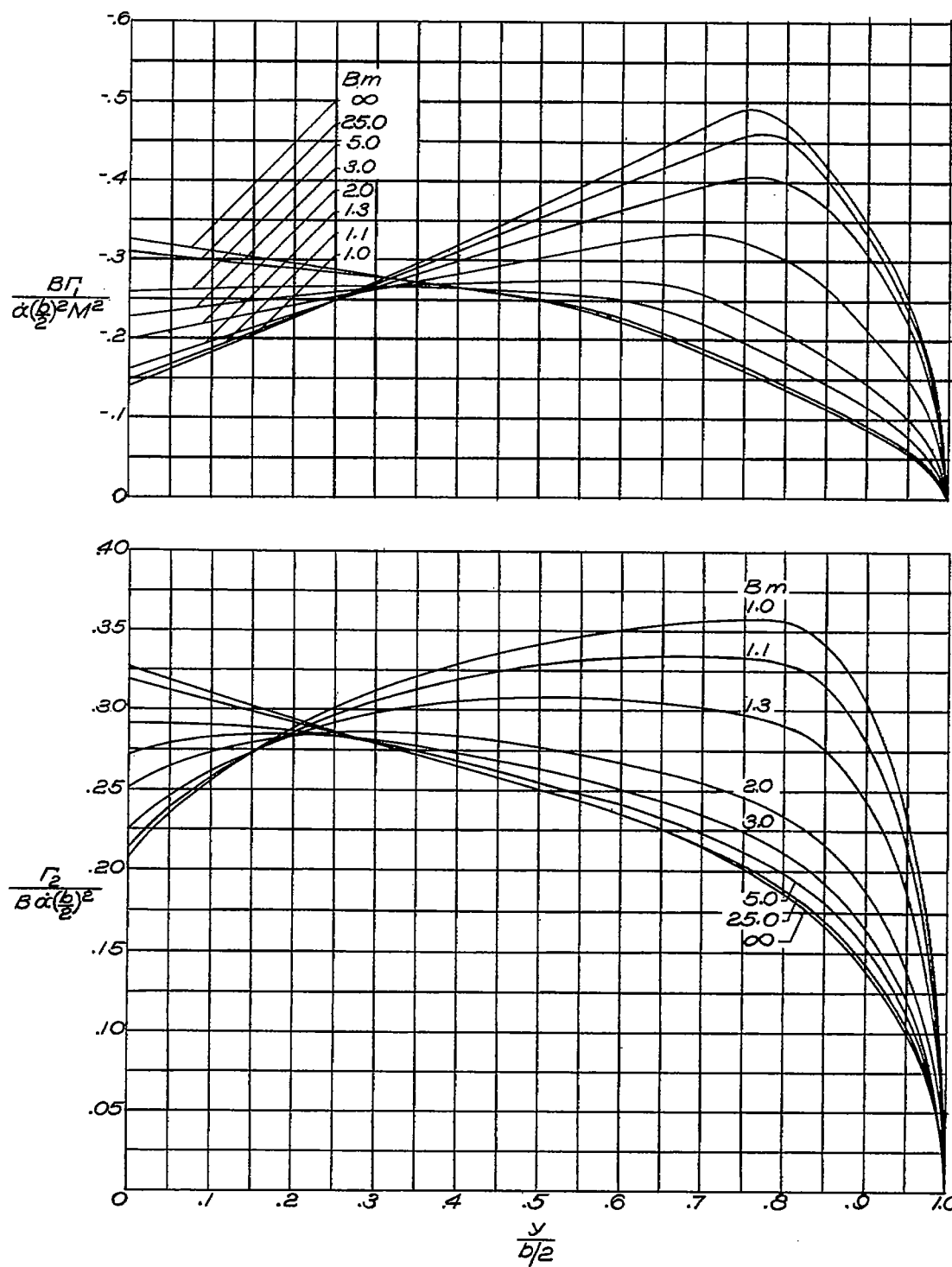
(f) $AB = 20$; $\lambda = 0.50$. Concluded.

Figure 7.- Concluded.



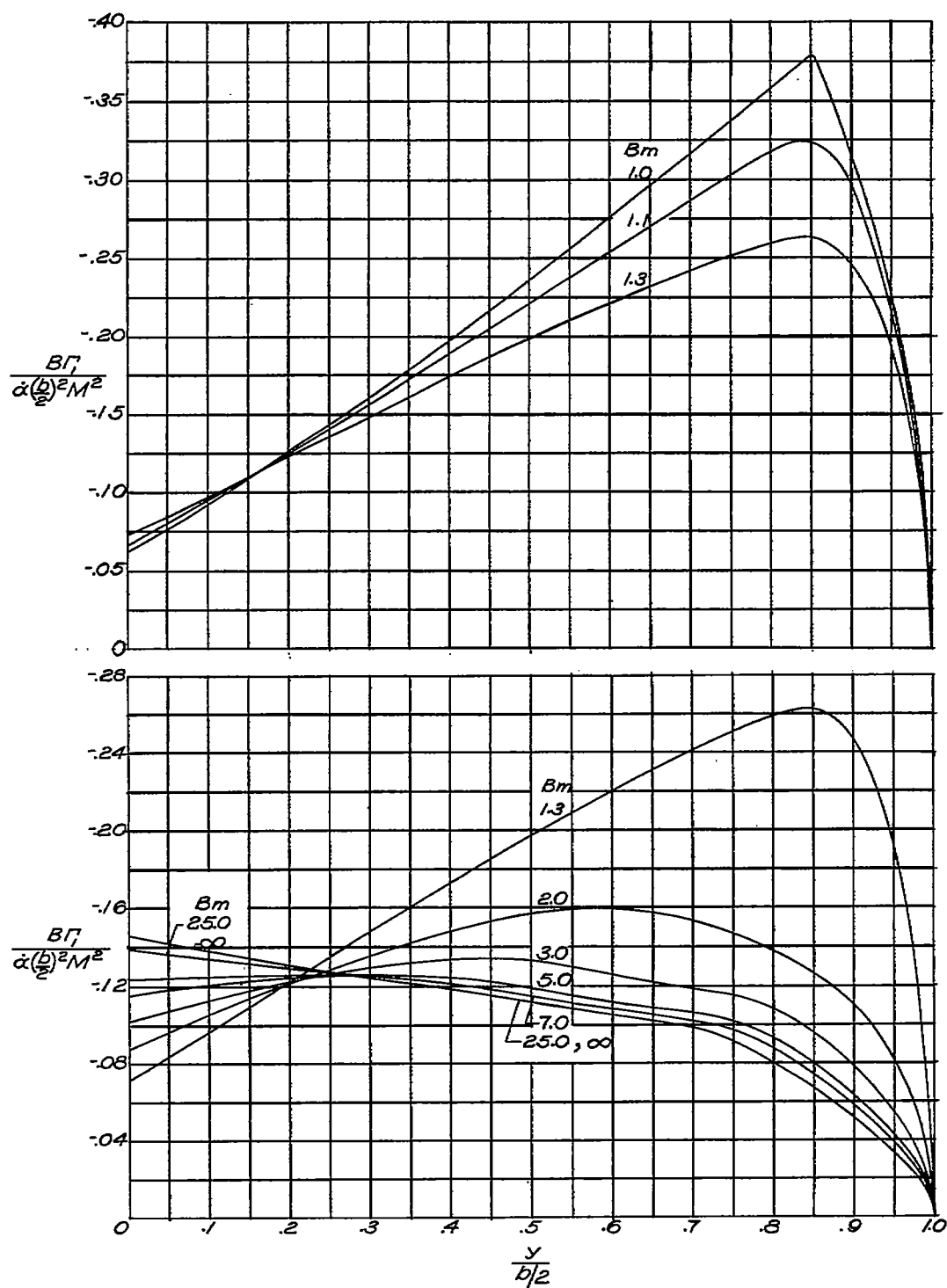
(a) $AB = 3$; $\lambda = 0.75$.

Figure 8.- Distribution of circulation along span for wings with $\lambda = 0.75$.
 $\Gamma = \Gamma_1 + \Gamma_2$.



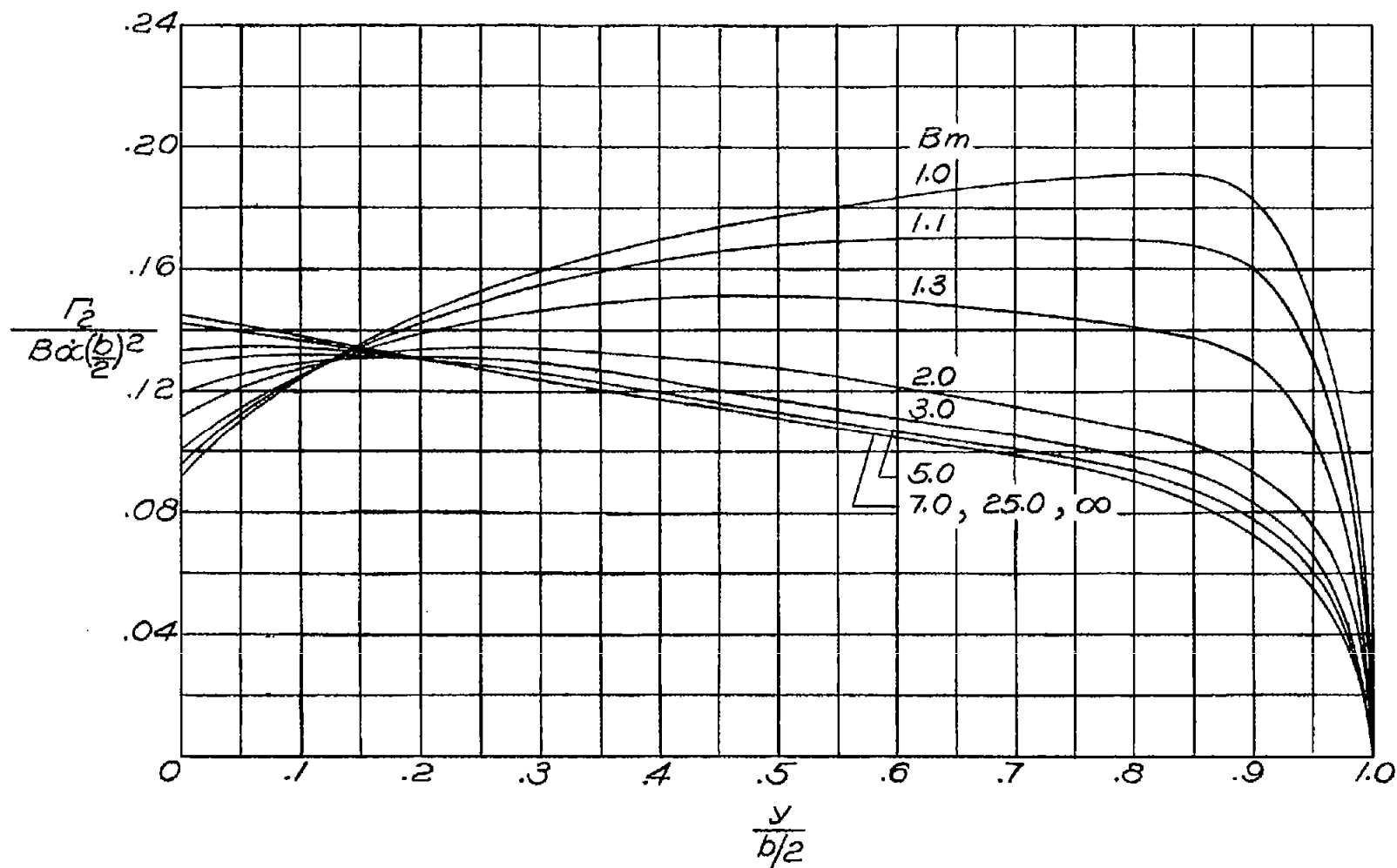
(b) $AB = 4$; $\lambda = 0.75$.

Figure 8.- Continued.



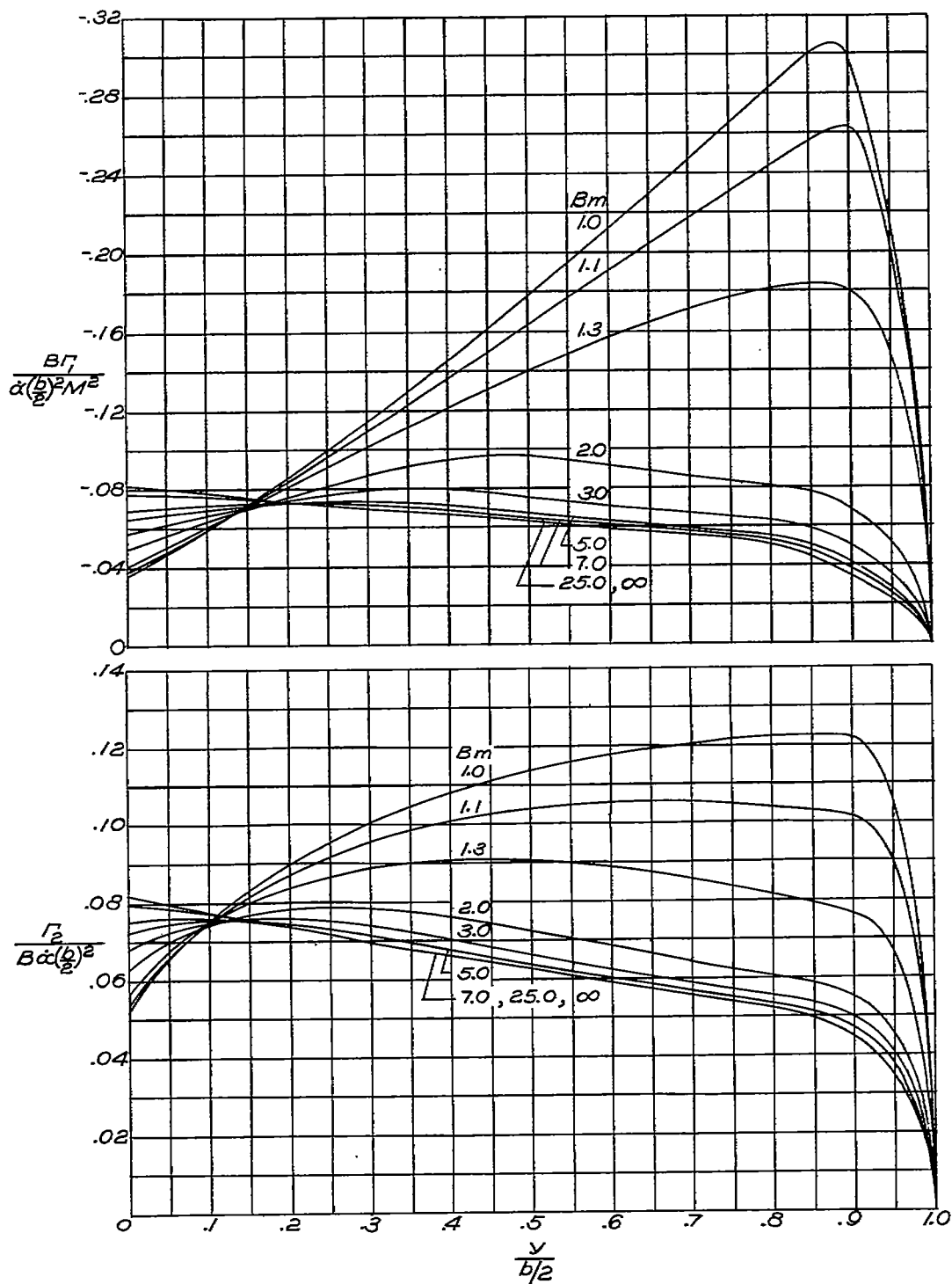
(c) $AB = 6$; $\lambda = 0.75$.

Figure 8.- Continued.



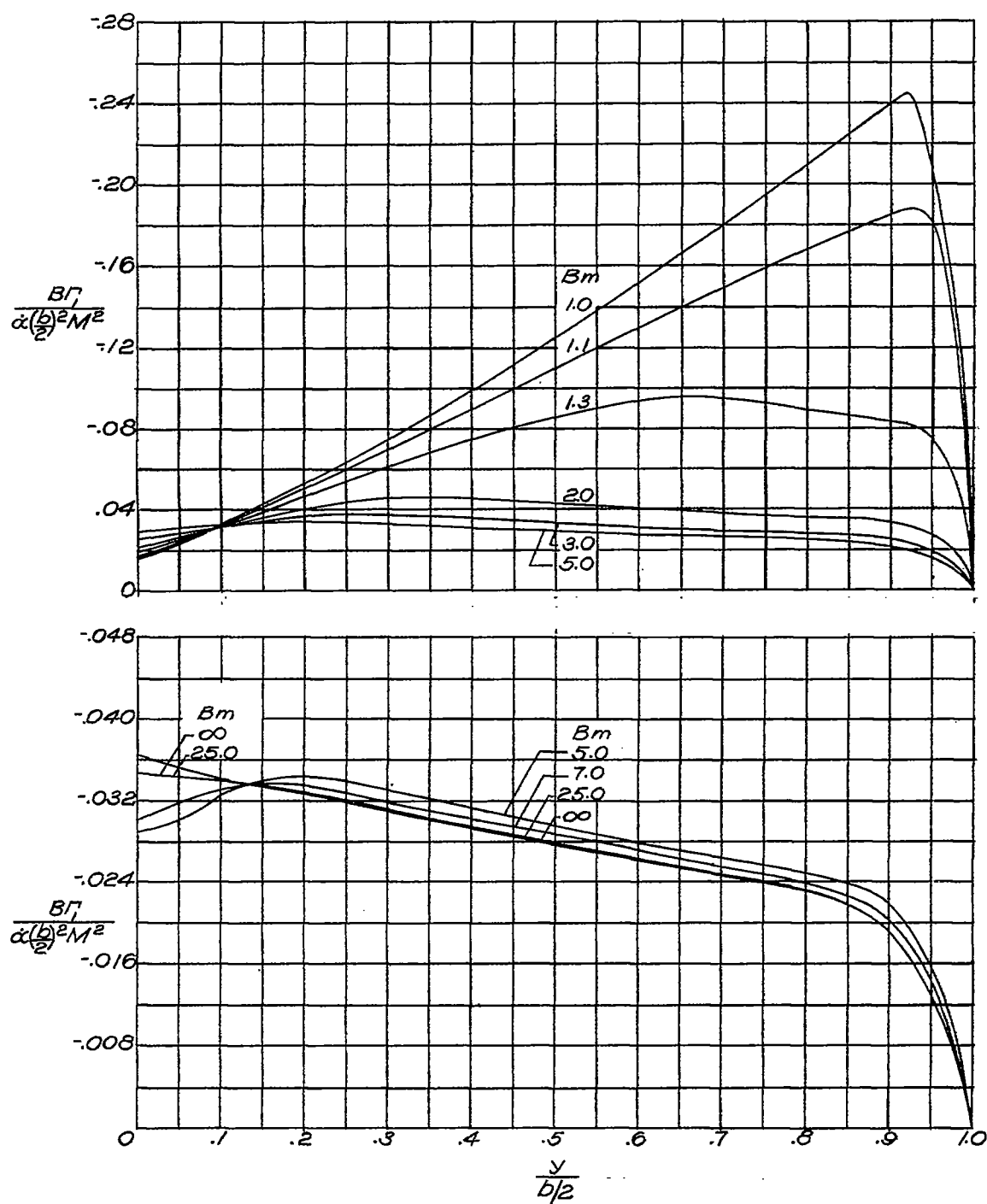
(c) $AB = 6$; $\lambda = 0.75$. Concluded.

Figure 8.- Continued.



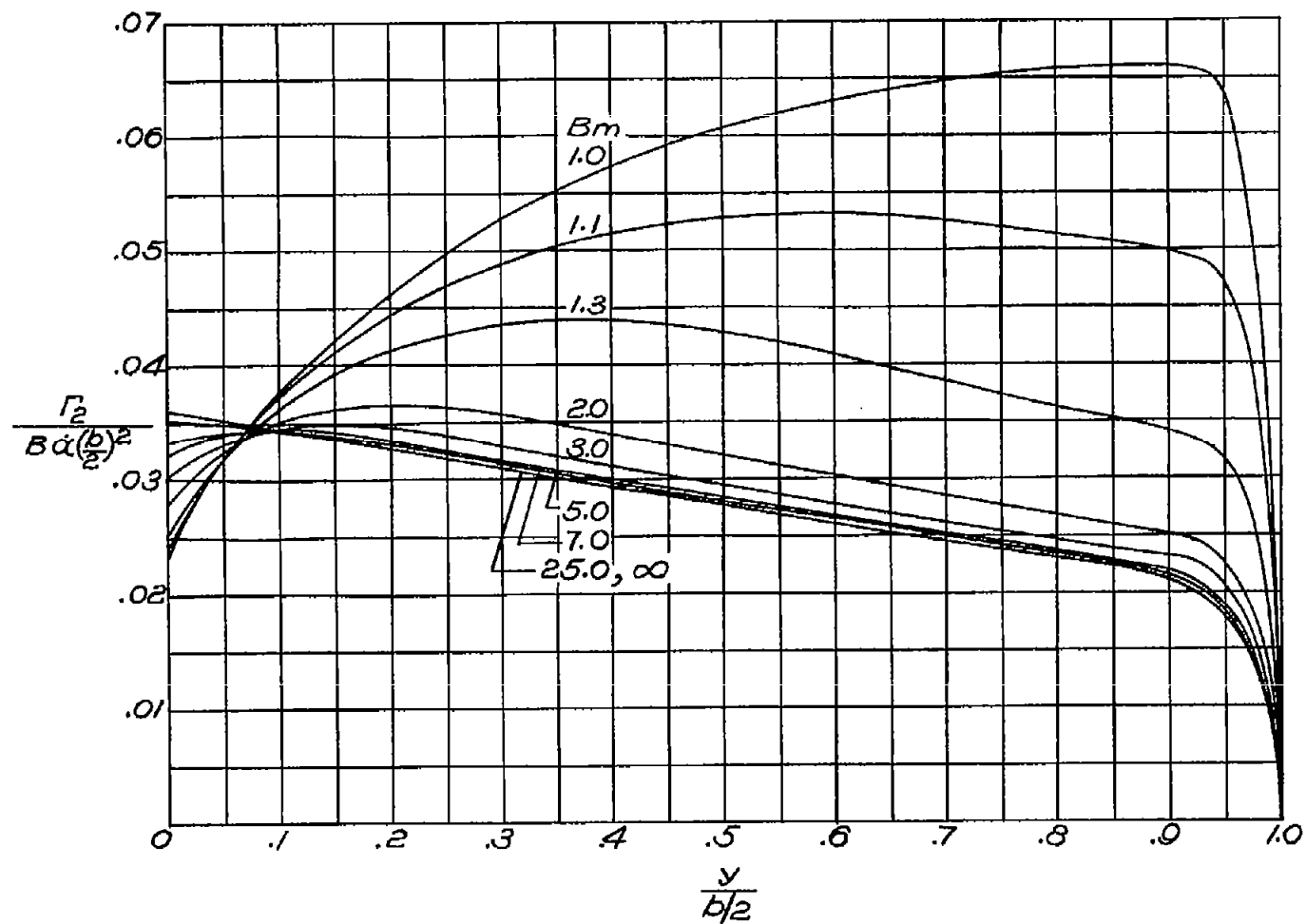
(d) $AB = 8$; $\lambda = 0.75$.

Figure 8.- Continued.



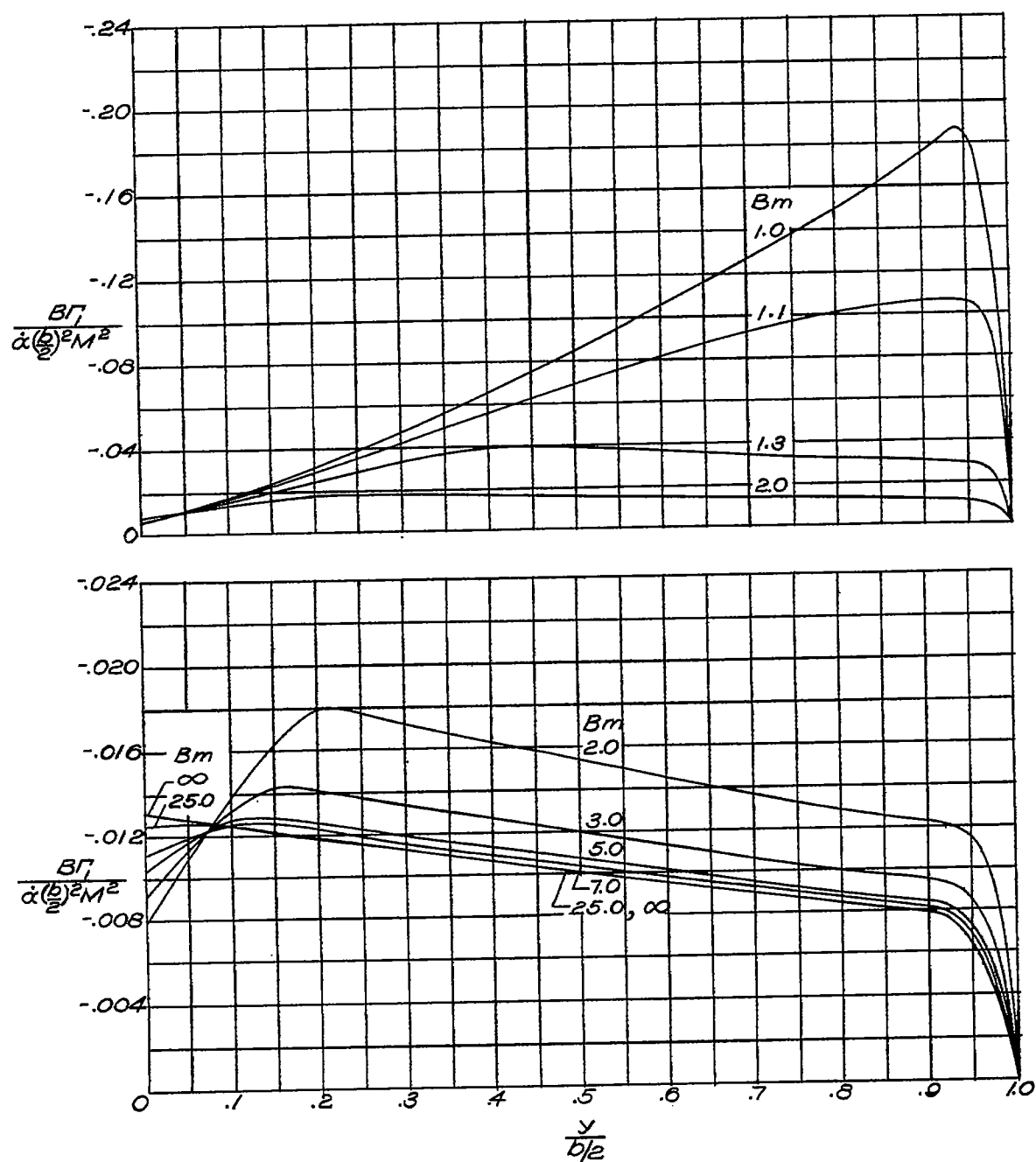
(e) $AB = 12$; $\lambda = 0.75$.

Figure 8.- Continued.



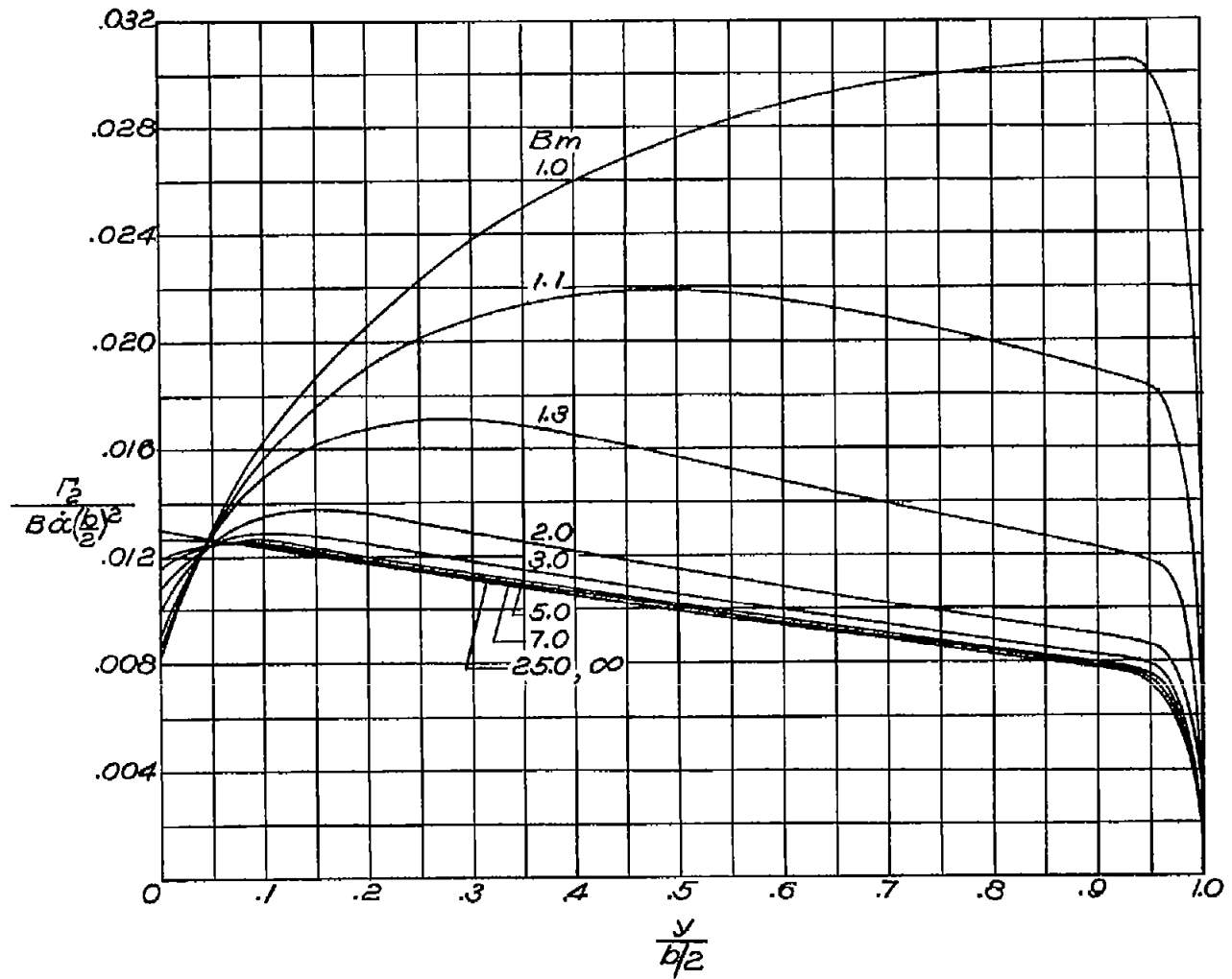
(e) $AB = 12$; $\lambda = 0.75$. Concluded.

Figure 8.- Continued.



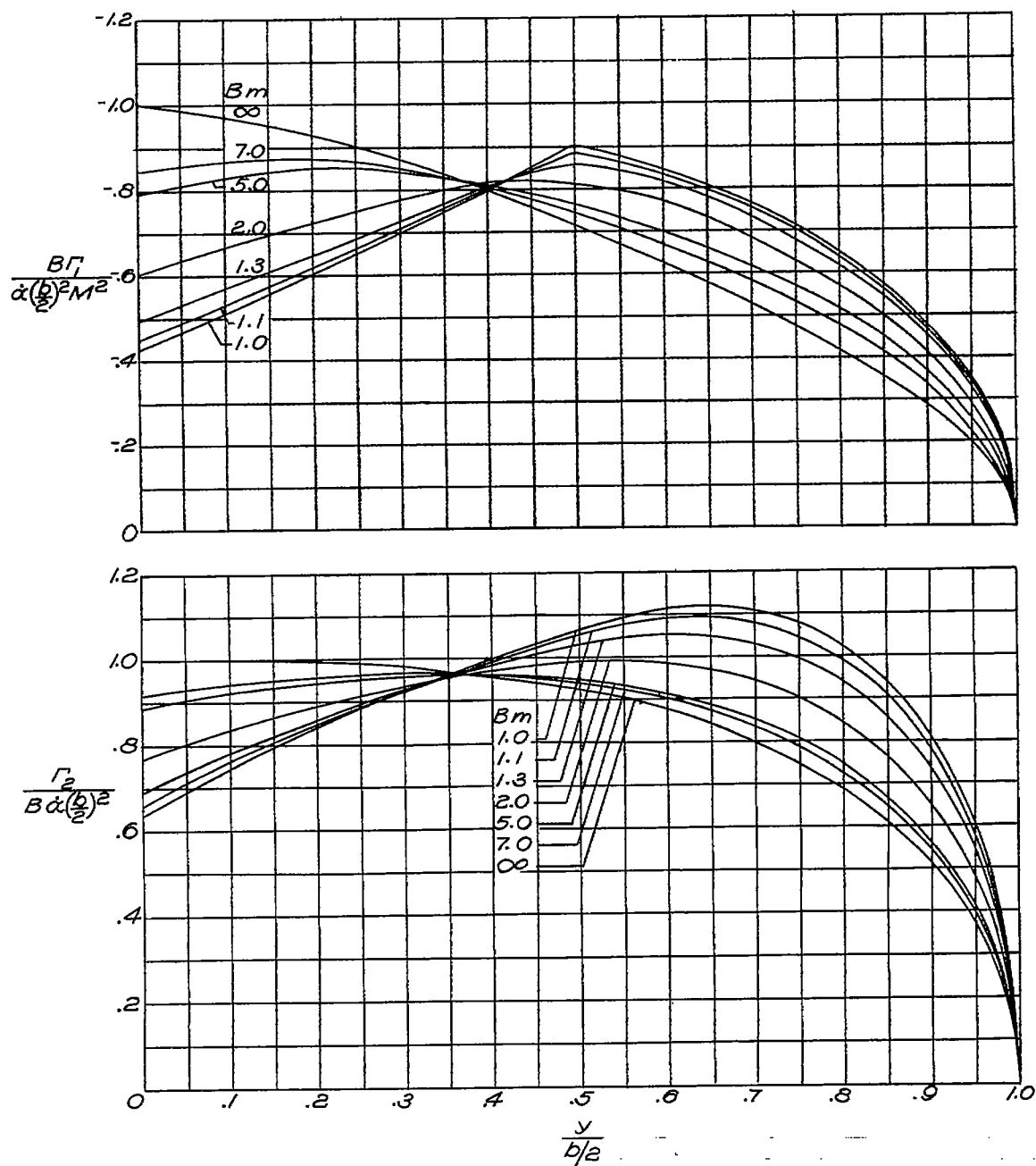
(f) $AB = 20$; $\lambda = 0.75$.

Figure 8.- Continued.



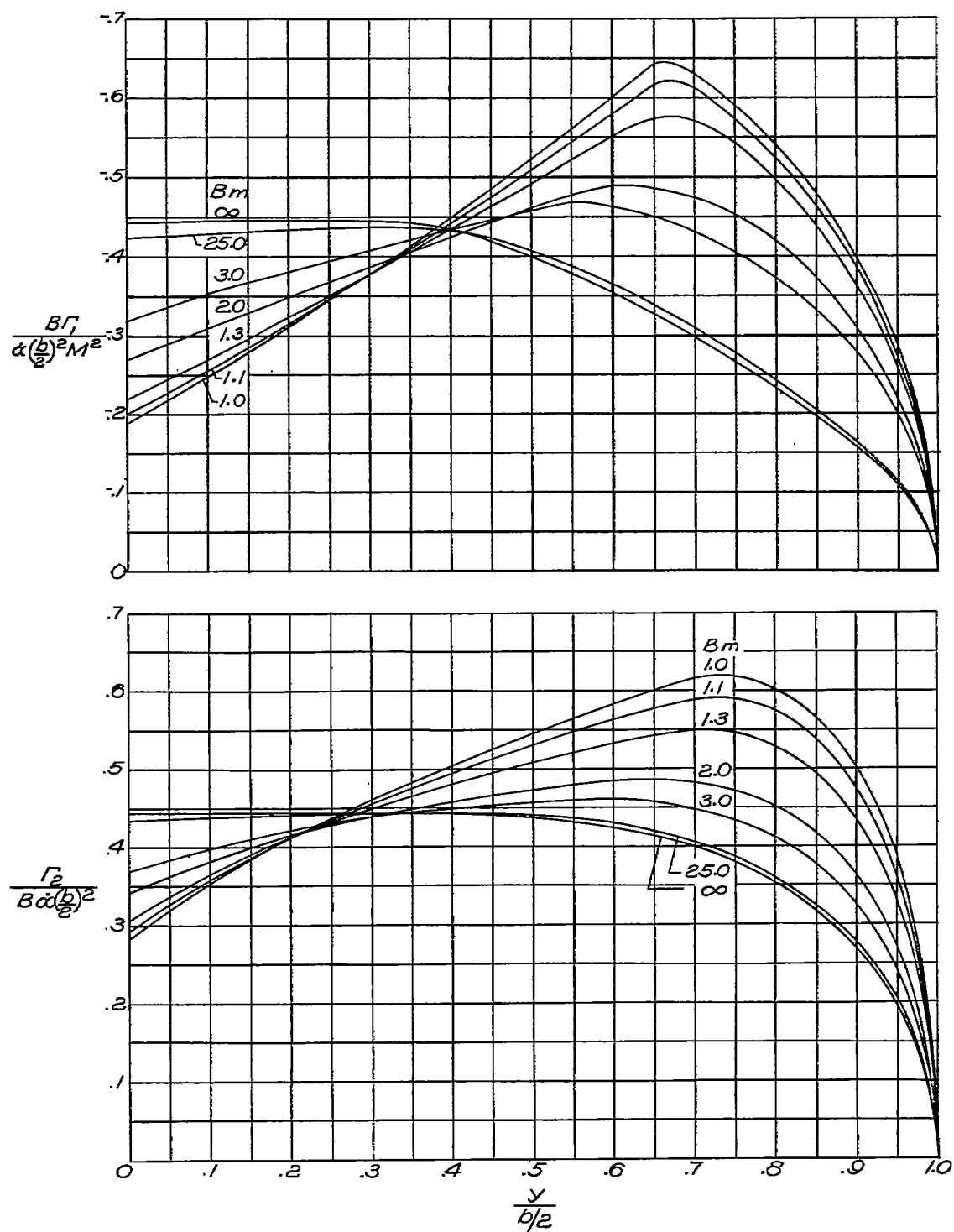
(f) $AB = 20$; $\lambda = 0.75$. Concluded.

Figure 8.- Concluded.



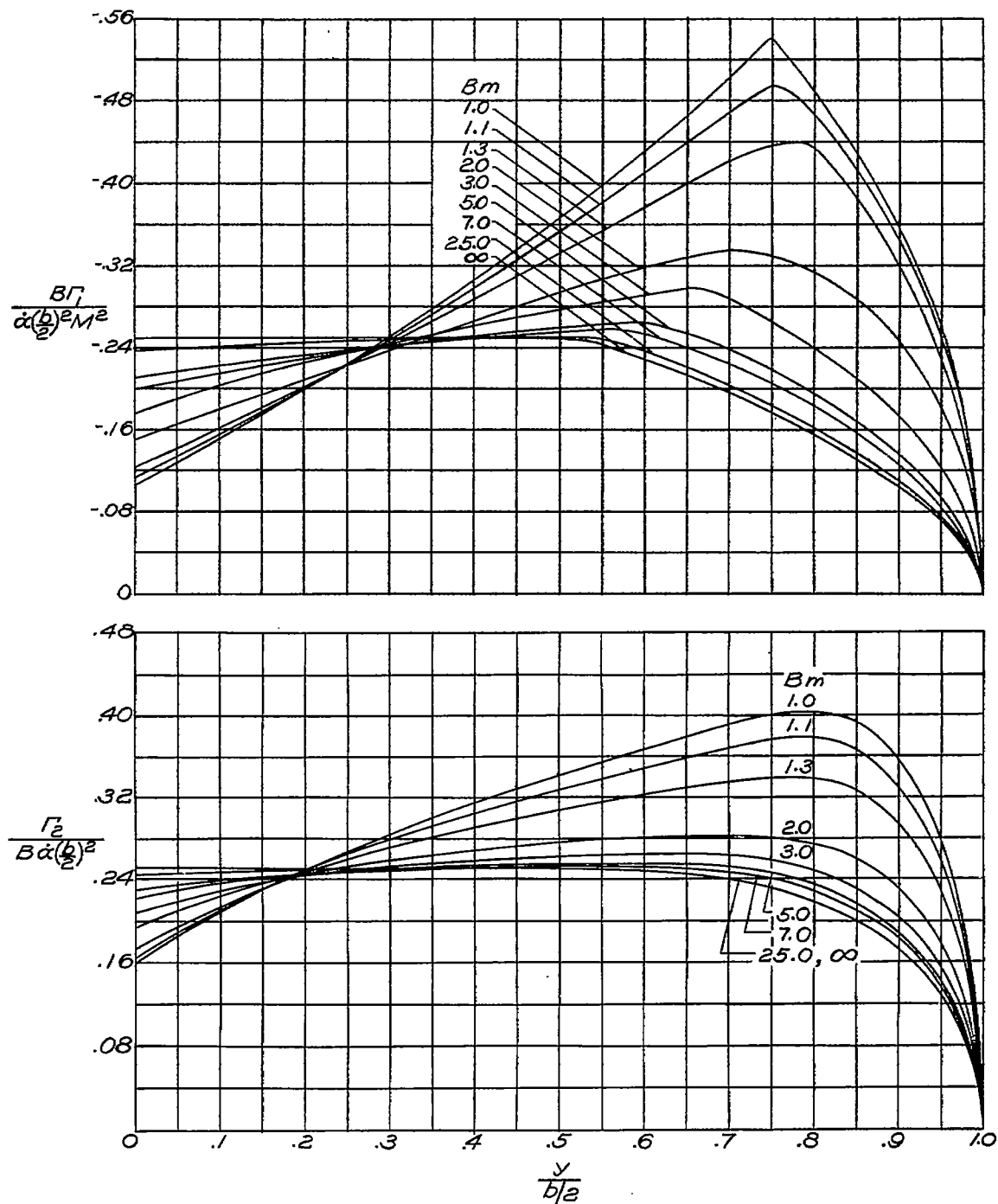
(a) $AB = 2$; $\lambda = 1.0$.

Figure 9.- Distribution of circulation along span for wings with $\lambda = 1.0$.
 $\Gamma = \Gamma_1 + \Gamma_2$.



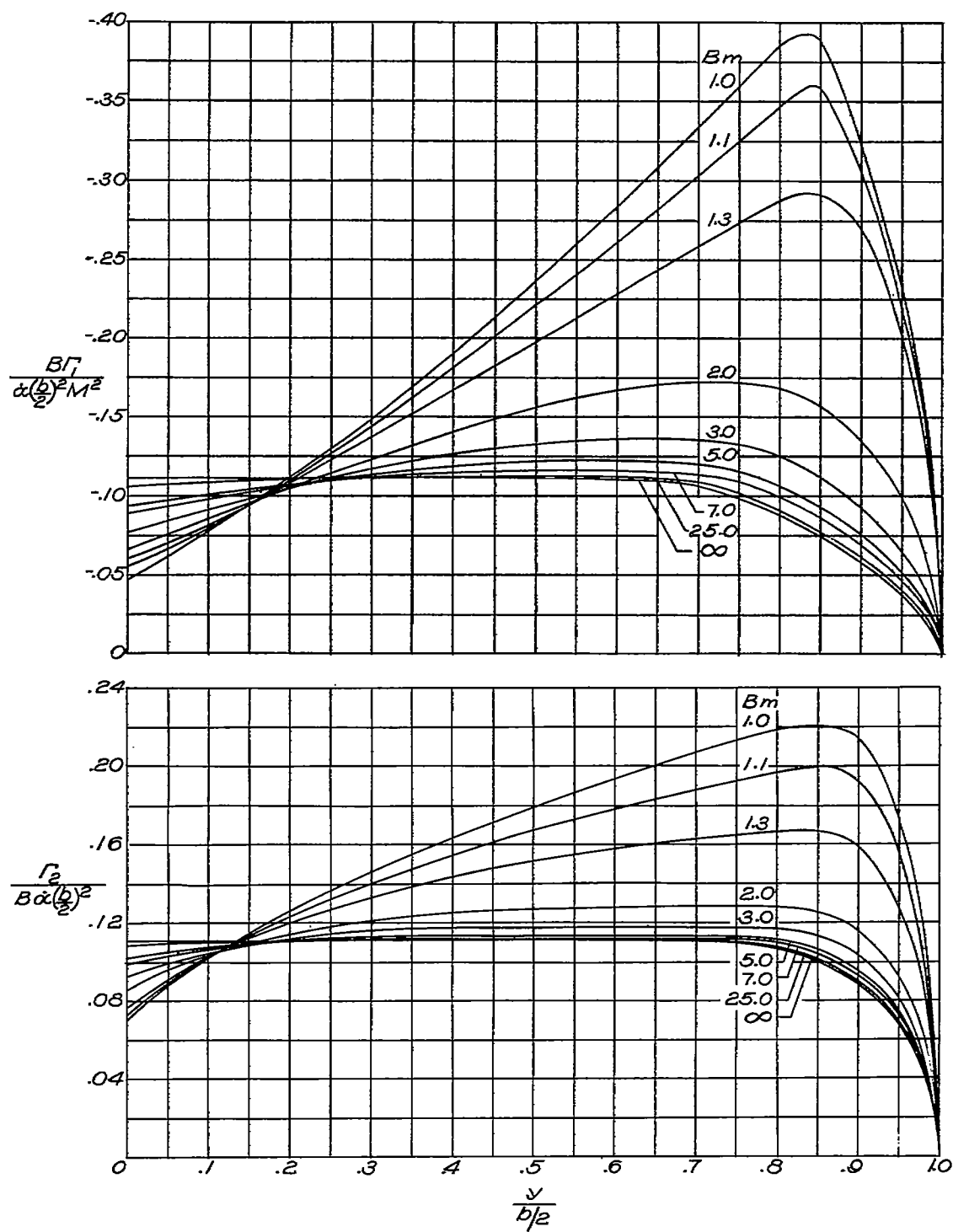
(b) $AB = 3$; $\lambda = 1.0$.

Figure 9.- Continued.



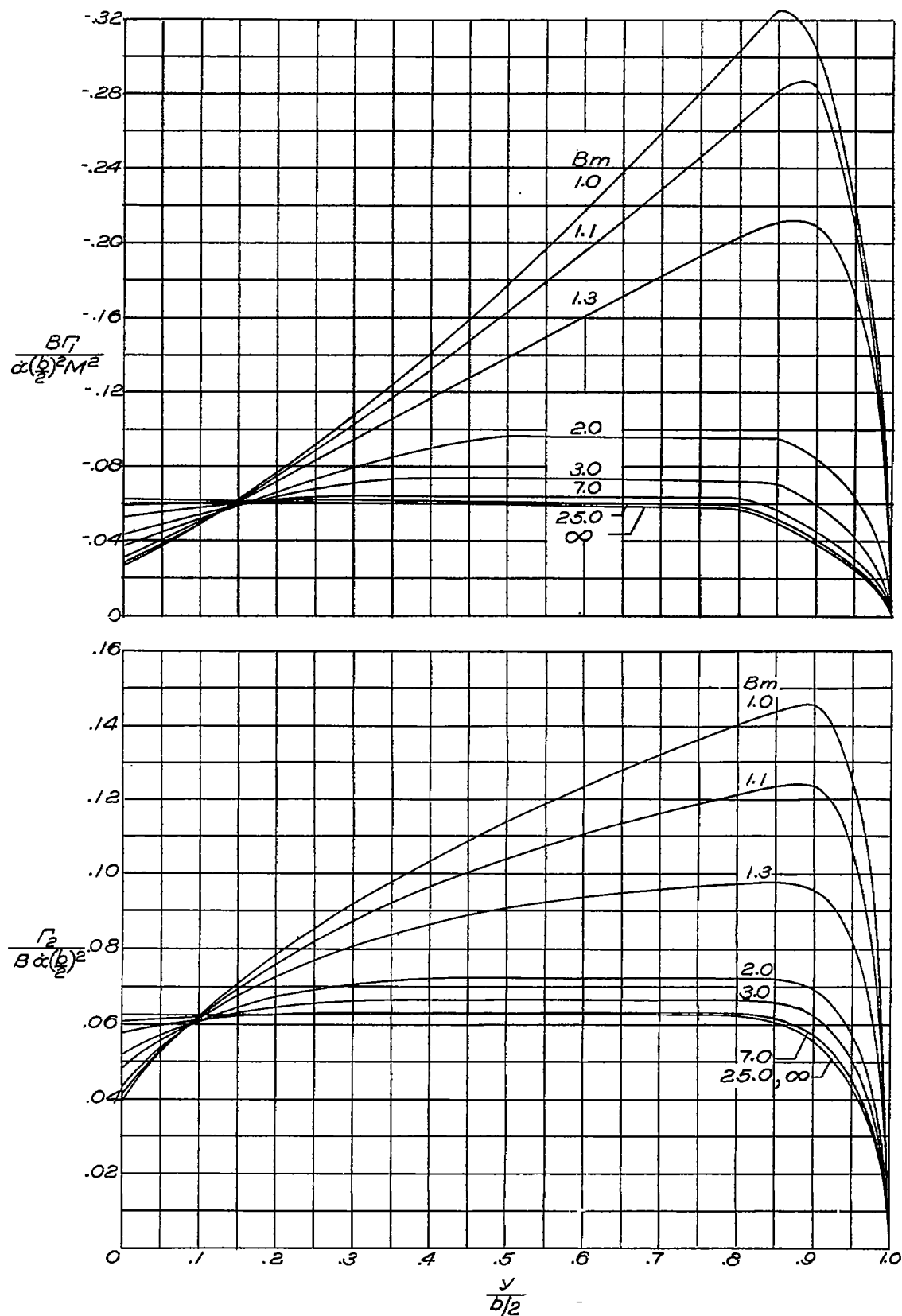
(c) $AB = 4$; $\lambda = 1.0$.

Figure 9.- Continued.



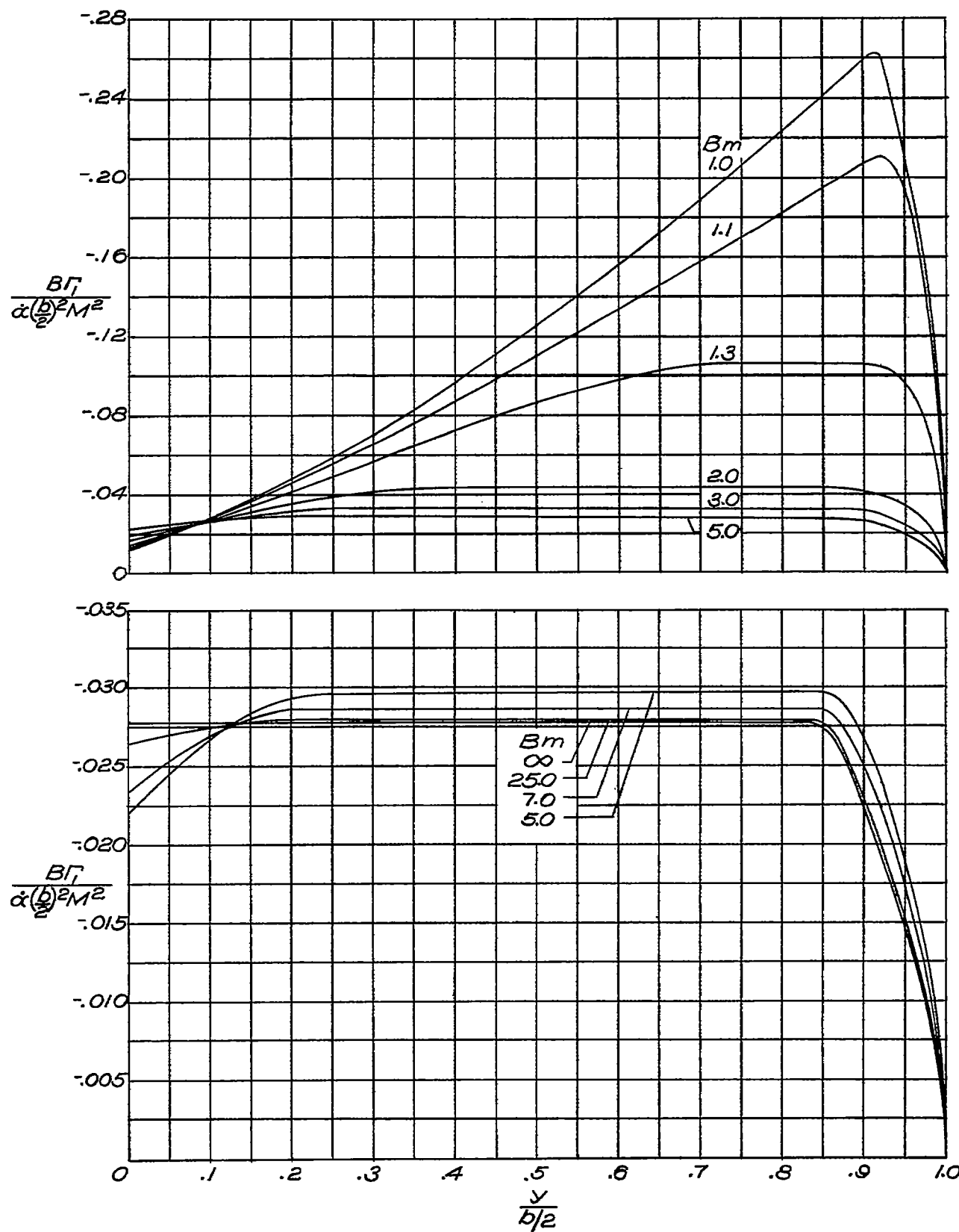
(d) $AB = 6$; $\lambda = 1.0$.

Figure 9.- Continued.



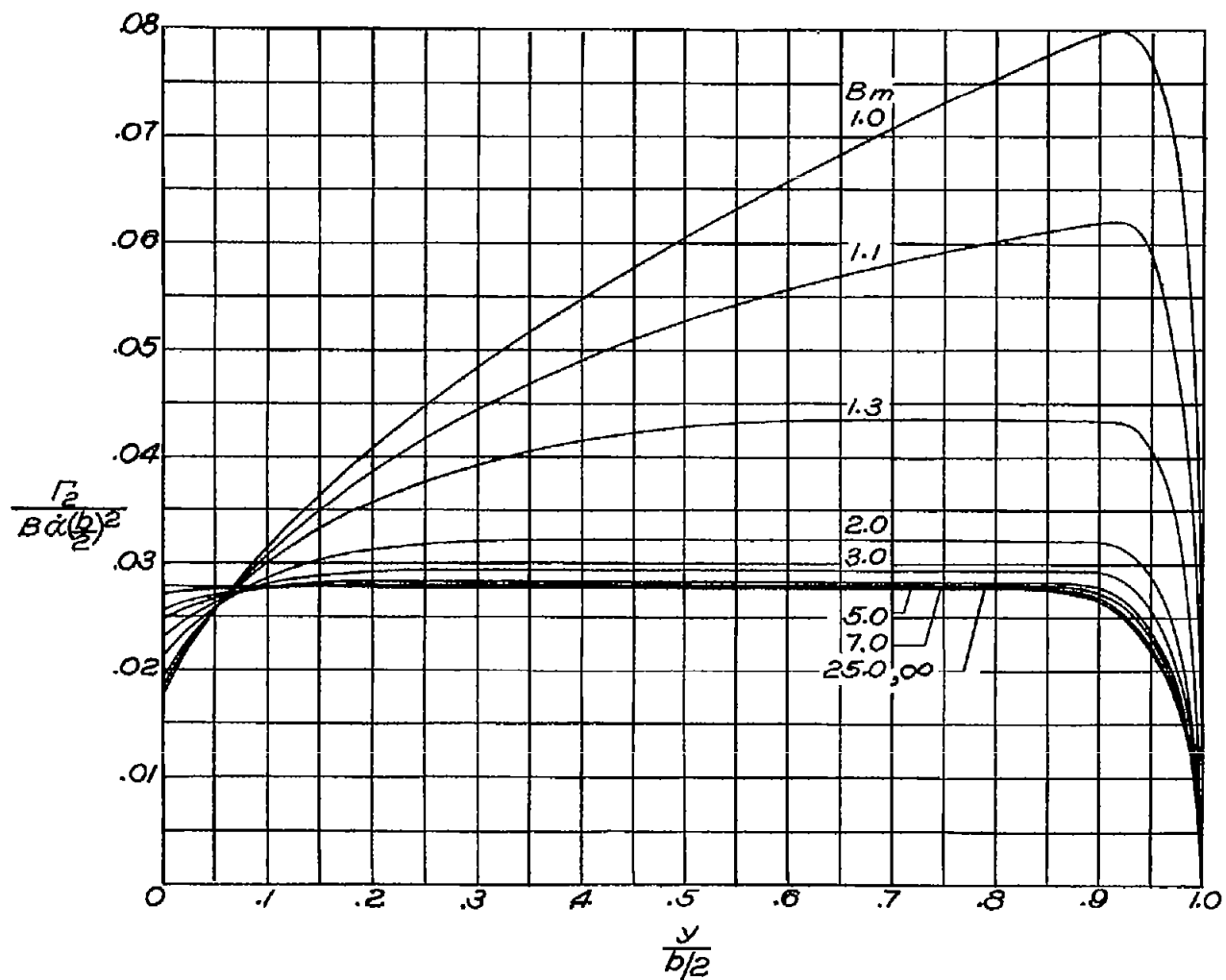
(e) $AB = 8; \lambda = 1.0.$

Figure 9.- Continued.



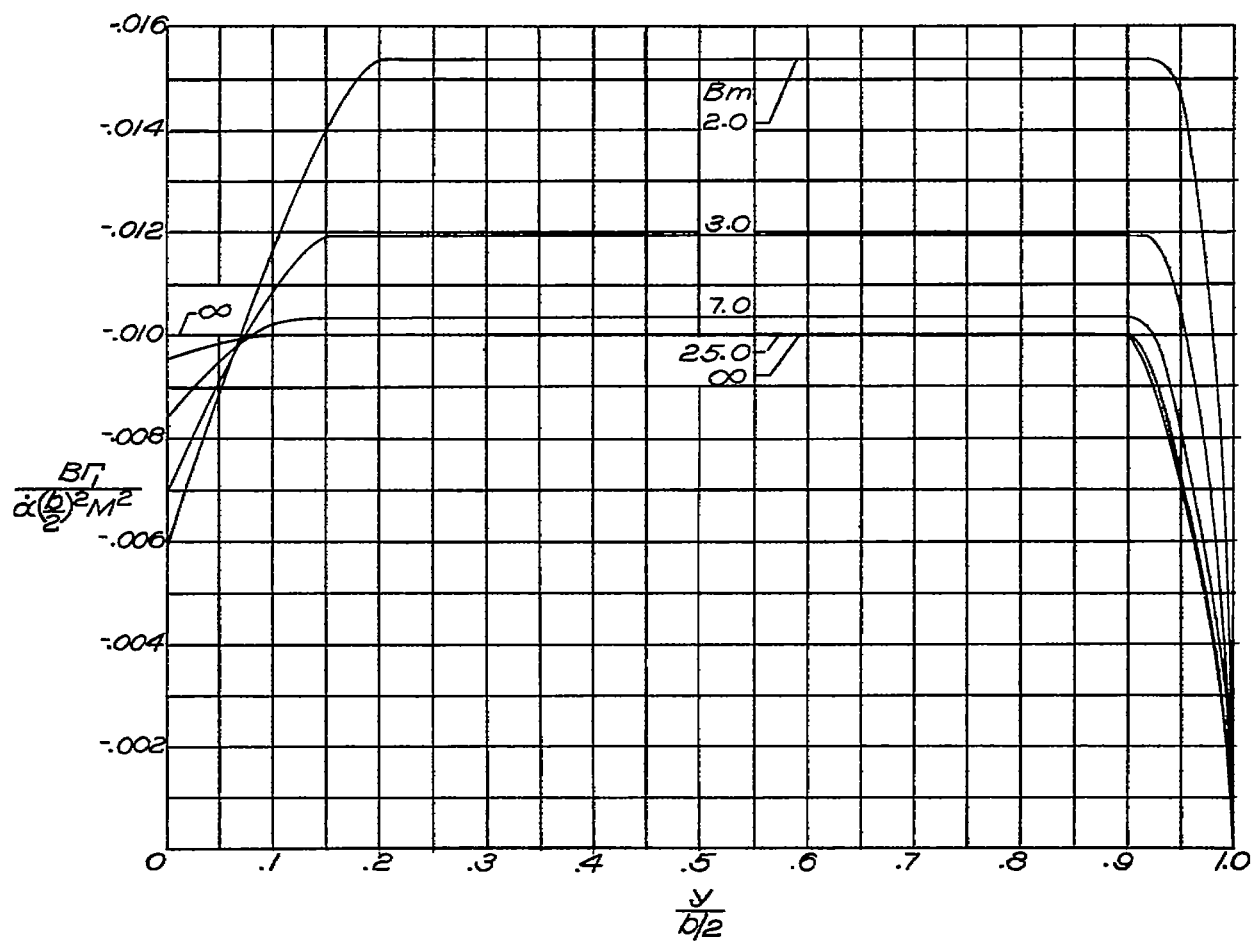
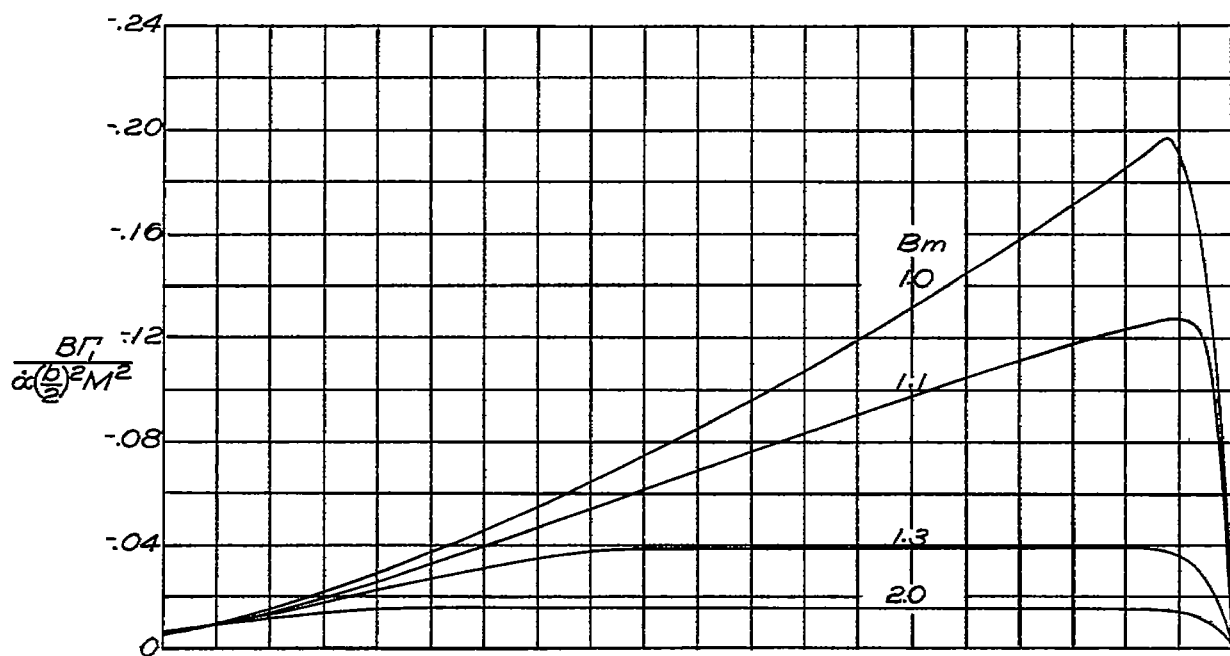
(f) $AB = 12$; $\lambda = 1.0$.

Figure 9.- Continued.



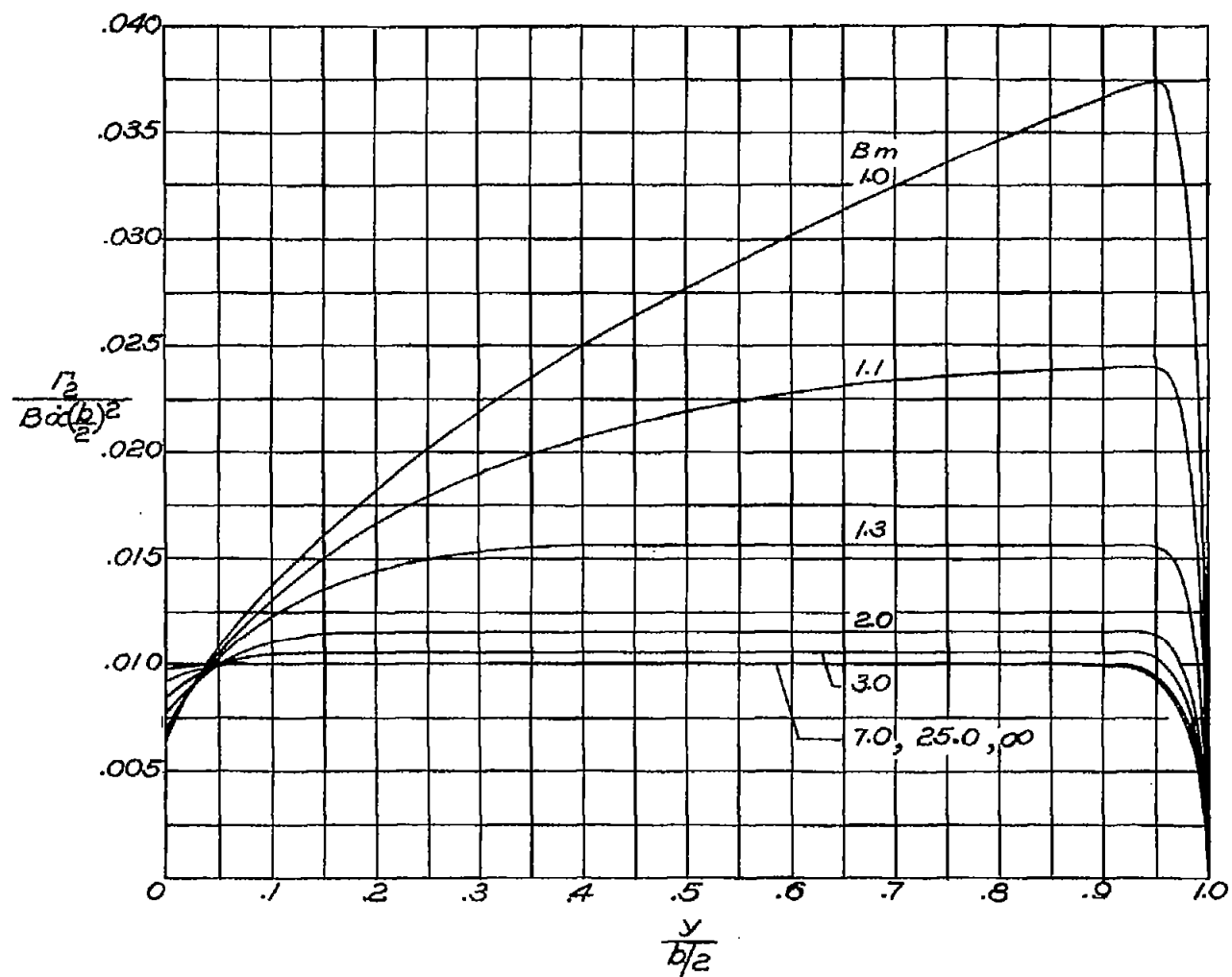
(f) $AB = 12$; $\lambda = 1.0$. Concluded.

Figure 9.- Continued.



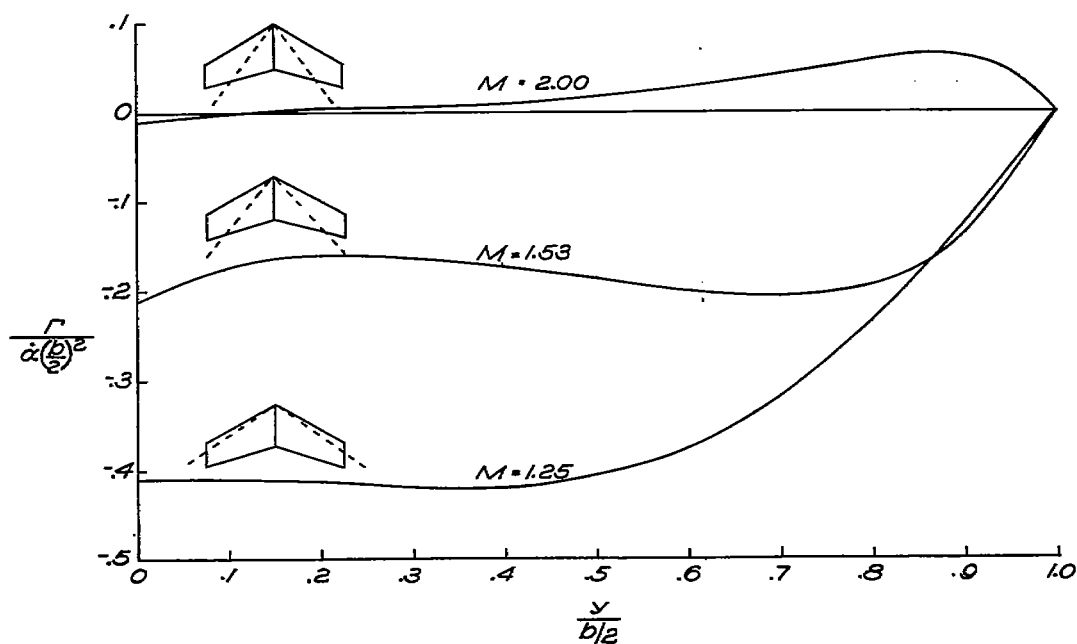
(g) $AB = 20$; $\lambda = 1.0$.

Figure 9.- Continued.

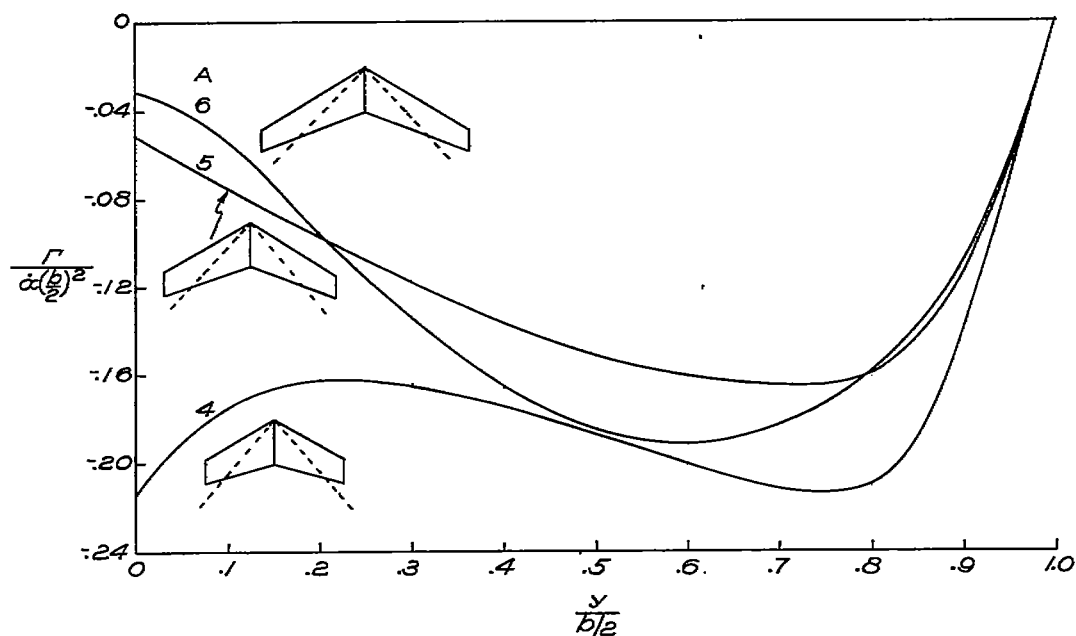


(g) $AB = 20$; $\lambda = 1.0$. Concluded.

Figure 9.- Concluded.

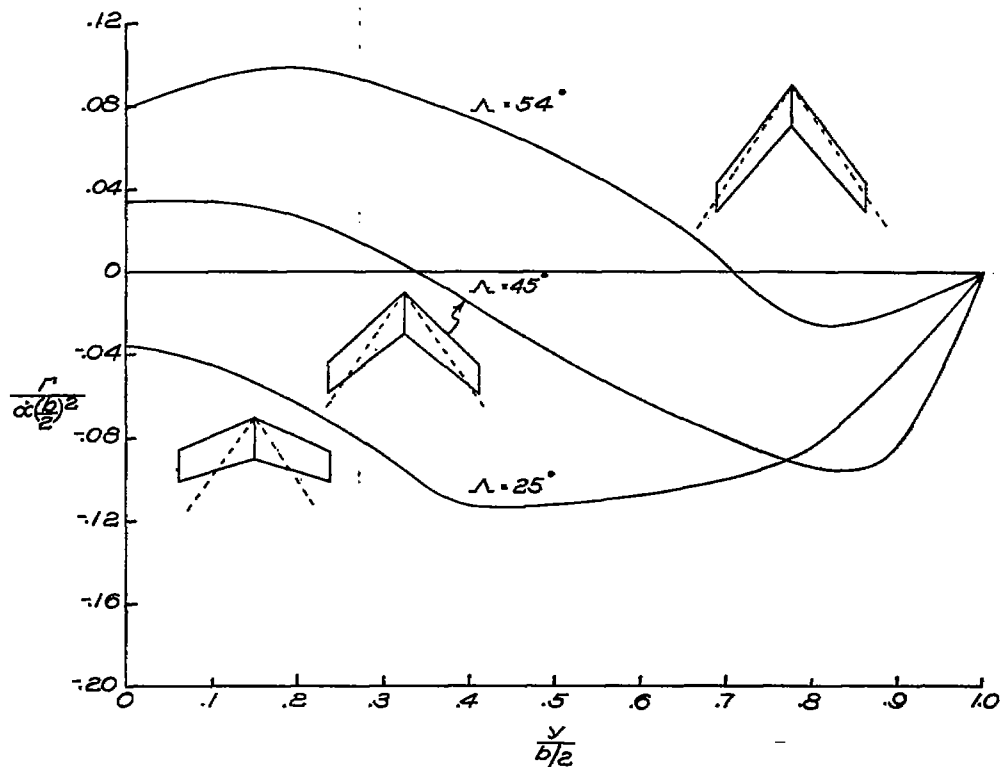


(a) Variation with Mach number. $A = 4$; $\Lambda = 30^\circ$; $\lambda = 0.50$.

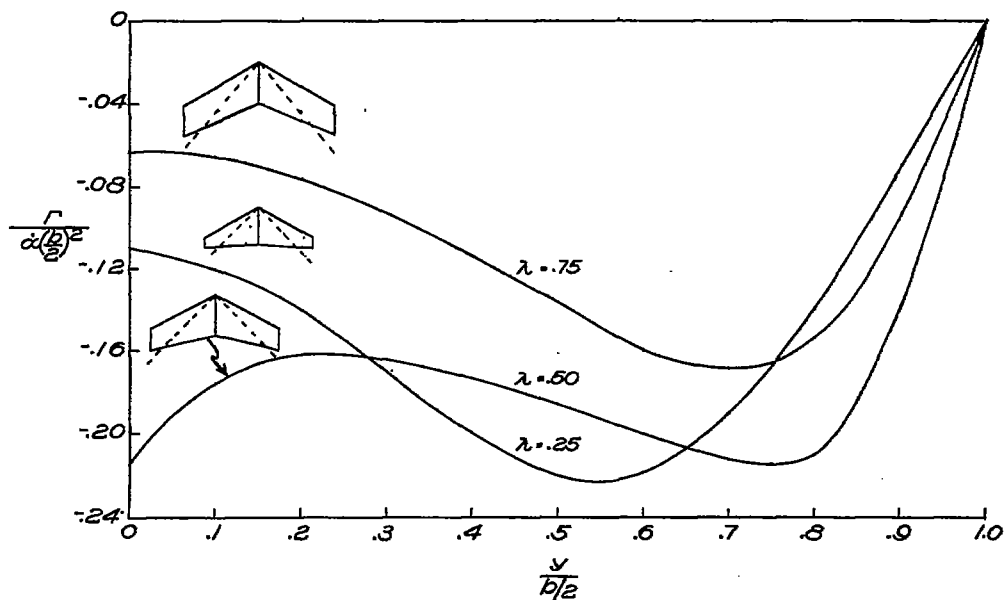


(b) Variation with aspect ratio. $M = 1.53$; $\Lambda = 30^\circ$; $\lambda = 0.50$.

Figure 10.- Some examples illustrating the variations of distribution of circulation along span with Mach number, aspect ratio, sweepback, and taper ratio.



(c) Variation with sweepback. $A = 4$; $M = 1.8$; $\lambda = 0.75$.



(d) Variation with taper ratio. $A = 4$; $M = 1.53$; $\Lambda = 30^\circ$.

Figure 10.- Concluded.